TUM

Analyzing Climate Adaptation and Heatwave Resilience in the Early-Stage Building Design

A Parametric Approach for Future-Proof Architecture

Scientific work to obtain the degree

M.Sc. Resource-efficient and Sustainable Building

at the TUM School of Engineering and Design

of the Technical University of Munich.

Supervisor   Michael Vollmer, Dr.-Ing.

                        Chair of Energy Efficient and Sustainable Design and Building

Author   Agata Dalach

                        Gärtnerstr. 62C

                        80992 Munich

Submitted   Munich, 01.01.2024

Vereinbarung

zwischen

der Technischen Universität München, vertreten durch ihren Präsidenten, Arcisstraße 21, 80290 München

hier handelnd der Lehrstuhl für Energieeffizientes und Nachhaltiges Planen und Bauen (Univ.-Prof. Dr.-Ing. W. Lang), Arcisstr. 21, 80333 München

– nachfolgend TUM –

und

Frau Agata Dalach, Gärtnerstr 62C, 80992 München

– nachfolgend Autorin/Autor –

Die Autorin / der Autor wünscht, dass die von ihr/ihm an der TUM erstellte Masterarbeit mit dem Titel

"Analyzing Climate Adaptation and Heatwave Resilience in the Early-Stage Building Design. A Parametric Approach for Future-Proof Architecture"

☒ auf mediaTUM und der Webseite des Lehrstuhls für Energieeffizientes und Nachhaltiges Planen und Bauen mit dem Namen der Verfasserin / des Verfassers, dem Titel der Arbeit, den Betreuer:innen und dem Erscheinungsjahr genannt werden darf.

☒ in Bibliotheken der TUM, einschließlich mediaTUM und die Präsenzbibliothek des Lehrstuhls für Energieeffizientes und Nachhaltiges Planen und Bauen, Studierenden und Besucher:innen zugänglich gemacht und veröffentlicht werden darf. Dies schließt auch Inhalte von Abschlusspräsentationen ein.

☐ mit einem Sperrvermerk versehen und nicht an Dritte weitergegeben wird.

(Zutreffendes bitte ankreuzen)

Vereinbarung

Zu diesem Zweck überträgt die Autorin / der Autor der TUM zeitlich und örtlich unbefristet das nichtausschließliche Nutzungs- und Veröffentlichungsrecht an der Masterarbeit.

Die Autorin / der Autor versichert, dass sie/er alleinige(r) Inhaber(in) aller Rechte an der Masterarbeit ist und der weltweiten Veröffentlichung keine Rechte Dritter entgegenstehen, bspw. an Abbildungen, beschränkende Absprachen mit Verlagen, Arbeitgebern oder Unterstützern der Masterarbeit. Die Autorin / der Autor stellt die TUM und deren Beschäftigte insofern von Ansprüchen und Forderungen Dritter sowie den damit verbundenen Kosten frei.

Eine elektronische Fassung der Masterarbeit als pdf-Datei hat die Autorin / der Autor dieser Vereinbarung beigefügt. Die TUM ist berechtigt, ggf. notwendig werdende Konvertierungen der Datei in andere Formate vorzunehmen.

Vergütungen werden nicht gewährt.
Eine Verpflichtung der TUM zur Veröffentlichung für eine bestimmte Dauer besteht nicht.

Die Autorin / der Autor hat jederzeit das Recht, die mit dieser Vereinbarung eingeräumten Rechte schriftlich zu widerrufen. Die TUM wird die Veröffentlichung nach dem Widerruf in einer angemessenen Frist und auf etwaige Kosten der Autorin / des Autors rückgängig machen, soweit rechtlich und tatsächlich möglich und zumutbar.

Die TUM haftet nur für vorsätzlich oder grob fahrlässig verursachte Schäden. Im Falle grober Fahrlässigkeit ist die Haftung auf den vorhersehbaren Schaden begrenzt; für mittelbare Schäden, Folgeschäden sowie unbefugte nachträgliche Veränderungen der veröffentlichten Masterarbeit ist die Haftung bei grober Fahrlässigkeit ausgeschlossen.

Die vorstehenden Haftungsbeschränkungen gelten nicht für Verletzungen des Lebens, des Körpers oder der Gesundheit.

Meinungsverschiedenheiten im Zusammenhang mit dieser Vereinbarung bemühen sich die TUM und die Autorin / der Autor einvernehmlich zu klären. Auf diese Vereinbarung findet deutsches Recht unter Ausschluss kollisionsrechtlicher Regelungen Anwendung. Ausschließlicher Gerichtsstand ist München.

München, den   München, den 01.01.2024

…………………………….   …………………………………….

(TUM)   (Autor:in)

Erklärung

Ich versichere hiermit, dass ich die von mir eingereichte Abschlussarbeit selbstständig verfasst und keine anderen als die angegebenen Quellen und Hilfsmittel benutzt habe.

München, den 01.01.2024

_____

Ort, Datum, Unterschrift

Table of Contents

Summary

In the near future, climate change will significantly impact people's lives, including their activities, comfort, and choices. Architecture, which primarily provides shelter, will face considerable challenges. According to the future climate scenarios of the IPCC, higher temperatures can be expected within the operational lifespan of the buildings built today.

For buildings equipped with air conditioning systems, this means increased energy demands for cooling during summer months. Buildings reliant on passive strategies, on the other hand, will be challenged in maintaining adequate thermal comfort. The capability to mitigate these effects and aim for informed decision-making in the design process is called climate adaptation or resilience.

This master's thesis focuses on the climate adaptation and resilience of buildings against the risk of overheating due to climate change. It explores the impact of early-stage design decisions through building performance simulations, to identify the most critical design parameters. The parametric approach makes this possible, and data visualization and analysis methods enhance the clarity and comprehension of the findings.

In this study, parameters such as building geometry, materials, shading, and glazing properties were analyzed. To assess the sensitivity of these parameters the workflow was divided into two parallel scenarios: buildings with mechanical conditioning, evaluated through indicators of total and peak energy demands, and buildings employing passive cooling strategies, assessed using thermal comfort indicators. In the future-updated environment, a large number of simulations were conducted over the two hottest months in order to reveal the most influential decisions to make the building future-proof, regardless selection of the future prognosis.

The main findings from this study indicate that the selection of shading devices, window dimensions, and glass properties are decisive in achieving climate resilience. In contrast, the choice of building materials and building orientation, while still relevant, play a minor role. Although parameter sensitivities showed differences across various scenarios and future predictions, the ranking of parameters from most to least efficient remained constant. Considering the significant differences among individual design

variants, especially in peak-value indicators, it becomes clear that a future-proof building will retain its resilience regardless of the specific future scenario that unfolds.

This study reveals the potential of early-design parametric simulations and their influence on the buildings, which will serve their users much longer than the norms and requirements are envisaged.

Kurzfassung

In naher Zukunft wird der Klimawandel das Leben der Menschen erheblich beeinflussen, einschließlich ihrer Aktivitäten, ihres Komforts und ihrer Entscheidungen. Die Architektur, deren Hauptaufgabe es ist, Schutz zu bieten, wird vor erhebliche Herausforderungen gestellt. Laut den Zukunftsszenarien des IPCC für das Klima können in der Betriebslebensdauer der heute gebauten Gebäude höhere Temperaturen erwartet werden.

Für Gebäude mit Klimaanlagen bedeutet dies einen erhöhten Energiebedarf für die Kühlung in den Sommermonaten. Gebäude, die auf passive Strategien angewiesen sind, werden dagegen Schwierigkeiten haben, ausreichenden thermischen Komfort zu gewährleisten. Die Fähigkeit, diese Auswirkungen zu mildern und auf informierte Entscheidungsfindung im Gestaltungsprozess abzuzielen, wird als Klimaanpassung oder Resilienz bezeichnet.

Diese Masterarbeit konzentriert sich auf die Klimaanpassung und Resilienz von Gebäuden gegenüber dem Risiko der Überhitzung aufgrund des Klimawandels. Sie erforscht den Einfluss von Designentscheidungen in der Frühphase durch Gebäudeleistungssimulationen mit dem Ziel, die kritischsten Gestaltungsparameter zu identifizieren. Der parametrische Ansatz macht dies möglich, und Methoden der Datenvisualisierung und -analyse verbessern die Klarheit und das Verständnis der Ergebnisse.

In dieser Studie wurden Parameter wie Gebäudegeometrie, Materialien, Beschattung und Verglasungseigenschaften analysiert. Um die Sensitivität dieser Parameter zu bewerten, wurde der Arbeitsablauf in zwei parallele Szenarien aufgeteilt: Gebäude mit mechanischer Klimatisierung, bewertet anhand von Indikatoren für den Gesamt- und Spitzenenergiebedarf, und Gebäude, die auf passive Kühlstrategien setzen, bewertet mit Hilfe von thermischen Komfortindikatoren. In der zukunftsorientierten Umgebung wurde eine große Anzahl von Simulationen über die zwei heißesten Monate durchgeführt, um die einflussreichsten Entscheidungen für die Zukunftssicherheit des Gebäudes aufzudecken, unabhängig von der Auswahl der Zukunftsvorhersage.

Die Haupterkenntnisse dieser Studie zeigen, dass die Auswahl von Beschattungen, Fensterabmessungen und Glaseigenschaften entscheidend für die Erreichung von Klimaresilienz ist. Im Gegensatz dazu spielen die Wahl der Baumaterialien und die Gebäudeausrichtung, obwohl immer noch relevant, eine untergeordnete Rolle. Obwohl die Sensitivität der Parameter Unterschiede in verschiedenen Szenarien und zukünftigen Vorhersagen aufzeigte, blieb die Rangfolge der Parameter von den effizientesten bis zu den am wenigsten effizienten konstant. Angesichts der signifikanten Unterschiede zwischen einzelnen Designvarianten, insbesondere bei Spitzenwertindikatoren, wird deutlich, dass ein zukunftssicheres Gebäude seine Resilienz beibehalten wird, unabhängig davon, welches spezifische Zukunftsszenario sich entfaltet.

Diese Studie zeigt das Potenzial von parametrischen Simulationen in der frühen Designphase und ihren Einfluss auf Gebäude, die ihren Nutzern viel länger dienen werden, als es Normen und Anforderungen vorsehen.

Abbreviations

ASHRAE	American Society of Heating, Refrigerating, and Air-Conditioning Engineers
AR5	IPCC Fifth Assessment Report
AR6	IPCC Sixth Assessment Report
BREEAM	Building Research Establishment Environmental Assessment Method
CMIP5	Coupled Model Intercomparison Project 5
CMIP6	Coupled Model Intercomparison Project 6
DGNB	Deutsche Gesellschaft für Nachhaltiges Bauen (German Sustainable Building Council) – DGNB e.V
EPW	EnergyPlus Weather File
ESPON	European Territory Observation Network
EUROCORDEX	European Contribution to the Coordinated Regional Climate Downscaling Experiment
IPCC	Intergovernmental Panel on Climate Change
GH	Grasshopper (visual programming tool)
HB, HB-Energy	Honeybee, Honeybee-Energy, elements of Ladybug Tools
HSP	Heat Sensation Percent
HVAC	Heating, ventilation, and air conditioning
LEED	Leadership in Energy and Environmental Design
OAT	One-at-a-time (sensitivity analysis)

PMV   Predicted Mean Vote

PPD   Predicted Percent of Dissatisfied

RCP   Representative Concentration Pathway

SSP   Shared Socioeconomic Pathway

UNFCCC   United Nations Framework Convention on Climate Change

WCRP   World Climate Research Programme

Glossary

Dry Bulb Temperature – temperature of a perfectly dry surface when exposed to convective heating of air (without the influence of humidity and radiation), ambient air temperature.

Grasshopper (GH) – a visual programming language plug-in included in Rhino 3D, enabling creation of parametric models, including generative architectures, as well as introduction of various advanced plugins and enhancements to Rhino 3D possibilities, such as physical simulations, advanced modeling or even machine learning.

Grasshopper definition – an algorithmic "script", made with the visual programming environment of Grasshopper.

Honeybee, Honeybee-Energy (HB, HB-Energy) – two of the Ladybug Tools plugins, designated for energy simulation. The particular elements of HB and HB-Energy enable creation of parametric building model, assigning zones, schedules and other properties as well as utilizing the earlier mentioned engines for energy-related calculations.

Ladybug Tools (LB) – a set of Grasshopper (and Dynamo) Python-written plugins for Grasshopper, enabling data analysis and visualization as well as communication with simulation engines, including RADIANCE and EnergyPlus.

Rhinoceros 3D, Rhino 3D – CAD/3D-modeling software, operating mainly on NURBS-surfaces (Non-Uniform Rational B-Spline Surfaces) and meshes, containing both a graphical user interface and command line input possibilities.

"Shoebox" model – a simplified rectangular-cuboid-shaped model of a building that resembles a shoe box.

1. Introduction

Addressing the sustainability challenges of today is crucial, but the objective of meeting future generations' needs demands that the strategies for building design and sustainable strategies in general must extend beyond the immediate present-day issues.

1.1. Motivation

The impact of global warming is becoming increasingly apparent in meteorological measurements. The year 2022 was the fifth warmest year recorded, and the last eight years preceding 2023 have been the warmest (C3S, 2023). Human activities are the primary cause of rising temperatures (Eyring et al., 2021), but even knowing this, we are not on track to meet the goals of the Paris Agreement (Chen et al., 2021). The then set goal of "*Holding the increase in the global average temperature to well below 2°C above pre-industrial levels and pursuing efforts to limit the temperature increase to 1.5°C above pre-industrial levels*" should be reached, among others, by measures of climate mitigation and adaptation (UNFCCC, 2016). Meanwhile, the current heatwaves in Europe are reaching temperatures even 10°C higher than averages (C3S, 2023).

Figure 1 presents the yearly trends in the global air temperature, with historical data spanning from 1940 till now. The interactive chart is available on the website Climate Reanalyser of the Climate Change Institute of the University of Maine (*Climate Reanalyzer*, n.d.) and the data is retrieved daily from the Copernicus Climate Change Service (C3S) (Hersbach et al., 2023). The orange line, representing the year 2022 was already alarming, but the thick black line, depicting the year 2023, may raise significant concern.
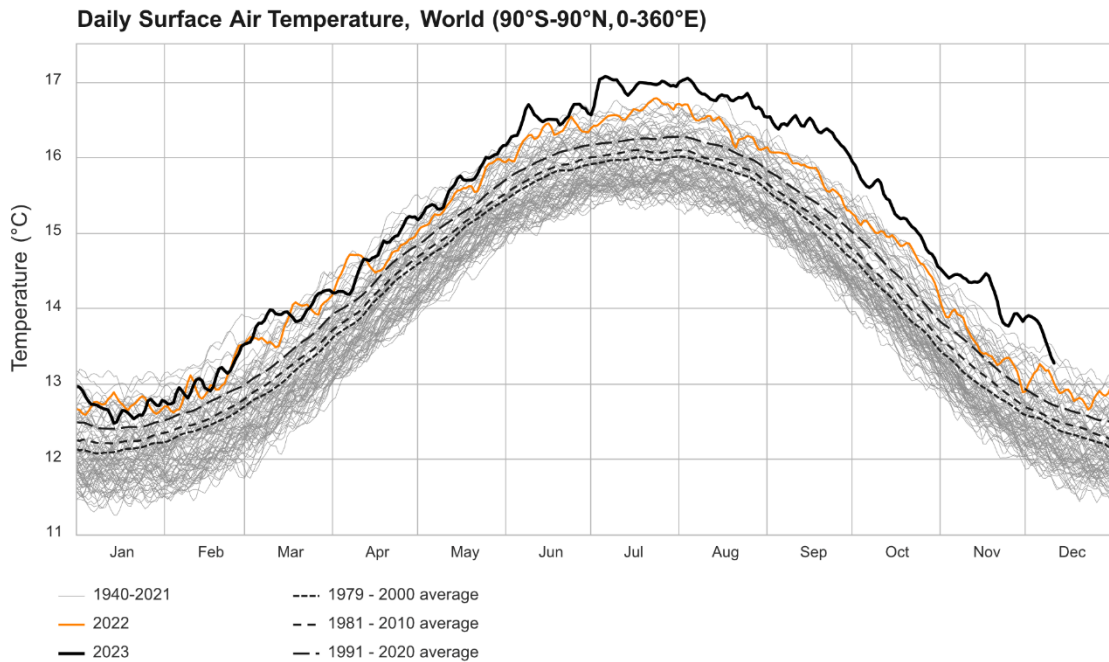
Figure 1 Global air temperatures spanning from 1940 till now (*Climate Reanalyzer*, n.d.)

Exposure to extreme events will grow in the future (Sharifi, 2022). Heatwaves, with higher intensity, longer durations, and appearing in unexpected locations, should be treated as one of the most important extreme events for which to prepare the built environment (Attia et al., 2021). August 2003's heatwave proved, that even Europe can be affected by their effects (Koppe et al., 2004). The summer of 2022 recorded unprecedented heatwaves, setting new temperature records among the historical data, which were subsequently surpassed by even higher temperatures observed in July 2023. Projections suggest that the occurrence of new temperature records will persist in the future (Seneviratne et al., 2021). Taking action against those predicted events is a valid objective. According to the EU Climate Adaptation Strategy, "*People, planet and prosperity are vulnerable to climate change, so we need to prevent the un-adaptable and adapt to the un-preventable*" (European Commission, 2021).

The implications arising from such extreme events on architecture affect all three dimensions of sustainability including social, environmental, and economic aspects (de Wilde & Coley, 2012). Resilient design strategies, therefore, aim to address human comfort and health, energy efficiency and the potential incurrence of additional costs.

1.2. Significance

The fundamental function of buildings is to provide shelter. Already in ancient times, people understood how to build structures to protect themselves from the surrounding conditions and make their space as comfortable as possible (Bougdah & Sharples, 2009). Examples of such approaches include using natural ventilation and shadows to chill the areas in warm periods (Candido, 2021).

Many modern examples of sustainable architecture are inspired by local and vernacular ways of building (Benslimane & Biara, 2019; Hamard, 2017; A. T. Nguyen et al., 2019; Seneviratne et al., 2021). On the other hand, the international style of architecture has fostered building practices and design choices, which could be described as non-sustainable. For example, fully glazed high-rise buildings require plenty of heating energy in winter and rely on air conditioning to cool the interiors in summer.

The lack of consideration for sustainability throughout the last decades can be considered a pattern of actions which contributed to climate change (Denton et al., 2022). Around 21% of global greenhouse gas emissions are generated by buildings (Cabeza et al., 2022), while up to 90% of those emissions may be caused during the building operation (de Wilde & Coley, 2012). The building sector is globally responsible for around 60% of world resource use and around 50% of produced debris (Sobek, 2022). Despite the fact, that in the EU, around 40% of the total energy is consumed by buildings, circa 50 million people are not able to sufficiently heat their houses in winter (The European Green Deal, 2019).

While sustainable architecture is a well-established building intention, it should be complementarily enhanced with parallel efforts in climate adaptation. Buildings must be prepared for the changing climate. Moreover, their design should not only include the strategies to deal with the current weather anomalies, but also, considering the long lifespan of buildings, additionally try to include the prognosed future characteristics of the environment surrounding the building. This means, that both its current as well as future performance should be evaluated (de Wilde & Coley, 2012). It is imperative that architecture serve its function effectively not only immediately after construction of a building, but also in the years leading up to its eventual vacation and demolition.

1.3. Research questions

Addressing the topics of the implications of climate change and increased temperatures on buildings and their users requires a comprehensive approach and understanding. The concept focusing on creating designs that maintain their performance despite fluctuating external conditions is referred to as climate adaptation. In the context of heatwaves, which are dangerous and deadly natural hazards, the chosen strategy is called resilience. This strategy targets the worst-case scenarios and provides the best protection and recovery in case of a danger. However, the true challenge lies in the uncertainty of future paths. Without precise knowledge of future conditions, it's difficult to make informed design decisions.

New technologies and digital tools enable predicting building performance under given conditions. Utilizing a parametric approach allows creating and analyzing the performance of variants of an early-design building, defined by a number of parameters. This way the most influential aspects of the design, when targeting climate adaptation and heatwave resilience, can be discovered.

Those considerations led to the formulation of two research questions guiding this thesis:

Can parametric early-stage simulations facilitate informed decision-making for future-proofing buildings?

Which parameters are the most decisive when aiming at climate adaptability and heatwave resilience?

1.4. Structure of the Thesis

The motivation described in Chapter 1.1 lead to the selection of this thesis topic, while its significance, elaborated in Chapter 1.2, explains why this topic is important. This section underscores the necessity of basing present-day architectural decisions on estimated future conditions, highlighting the relevance of sustainability, resilience, and climate adaptation, particularly in the context of climate change and the increasing frequency of heatwaves in summer.

In the Literature Review section of this thesis, those topics are deeply studied, along with the state-of-the-art solutions to these challenges, including building performance simulations and parametric design. The section also examines the possibilities of predicting future climate conditions and incorporating future-updated weather data into building design, particularly in the early design stages.

The Methodology section introduces a study that investigates this topic further. Utilizing a parametric approach for early-design performance simulation, it considers future-updated weather data and various scenarios to identify critical parameters for building climate adaptability and heatwave resilience. This section details the entire process, including the identification of main parameters and performance indicators, the setup of simulations, and the methods used for data visualization and interpretation.

Following the Methodology section, the Results section presents the substantial effects of this study. It includes creating a database, plotting, and analyzing charts, inspecting extreme and average values, as well as extracting valuable information from the dataset. This part, considering various scenarios and simulation setups, comprises several sub-chapters, each providing valuable insights into different aspects of the topic. The sensitivity analyses conducted in this section help determine which parameters are most influential in terms of building design's heatwave resilience and climate adaptability.

The Discussion section contains a summary and evaluation of all the study's findings as well as its main limitations. In the Outlook section, potential further research steps to build on these findings and to expand scientific knowledge are proposed. The thesis concludes with lists of bibliographic sources, images, tables, and all appendices.
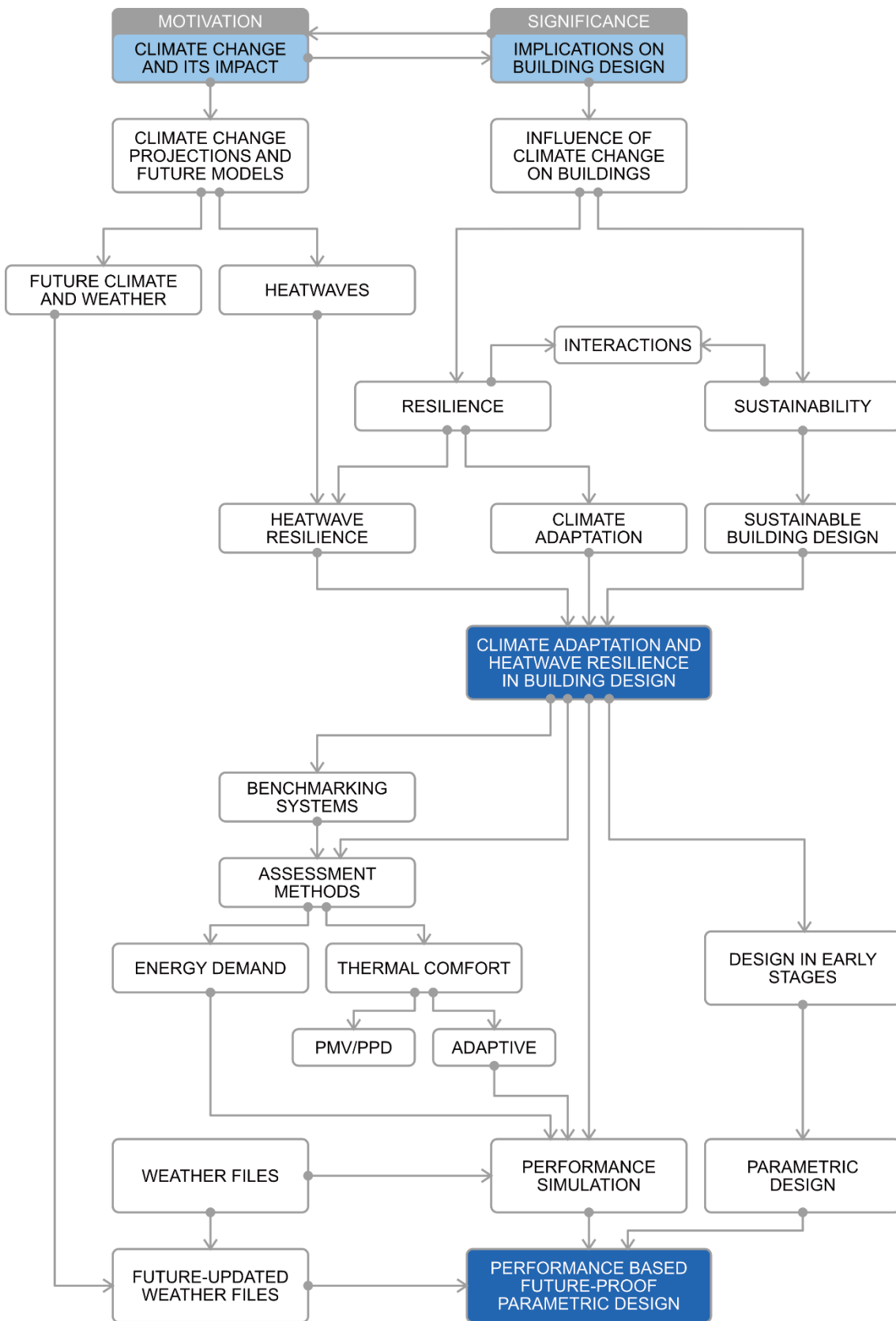
Figure 2 Framing the topic of the master's thesis – a flowchart of the Literature Review

2. Literature Review

In preparation for assembling the methodology for this topic, an in-depth review of established knowledge sources and current research was undertaken to build a robust knowledge base, thereby maximizing the study's quality. Figure 2 organizes the topics included in this section, presenting the relationships between them.

2.1. Climate Change and Its Expression

Considering climate being a key focus of this thesis, comprehending its complexities is crucial. The IPCC (Intergovernmental Panel on Climate Change) characterizes it as: *"Climate in a narrow sense is usually defined as the average weather, or more rigorously as the statistical description in terms of the mean and variability of relevant quantities over a period of time ranging from months to thousands or millions of years"* (IPCC, 2021) It contains average temperatures, precipitation, wind velocity and direction over ranges of time, specific for a particular area. Climate changes and this variability can be dependent on natural fluctuations, as well as various natural or anthropogenic impacts, what is referred to as forcing (IPCC, 2021).

The basic knowledge on the topic of natural climate change was formed already in the 19th century, when observations of the natural processes brought scientists to the conclusion, that the Earth's temperature was increasing (Arrhenius, 1896; Chen et al., 2021) The factors influencing those changes are natural and anthropogenic influences, referred to as "drivers". The natural influences include changes in natural conditions, such as solar irradiance, amount of water vapor in the atmosphere or water currents in oceans. The anthropogenic influences refer mostly to the increase of CO_2 concentration in the atmosphere caused by human activities, for example, combustion of fossil fuels (Chen et al., 2021). The current understanding of climate change, thanks to modern observation tools, the possibility of collecting big data and making complex calculations, is very advanced and well-established. It became clear, that despite natural processes also having their impact on global warming, the impact of human activities is the dominant factor (Eyring et al., 2021).

Since the industrial revolution, anthropogenic drivers have led to the increase of greenhouse gases – especially CO_2, methane and nitrous oxide (Gulev et al., 2021).

The observed consequences are temperature increase, reduction in ice coverage of the Arctic Sea, rise of the ocean levels and significant changes in entire ecosystems (Gulev et al., 2021). Moreover, the temperature increase contributes to the emergence of dangerous natural events, such as heavy rains and storms, floods and extreme temperatures (Seneviratne et al., 2021). As climate change progresses, the intensities, frequencies, and durations of these natural hazards are predicted to increase (Ranasinghe et al., 2021). Since each of these events has a different character, the focus of this thesis has to be limited to only one type of hazards, particularly heatwaves.

2.1.1. Climate Change Projections and Future Climate Models

Because of a large number of factors influencing climate, it is not possible to effectively predict its changes in the future and states in particular years or places. It is though possible to create comprehensive models, including as many factors as possible and to project the physical and socioeconomic processes on this model in order to achieve realistic simulation of how the climate could look in the future. The most significant approach to this topic is the Coupled Model Intercomparison Project (CMIP) of the World Climate Research Programme (WCRP), which coordinates physical models of the Earth's climate, including past, present, and future (Eyring et al., 2016). The project is currently in Phase 6, federating modeling institutions to conduct experiments, which are climate studies of various forcings, together creating WCRP, World Climate Research Programme.

Those efforts are scoped, summarized, and commented in Assessment Reports. The IPCC AR5 (Fifth Assessment Report) from 2014 based the future climate predictions (CMIP5 models) on Representative Concentration Pathways (RCPs), which are the predicted greenhouse gas concentrations, or radiative forcings, ranging from 2.6 to 8.5 W/m^2 in the year 2100 (Lee et al., 2021; Van Vuuren et al., 2011).

The new guidelines for experiments, CMIP6, use a set of scenarios called Shared Socioeconomic Pathways (SSPs), whose additionally include socioeconomic factors influencing climate which contains various anthropogenic factors influencing the climate, such as greenhouse gas emissions, land use, as well as mitigation strategies (O'Neill et al., 2016). Those factors along with RCPs, define a selection of possible futures in the AR6, called scenarios.

The Scenario Model Intercomparison Project (ScenarioMIP) identifies four main future pathways (SSP-RCP) (Lee et al., 2021):

- SSP1-2.6 – "Sustainability" – sustainable development,
- SSP2-4.5 – "Middle of the road" – continuation of historical path,
- SSP3-7.0 – "Regional rivalry" – prioritization of country security,
- SSP5-8.5 – "Fossil-fueled development" – energy-intensive economic growth.

The members of the IPCC Working Group I used these models to comprehensively analyze and describe the possible future climates. Their Report confirms that global warming is expected to continue regardless of the scenario (see Figure 3). Together with those changes, the global precipitation is also expected to increase and the Arctic Sea ice coverage is expected to decrease (Lee et al., 2021).
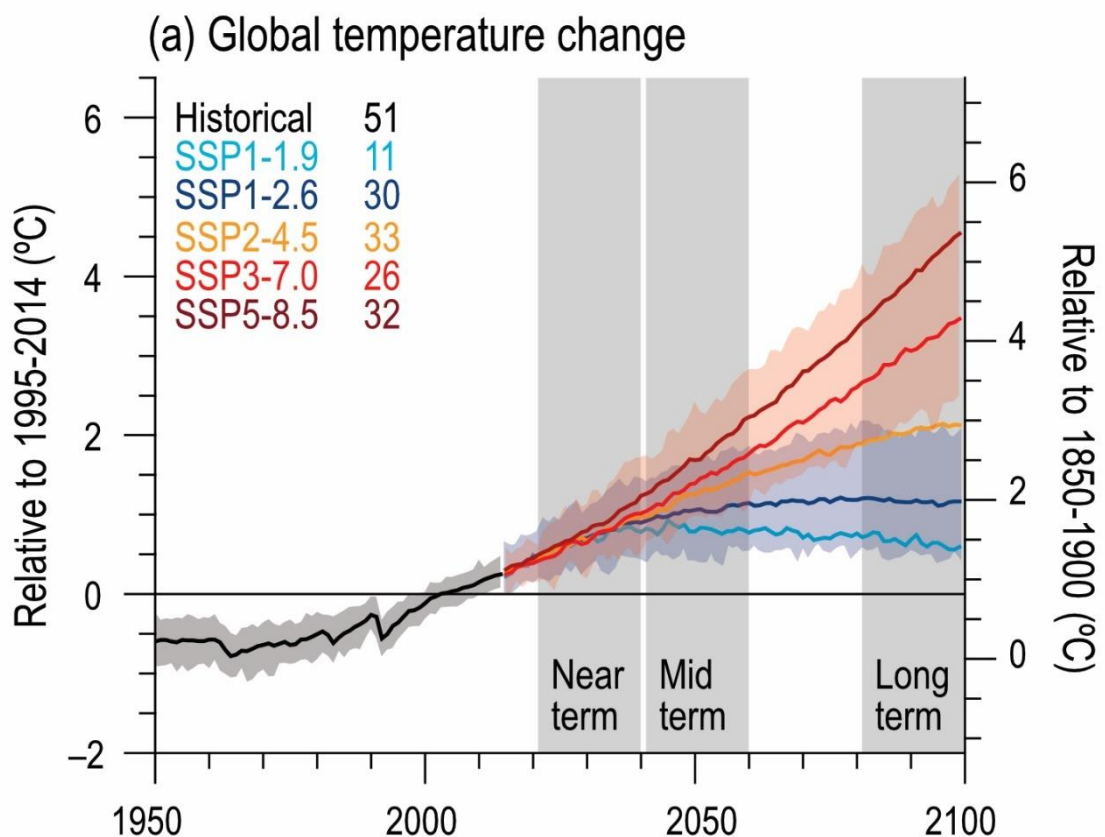
Figure 3 Projected temperature change according to scenarios (Lee et al., 2021)

Table 1 compares the predicted temperatures for future time ranges depending on the selected SSP-RCP scenario.

Table 1 Air temperature anomalies in relation to 1850-1900, averages from selected CMIP6 experiments, adapted from Lee et al. (2021)

	SSP1-1.9 (°C)	SSP1-2.6 (°C)	SSP2-4.5 (°C)	SSP3-7.0 (°C)	SSP5-8.5 (°C)
2021-2040	1.5	1.6	1.6	1.6	1.7
2041-2060	1.7	1.9	2.1	2.3	2.6
2081-2100	1.5	2.0	2.9	3.9	4.8

2.1.2. Future Climate-Change-Related Natural Hazards Risk Prediction

The anthropogenic greenhouse gas emissions lead to the increase of intensity and frequency of natural hazards, such as temperature extremes, massive precipitation events, floods and droughts (Seneviratne et al., 2021).

One significant representation of the risk predictions is the report published by the European Territory Observation Network (ESPON) in 2022: "Updating and Integrating CLIMATE Datasets and Maps" (Navarro et al., 2022). Based on a comprehensive methodology, it develops risk scenarios related to the climate change impacts, considering hazard type, exposure, and vulnerability of a particular region, consisting of its sensitivity and adaptive capacity. One of them is "Heat stress on population". The impact chains are then analyzed in the context of future scenarios and types of exposure.

In the EPSON project's results, one can find detailed maps representing the risk of heat stress on population in high-concentration scenario RCP8.5, considering relative and absolute population exposure to the risk (see Annex 1). In both cases, the maps show a significant increase of the impact chain risk. Even though the southern regions of Europe are the most affected, Central Europe is expected to experience a category change from "very low or low risk" to "medium or high risk".

2.1.3. Heatwaves

Heatwaves are natural hazards characterized by extreme elevations in temperature, resulting in thermal stress that brings significant health risks, or even death (Gosling et al., 2009). P. J. Robinson, (2001) defined heatwaves as follows:

"*A basic definition of a heat wave implies that it is an extended period of unusually high atmosphere-related heat stress, which causes temporary modifications in lifestyle and which may have adverse health consequences for the affected population. Thus, although a heat wave is a meteorological event, it cannot be assessed without reference to human impacts.*" (P. J. Robinson, 2001)

For a long time, heatwaves have been receiving less attention than other natural hazards and were considered less deadly, therefore less important in decision making (Koppe et al., 2004). However, this assessment may be not accurate, considering events such as the summer of 2003, where heatwave led to the death of tens of thousands of people, mostly in Italy, France, the United Kingdom, Germany and Portugal (Gosling et al., 2009; Koppe et al., 2004). The danger of high temperatures on the human body results from the fact, that the thermoregulatory mechanism becomes unable to remove the excess heat, which leads to the overheating of the organism (P. J. Robinson, 2001).

Heatwaves are expected to intensify in the future, meaning their longer expected duration, frequency and severity (Attia et al., 2021; Gosling et al., 2009; Rahif et al., 2022; P. J. Robinson, 2001; Seneviratne et al., 2021). Moreover, considering the fact, that elderly people are more prone to suffering from the negative effects of elevated temperatures, the aging society is endangered (Gosling et al., 2009). Economically disadvantaged individuals, who may not have access to air conditioning systems, are also at risk (Escandón et al., 2019). Furthermore, the accompanying air pollution and increased disease risk due to higher temperatures will make hot summers especially hazardous for human health (Hunt & Watkiss, 2011).

The understanding of the issue and knowledge of the inevitability of its effects, should motivate corresponding actions. In the case of architectural design, in parallel to sustainability, is the mitigation of those effects on the building energy performance and thermal comfort of its users.

2.1.4. Influence of Climate Change and Heatwaves on Cities and Buildings

The topic of influence of climate change on architecture and cities has already been well studied (Stagrum et al., 2020). The implications of climate change, which should be targeted by architecture, include temperature change, precipitation patterns, and wind changes (Bougdah & Sharples, 2009; Hunt & Watkiss, 2011). Global warming will highly influence the energy performance of buildings (de Wilde & Coley, 2012) and urban areas (Hunt & Watkiss, 2011; Tyler & Moench, 2012), affecting energy demands for heating and cooling (Wang & Chen, 2014). Buildings in Europe will experience a reduction of heating energy demand in winter, but an increase in cooling energy demand in summer (Hunt & Watkiss, 2011). Simultaneously the provision of indoor (Bougdah & Sharples, 2009; Escandón et al., 2019; Stagrum et al., 2020) (Alrasheed & Mourshed, 2023; Attia et al., 2021) and outdoor/pedestrian comfort (D. Robinson & Bruse, 2012) will become challenging.

Cities, and thus also the buildings in urban areas are especially prone to those changes due to the urban heat island effect (Bougdah & Sharples, 2009). Because of larger rugosity of urban areas, and inter-reflections between objects, more solar shortwave radiation is being absorbed, while the high building density reduces the longwave radiation loss (Rasheed & Robinson, 2012). Moreover, many common urban forms enable wind to be trapped in the urban canopy layer, thus weakening the airflow and temperature exchange further (Okeil, 2010). Those effects may lead to cities' temperature being higher by 2-5°C than their surroundings (Bougdah & Sharples, 2009).

Heatwaves, along with the accompanying overheating of buildings, constitute especially significant challenge to architecture. Depending on the character of heatwaves – their duration and intensity – buildings may perform differently in their mitigation. For example, shorter heatwaves might be absorbed by building materials (Flores-Larsen et al., 2022), while longer and more intense heatwaves will lead to overheating and decrease of user comfort. Moreover, in the event of a power shortage coinciding with a heatwave, mechanical ventilation fails to maintain comfortable interior conditions (Flores-Larsen et al., 2023).

The far-reaching impacts of climate change additionally encompass indirect implications on the built environment, including social and economic changes as well as land-use changes due to the transformations of ecosystems (de Wilde & Coley, 2012). On a

bigger scale, the interdependencies between city elements will also be affected (Hunt & Watkiss, 2011).

Coinciding with the occurrence of climate change, future policies and laws will impose more rigorous requirements on the energy performance of buildings (Kotireddy, 2018). However, it is impossible to accurately predict the extent and effectiveness of those policies due to the complexity of climate change and the nature of societal factors (Kotireddy, 2018). In Germany, according to a study by Olonscheck et al. (2011), the decrease in heating energy in winter will be dependent mostly on the share of renovated buildings, while the cooling energy demand – on the switch to mechanical air conditioning. The research team estimated the reduction of heating energy demand to reach around 44-47% between the periods of 1961-1990 and 2031-2060.

2.2. Sustainability, Climate Adaptation and Heatwave Resilience

As described in Chapter 2.1.4, buildings not only contribute to climate change but are also directly influenced by its consequences. Therefore, building design should, already in the planning phase, consider that it can be exposed to extreme temperatures, and be planned in such a way, that it is still able to completely fulfill its function, without the need for additional building systems. Sustainable architectural and urban design, which aims towards reduction of the building's negative influence on the environment, may be also a solution to this issue.

2.2.1. Sustainability Targets and Goals

Sustainability, or sustainable development, is not a new concept. The first traces of the first definitions of sustainability may be traced back to 250 years ago (Grober, 2013). One of the most significant definitions, however, was formed in the "Our Common Future" report published by the United Nations in 1987, usually referred to as "Brundtland's Report". The publication stressed the importance of environmental issues in policymaking and defined concrete steps towards sustainable development (United Nations, 1987). It implied that economic growth has limits, but also a goal, which focuses on (usually quoted) present and future generations. This goal includes all people, which makes it crucial to fight poverty (United Nations, 1987). It also clearly states that sustainable development is not a static condition that can be met, but an ongoing process.

Since then, other policies and actions were taken towards communicating the significance, drawing the development directions, and defining particular development goals. One of the most important climate accords was the Paris Agreement adopted in 2015 by the United Nations Framework Convention on Climate Change (UNFCCC, 2016). The treaty focuses on climate adaptation and mitigation through the reduction of temperature increase to well below 2 °C, possibly even below 1.5 °C of the levels before the Industrial Revolution.

The United Nations General Assembly in 2015 created a framework of 17 objectives known as Sustainable Development Goals, which target issues related to climate change and formulate guidelines in corresponding aspects. Among them, Goal 11 is called "Sustainable Cities and Communities" and aims to "*Make cities and human settlements inclusive, safe, resilient and sustainable*" (United Nations, 2015). This also includes the following goal:

"*11.b By 2020, substantially increase the number of cities and human settlements adopting and implementing integrated policies and plans towards inclusion, resource efficiency, mitigation and adaptation to climate change, resilience to disasters, and develop and implement, in line with the Sendai Framework for Disaster Risk Reduction 2015–2030, holistic disaster risk management at all levels.*" (United Nations, 2015)

In 2020, the European Commission approved the European Green Deal aiming to achieve climate neutrality by the year 2050 (The European Green Deal, 2019). Among the target areas, the emphasis lays on sustainable building and renovation and circular economy. It does also include the climate adaptation and mitigation strategies, claiming that "*Strengthening the efforts on climateproofing, resilience building, prevention and preparedness is crucial*".(The European Green Deal, 2019)

The European Union is committed to tackling climate change issues and aims at facilitating investments focused on climate resilience and adaptation (European Commission, 2021). All the EU Member States have already developed their national adaptation strategies, also including solutions applicable on international scales (European Commission, 2021).

2.2.2. Sustainability in Building Design

Sustainable development became a direction for the built environment, influencing the performance of newly built objects. This change is driven either by the ecological aspirations of the designers and their clients, or by stronger design requirements. Consequently, building design aims towards the reduction of the heating and cooling energy demand in order to meet the demands of building codes and regulations (Kotireddy, 2018), but often not surpassing the required values (de Wilde & Coley, 2012). This complex issue usually involves balancing the environmental targets with social and economic aspects (Lützkendorf, 2019).

The actions aiming to improve sustainability are usually focused on enhancing the energy efficiency of buildings, increasing the comfort of their users, or reducing the emissions and use of resources. An example of such approaches is bioclimatic design, which utilizes the site microclimate to achieve the best comfort and thus reduce the energy demand (Bougdah & Sharples, 2009), for examples the use of wind for natural ventilation and thus reduction of the need for air conditioning (Candido, 2021). Additionally, objects and greenery especially influence the site by providing shadows and influencing the wind flow (Bougdah & Sharples, 2009).

Modern approaches to sustainable architecture include passive houses (Hasper et al., 2021), high-performance buildings (Attia et al., 2013), including low- or zero-energy buildings (Manzoor et al., 2022; Omrany et al., 2022; Rey-Hernández et al., 2018) and plus-energy buildings (Hawila et al., 2022), also called positive energy buildings (Hasan & Reda, 2022). The research focuses on evaluation and decrease of the environmental impact of buildings, through the choice of materials and use of energy (Omrany et al., 2022), or even on achieving a positive annual energy balance (Hawila et al., 2022).

One of the concepts within sustainability is sufficiency, which means limiting the amount of materials and energy needed throughout the entire lifecycle of a building (Cabeza et al., 2022). Especially in the context of rising temperatures, it will mean more thoughtful design (choice of building form, properties, size of openings and orientation) over equipping it with energy-intensive cooling systems (Cabeza et al., 2022).

Sustainability Assessment systems, such as BREEAM, LEED and DGNB offer performance metrics, focusing on various aspects of the design (Ferreira et al., 2023).

By granting points or percentages, buildings may receive special certificates informing about their sustainability.

On the urban or neighborhood level, sustainable development usually involves public participation and involvement of additional, professional actors (Lützkendorf, 2019). Moreover, similarly to buildings, urban areas can be also assessed in terms of sustainability (Ehlers et al., 2023) and energy efficiency (Litsa & Giarma, 2023).

2.2.3. Climate Adaptation

The building response to changing temperatures is usually referred to as climate adaptation (Stagrum et al., 2020). As defined by Working Group II of IPCC Report, "*In human systems, the process of adjustment to actual or expected climate and its effects, in order to moderate harm or exploit beneficial opportunities. In natural systems, the process of adjustment to actual climate and its effects; human intervention may facilitate adjustment to expected climate and its effects*" (Möller et al., 2022a).

In building design, climate adaptation strategies are the measures taken in order to reduce the risks and vulnerability to climate change (Ara Begum et al., 2022). They encompass the influence of raising temperatures, changes in precipitation and wind direction on the built environment and the actions that can be undertaken to improve the conditions during this kind of stress. Those strategies aim to ensure, that in context of extreme events, buildings are still able to provide comfort internal conditions to their users (Dodman et al., 2022). Those strategies include above all the provision of shading from the sunlight, proper selection of materials in terms of insulation and thermal mass, as well as possibilities of natural ventilation and nighttime cooling (Dodman et al., 2022). This technology, known as passive cooling, is a method of lowering the indoor air temperature through natural air circulation. Although it was already known in ancient times in warm regions (Di Turi & Ruggiero, 2017), is still used in low-tech architecture and explored in the context of the climate change and elevated outdoor temperatures (Gilani & O'Brien, 2021).

Climate adaptation is aligned with the aforementioned Sustainable Development Goals (Fuldauer et al., 2022) in the goal of targeting the climate change and its possible influence on people and their environment. Even though climate adaptation strategies are in a focus of current research, they are not yet sufficiently explored (Stagrum et al., 2020).

2.2.4. Definition of Resilience

In the field of sustainability, one of the often-discussed concepts is resilience (Attia et al., 2021; Moench, 2014; Rodriguez-Nikl, 2015). There is no consensus on its definition in the literature (Burman et al., 2014; Sharifi, 2022), nor its established universal assessment methodology (Burroughs, 2017). It is usually linked with the concepts of vulnerability (sensitivity to external stress or events) and adaptive capacity/adaptability (ability to adjust to climate change) (*DGNB System. New Construction, Buildings, Criteria Set. Version 2023 International*, 2023; Gallopín, 2006). Other similar terms used to describe the building response to extreme events are resistivity (Rahif et al., 2022), or robustness (Chinazzo et al., 2015; Kotireddy, 2018). Moreover, Attia et al., (2021) point out, that a building or system can be only named resilient, when it is vulnerable and experiences a failure, for example overheating due to a heatwave.

Attia et al., (2021) collected almost 90 publications focused on overheating and power outages resilience, coding them with themes: vulnerability, resistance, robustness, recovery, and resilience. Based on this review they were able to conclude, that "*The definitions of resilience concern with the interplay of continuity and change of objects/systems subject to internal or external disruption(s)*" (Attia et al., 2021). They also noted that the understanding of resilience is different in various research disciplines, but it does always contain "a shock", to which the object or system is exposed. Most literature sources, when addressing resilience, describe the bigger-scale influence of extreme events (Attia et al., 2021). Ernstson et al., (2010) addressed the uncertainty of the future of urban areas and the resilience of the ecological economy.

According to the IPCC, "*Resilience is (…) the ability of a social, ecological, or socio-ecological system and its components to anticipate, reduce, accommodate, or recover from the effects of a hazardous event or trend in a timely and efficient manner*" (Denton et al., 2014) or "*The capacity of interconnected social, economic and ecological systems to cope with a hazardous event, trend or disturbance, responding or reorganising in ways that maintain their essential function, identity and structure. Resilience is a positive attribute when it maintains a capacity for adaptation, learning and/or transformation*" (Möller et al., 2022b).

The properties of a resilient physical or social system are, according to Bruneau et al., (2003): robustness (ability to withstand), redundancy (ability to substitute system

elements), resourcefulness (ability to utilize possessed material and human resources) and rapidity (short time of recovery). Considering the agents, stakeholders and policymakers, the most important aspects of resilience are, according to Moench, (2014) the ability to learn (willingness to reflect on past experiences), resourcefulness (provision of assets and skills) and responsiveness (ability to physically recover).

2.2.5. Resilience in Building and Urban Design

The goal of resilient building design is to ensure that in the context of climate change, the safety of people and their belongings is preserved, but also to make sure that buildings can be used according to their purpose, without the increase of costs of their operation (*DGNB System. New Construction, Buildings, Criteria Set. Version 2023 International*, 2023).

In building design, parameters and approaches which can be related to resilience are targeting possible risk, adaptability, self-sufficiency, and durability of the structures. There are examples of targeting the topic of building resilience in architecture, including building redesign and conversion to a hotel with durability and resilience on mind, especially including protection of vulnerable structures (Sijakovic et al., 2021)

There are more examples of approaches to describing or improving resilience in urban design. Disaster resilience of cities, on an example of Sri Lanka, was studied by Malalgoda et al., (2014), including the analysis of the most important challenges to the built environment. Sharma et al., (2014) investigated possible methodologies for resilience of urban systems, agents and institutions of seven Indian cities (Sharma et al., 2014). Social aspects of urban resilience were described by Ernstson et al., (2010) in context of the cities of New Orleans, Cape Town and Phoenix. Stead, (2014) focused on resilient water management in the Netherlands when faced with climate change issues, including the case study of Rotterdam's vulnerability to floods.

2.2.6. Resilience Assessment Approaches and Measures

In contrast to the well-established sustainability evaluation frameworks, resilience assessment tools and methodologies are still in the experimental stage. Despite the availability of many guidebooks, practical measurements of resilience are still missing (Tyler & Moench, 2012). Furthermore, a universal, overall assessment framework might be inadequate, as every case is different and such an approach could lead to the

undermining of the significance of particular factors (Moench, 2014). Every location is prone to different hazards, which has posed the key question, after (Moench, 2014): "*Resilient to what?*".

The approaches to creating non-overall resilience assessment include frameworks for climate resilience of urban areas (Moench, 2014) and hydro projects (Bourgin & Le-Clerc, 2022), flood resilience of cities or coastal areas (Karamouz & Zahmatkesh, 2017), hurricane resilience (Tokgoz & Gheorghe, 2013) or seismic resilience of buildings (Takewaki et al., 2013) and communities (Bruneau et al., 2003), disaster management of civil infrastructure (Bocchini & Frangopol, 2011). Homaei & Hamdy, (2021), on the other hand, focused on the thermal resilience of buildings after disruptive events.

What is common for all those approaches is the existence of a negative event, a shock or disruption, to which an object or system should respond. Various studies tried to quantify this response, usually comparing the state before and after the disruptive event. Bruneau et al., (2003)'s approach included measuring the percentual degradation of performance due to a seismic event and the restoration of the recovery over time:

$$R = \int_{t_0}^{t_1} [100 - Q(t)]dt$$

Equation 1 Resilience equation, according to Bruneau et al. (2003)

In Equation 1, R is resilience, $Q(t)$ is the quality of the object or system, t_0 is the time of shock beginning, and t_1 is the time when the initial state has been restored. Further developments of this formula, as well as a description and discussion of the so-called "resilience triangle" can be found in studies of Bocchini & Frangopol, (2011). In said studies, several recovery strategies in terms of disaster resilience were compared and assessed, considering parameters such as total cost of intervention, time required for recovery, minimum acceptable functionality etc.

2.2.7. Heatwave Resilience

Considering heatwaves as types of natural hazards, response to them can still be referred to as resilience, in this case heatwave or overheating resilience.

Overheating resilience is currently receiving plenty of attention, reflecting its significance in the context of climate change and resulting global warming. Gremmelspacher et al.,

(2020) focused on building retrofit in Denmark and Germany and based on four case studies in the years 2010-2099 with 30-year intervals, they concluded the urgency of the use of future climate projections in order to increase their climate resilience. Rahif et al., (2022) introduced a framework for evaluating cooling strategies against overheating due to climate change. They introduced a measure named "Climate Change Overheating Resistivity (CCOR)", describing it as: (it) "*shows to what extend the indoor overheating risk will increase with the increase of outdoor thermal stress under future climate scenarios*", therefore focusing on the change of indoor comfort due to extreme temperatures outside.

The most important actions, which can be taken against the heatwaves are provision of green areas and water, as well as providing shade and natural ventilation with building design (Bougdah & Sharples, 2009). The choice of building materials, including reflective surfaces and thermal insulation as well as thermal mass, also plays a major role (Bougdah & Sharples, 2009). Massive buildings, due to their thermal mass, are able to postpone the effects of a heatwave on the indoor environment by up to two days (Flores-Larsen et al., 2022).

2.2.8. Resilience and Climate Adaptation in Benchmarking Systems

The topics of resilience and climate adaptations more and more often appears in sustainability benchmarking systems, including DGNB in Germany.

While resilience was only a contributing factor to the Biodiversity category in 2020 the DGNB criteria set (*DGNB System. New Construction, Buildings, Criteria Set. Version 2020 International*, 2020), it has its own category in the 2023 version (*DGNB System. New Construction, Buildings, Criteria Set. Version 2023 International*, 2023), under the economic quality main topic. The criterion includes the building resilience to climate and environmental risks (noise, air quality, radon) and requires the so called "Basic resilience" to be possessed by all the buildings. Climate change adaptation is the second feature indicator within the Resilience criterion and includes the measures of effectiveness and alignment with local, regional and national adaptation plans or strategies. Moreover, additional points can be received for the "AGENDA 2030 Bonus" if measures against heat stress were made to the project, including minimizing or converting solar input, warm air removal and introduction of cool air from sustainable technical solutions. Resilience is also assessed in the Districts catalog (*DGNB System.*

Districts Criteria Set. Version 2020, 2020). In both cases, to receive points for resilience, planners must prove, that buildings or districts are not exposed to natural hazards or if so, that they are technically resistant.

In BREEAM (Building Research Establishment Environmental Assessment Method in the United Kingdom), Resilience is characterized by four focus points: Resistance (prevention), Reliability (mitigation), Redundancy (availability of alternatives) as well as Response and Recovery (*Encouraging Resilient Assets Using BREEAM*, n.d.).

LEED (*Leadership in Energy and Environmental Design*) green building certificate awards certification credits to buildings, whose designers utilized the LEED Climate Resilience Screening Tool for identification of climate sensitivities and enhancements for the resilient design (*LEED Climate Resilience Screening Tool for LEED v4 Projects | U.S. Green Building Council*, n.d.).

2.2.9. Interdependencies Between Sustainability and Resilience

The interdependencies between sustainability and resilience are a subject requiring additional attention. According to (Rodriguez-Nikl, 2015), "*Resilience is a necessary condition for sustainability*", even though in his paper he refers to disaster resilience. Burman et al., (2014) claim, that there should be a strong distinction between those two terms, as resilience measures do not necessarily need to be sustainable. Sustainability usually refers to consistent and long-term decisions, while resilience focuses on short-term extreme events.

The achievement of resilience does not inherently contribute to the overall sustainability of a building, as the actions undertaken to mitigate an anticipated risk may compromise the overall performance of the building and, consequently, its sustainability (Burman et al., 2014). Conversely, by aiming at sustainability, building resilience can be reduced. One of such examples is the Passivhaus standard, in which a highly-insulated building envelope may contribute to building overheating, trapping the heat inside (Kotireddy, 2018). Nevertheless, both sustainability and resilience share the mutual goal of provision of the best-performing design in the uncertain future (Rodriguez-Nikl, 2015). Achieving both requires a thoughtful design, analysis of external conditions and building performance simulations, estimating both the energy performance, as thermal comfort of the building's users in its interior spaces.

2.3. Thermal Comfort

One of the most important aims of architecture is to create indoor spaces, which are comfortable for their users (Bougdah & Sharples, 2009).

2.3.1. Thermal Comfort and the Human Body

The perception of comfort is linked to the human body's thermal state and its internal mechanisms (Van Treeck, 2011). The body regulates its temperature by balancing the heat generated by metabolic activities with the heat released to its surroundings.

Thermal comfort defined as satisfaction with the ambient climate (*DIN EN ISO 7730*, 2006) occurs when the body's heat balance maintains a constant temperature. The sensible and latent heat exchange with the environment depends on the air temperature and relative velocity, the mean radiant temperature, and the water pressure in the atmosphere. Some of those relations are depicted in Figure 4, based on the ISO Standard 7730 and ASHRAE Standard 55. A person's clothing and activity level significantly affect their thermal energy balance (ASHRAE, 2021). While the perception of comfort is generally consistent across cultures and climates (ASHRAE, 2021), studies have shown that women and the elderly prefer slightly warmer environments than younger men (Schaudienst & Vogdt, 2017). Moreover, research by Wu et al. (2023) suggests, that upper body thermal conditions impact comfort more than lower body conditions.

Extreme temperatures can lead to either excessive heat loss, causing hypothermia, or overheating, leading to hyperthermia. Both conditions can decrease work performance and pose health risks (ASHRAE, 2021). In case of elevated temperatures, the human body produces sweat to cool the skin's surface through evaporation.

2.3.2. Thermal Comfort Measures for Building Design

Thermal comfort can be influenced by design decisions and actions of the building users. Orosa & Oliveira (2011) found that building construction significantly influences thermal comfort and sensation, with internal cladding permeability affecting indoor air humidity and comfort. On the other hand, the choice of flooring materials does not significantly influence the thermal comfort of people wearing shoes (ASHRAE, 2021).

Increasing air velocity can enhance thermal comfort, both in the case of mechanical ventilation as well as in the case of opening the windows.

While it is impossible to create universally satisfying thermal conditions, numerous measures exist for comparing or numerically expressing thermal comfort. If one or more of such conditions have been specified to meet a specific value, it can make an impact on the project, its energy demands and the costs of operation.

Thermal comfort measurement and prediction have already been extensively studied. Some of those studies include thermal manikins, which model different parts of the human body against its environment (Van Treeck, 2011). Predictive models for thermal comfort inside spaces include rational (including PMV and PPD models) and adaptive models (Djongyang et al., 2010). Rational models suit static conditions, like those regulated by air conditioning, while adaptive models consider occupant behavior, outdoor environment, and personal expectations.
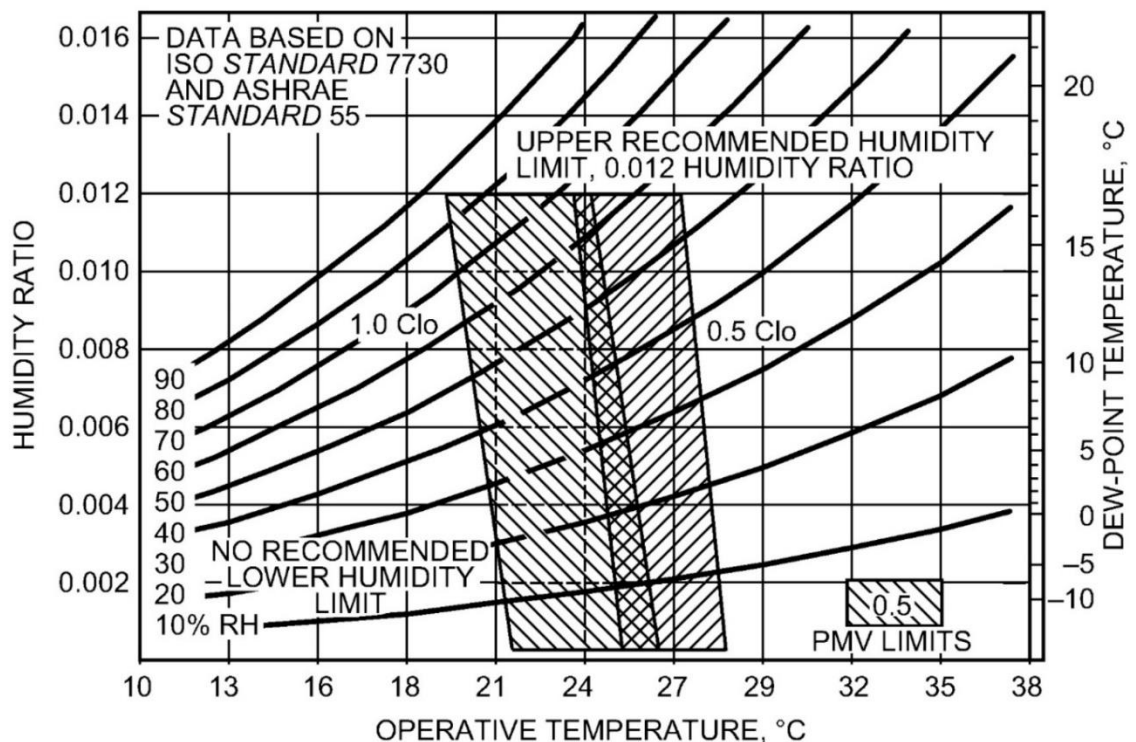

Figure 4 Comfort areas for 1.0 and 0.5 clothing rates (clo) depending on operative temperature and humidity by low air speed of less than 0.2 meters per second (ASHRAE, 2021).

2.3.3. PMV / PPD Thermal Comfort

Developed in the 1970s by Ole Fanger using climate chamber experiments with college students, the PMV (Predicted Mean Vote) model integrates key thermal conditions into an equation. This equation rates comfort on a scale of +3 (hot) to -3 (cold), and a subsequent equation calculates the PPD (Predicted Percent of Dissatisfied) (Cheung et al., 2019; Fanger, 1970; Schaudienst & Vogdt, 2017; Van Hoof, 2008). Since then, Fanger's methodology has been adapted by various international standards and norms and was used in numerous projects and studies.

The EN ISO 7730:2005 norm describes this calculation method but limits its use to indoor temperatures below 30 degrees Celsius. According to the norm, PMV assesses median comfort levels, while PPD estimates the percentage of people likely to find a space too hot or cold. It can be calculated with the direct use of complex equations, or with tabular values within the norm, or with the use of a sensor device with integrated PMV calculator (*DIN EN ISO 7730*, 2006). The American Society of Heating, Refrigerating and Air-Conditioning Engineers ASHRAE developed its thermal sensation scale, based on studies by Fanger, which – similarly to PMV – includes a rating from +3 (hot) to -3 (cold) (ASHRAE, 2021). The answers +3, +2, -2 and -3 count as being dissatisfied.

Even though PMV and PPD are the most often chosen indicators to predict the thermal comfort, some authors argue, that their accuracy is low and not applicable to all models and scenarios (Cheung et al., 2019; Van Hoof, 2008). Even though the PPD model has been discarded by the ASHRAE standard, some authors suggest, that also the PMV is the source of inaccurate predictions (Cheung et al., 2019) and climate chamber experiments do not correspond to the human behavior in real conditions (Djongyang et al., 2010). Fanger himself noted that his model is best for mechanically-controlled indoor conditions, not naturally ventilated spaces (Van Hoof, 2008). Further research on this topic led to the conclusion, that in naturally ventilated buildings in warmer climates the comfortable temperature may be higher, and in colder climates, the comfortable temperature may be lower than what would be indicated by those models (Van Hoof, 2008). This way, adaptive models have been introduced and used for such cases, alone or in combination with rational models to create a more accurate prediction of thermal comfort inside a building (Orosa & Oliveira, 2011).

2.3.4. Adaptive Thermal Comfort

The adaptive thermal comfort model assumes that people can adapt to their thermal environment. This model It acknowledges the human influence on its surroundings, such as changing clothes and opening windows and use the outdoor air temperature in the calculations (Orosa & Oliveira, 2011).

To address the topic of comfortable indoor temperature, in relation to the outdoor temperature, the German national appendix to the Norm DIN EN 15251 can be consulted (*DIN EN 15251*, 2012). It defines the comfortable interior air temperature $\theta_{Ra,C}$ and the border deviations of ± 2 K:

- For outdoor temperature below 16 °C: $\theta_{Ra,C}$ = 22 °C
- For outdoor temperature above 32 °C: $\theta_{Ra,C}$ = 26 °C
- For outdoor temperature between 16 °C and 32 °C: $\theta_{Ra,C}$ = 18 °C + 0,25 * AT
   (where AT is the outdoor temperature in °C) (*DIN EN 15251*, 2012)

Numerous research studies currently involve developing models and methodologies for adaptive comfort prediction or assessment (Djongyang et al., 2010). However, the importance of "people factor" within the building simulation is sometimes undervalued despite having major influence on the overall building performance (Mahdavi, 2011). This influence results from both their actions and behavior, as the space occupancy itself. The user adapts the building systems to fit their comfort needs, which leads to interrelation between the user and the building.

The adaptive model focuses on "*real acceptability of thermal environment*" (Djongyang et al., 2010), what means that it also includes the behavioural, physiological and psychological adaptation aspects (de Dear et al., 1997). Moreover, the possibility to control the interior spaces leads to the user's feeling of satisfaction (Wagner et al., 2007), which could potentially balance the negative effects of too high or low temperature of the building interiors. Djongyang et al., (2010) presented those aspects on a Flowchart cited here as Figure 5.
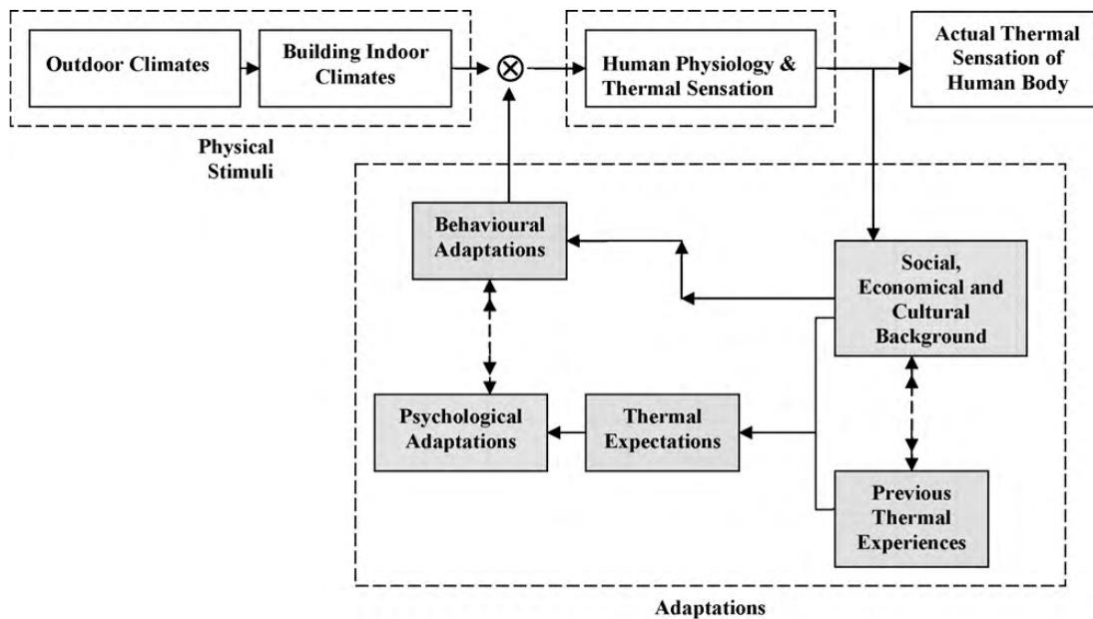
Fig. 2. The thermal comfort adaptive model mechanism.

Figure 5 Adaptive Thermal comfort model summarized by Djongyang et al. (2010)

2.3.5. Heatwave Resilience Related Comfort Models

There is no established methodology nor models described in norms, which can be directly utilized to measure the comfort in case of heatwave exposition. This topic, however, raised a broad interest among researchers.

D. Robinson & Haldi, (2008) proposed a methodology of predicting overheating, which considers the fact, that to some extent the human body can tolerate hot temperatures, providing they will be followed by a cooler period. They compared this ability to discharging and recharging of an electrical capacitor. Flores-Larsen et al., (2023), on the other hand, introduced measures like Indoor Overheating Degree (IOD) and Ambient Warmness Degree (AWD) as well as their ratio, called Overheating Escalation Factor, that can be used to estimate heatwave-exposition-related user comfort.

Independent on the measurement methods, thermal comfort is a crucial building performance metric, which should be considered already in the early stages of design.

2.4. Early Stages of Design

The building design process can be divided into phases, from preliminary sketches up to construction administration and error correction. Figure 6, an adaptation based on the Paulson curve, visualizes the building design process with the original Paulson's idea that early design stages have the biggest impact on the design while representing the lowest costs of changes (Paulson, 1976). The predesign and schematic design are the time when the influence on the project is the highest and at the same time, the costs of introduction of those changes is the lowest. At the same time, the smallest amount of information is available at that time (Negendahl & Nielsen, 2015), this is additionally presented additionally in the Figure.
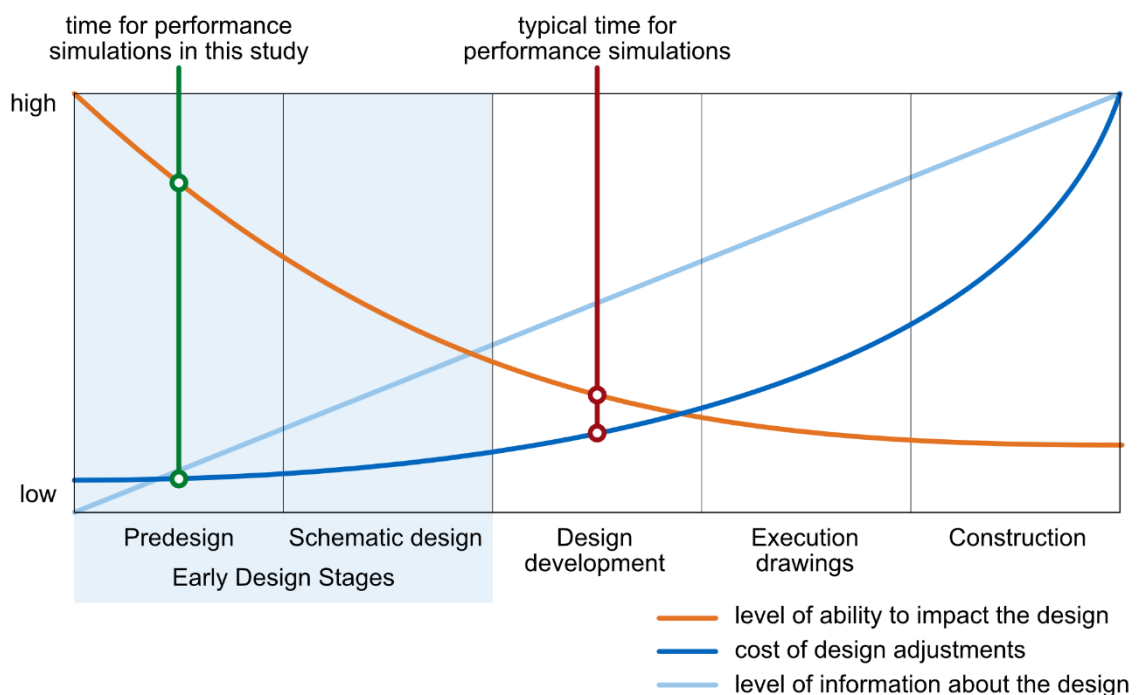
Figure 6 Building design process divided by phases - own adaptation based on the Paulson curve

This scarcity of information is one of the reasons why building performance simulation tools are rarely used at the beginning of the design process (Aksamija, 2018; Augenbroe, 2011; Negendahl & Nielsen, 2015; Rentfro & Gumpertz, 2020). Another reason may be that the vision of upcoming changes and adjustments to the design discourages the use of time-intensive and computationally demanding simulations.

However, the potential benefits of incorporating such simulations are often discussed in literature (Clarke, 2001).

The reduced level of detail should not be the biggest issue of the simulation. According to Augenbroe, (2011), model complexity is less important than well-informed decisions and criteria trade-offs. Rentfro & Gumpertz, (2020) argued that using parametric tools, like Grasshopper plugin for Rhinoceros, may increase the efficiency of the design in the early stages. Thanks to the ease of design manipulation using a parametric workflow, a multitude of versions can be analyzed and compared, even if – or especially if – most of the design decisions have not yet been made.

2.5. Parametric Design

Parametric design, often also referred to as algorithmic design, is a term inseparable from the development of computers and digital tools. The first programs developed for architects, for example Sketchpad in 1963, were purely parametric (Frazer, 2016). There are various definitions of parametric design, but most of them focus on highlighting the algorithmic process of iterative generation of the design.

Buildings can be characterized by a multitude of parameters, defining for example its geometric quantities and material attributes. Other parameters may be related to particular properties of building systems (for example the ventilation rate) or of the planned functional program (number of potential users). The number of possible variants of a building is $n!$, where n is the number of parameter values (Clarke, 2001). Considering the number of building variables, one can assume that it is not possible to evaluate all parameter combinations in a reasonable amount of time, even with the fastest computers.

In the past, a more advanced parametric approach to building design was used mostly for aesthetic purposes (Schwartz et al., 2021), enabling the generation of complex forms, and simulating biological patterns (Phillips, 2010). Now, the parametric approach is experiencing its revival, due to its possibility to address much more complex problems (Frazer, 2016). Parametric design now enables rapid creation of a multitude of design variations, allowing for comparing and optimizing (Hollberg, 2017; Schwartz et al., 2021).

Thanks to those advancements in research and technology, architects and engineers can now use parametric design also as tools that can help address the issue of climate change (Aksamija, 2018; Li, 2017; Sheil, 2020). The current research usually focuses on thermal and daylighting simulation (A.-T. Nguyen et al., 2014; Wetter, 2004) or life cycle assessment (Hollberg, 2017; Vollmer et al., 2023), often also suggesting methods of energy optimization (Hopfe et al., 2012; Negendahl & Nielsen, 2015). What is the most meaningful here, though, is that parametric design enables optimizing the sustainability of the design in the early stages (Ahuja et al., 2015; Hollberg, 2017; Negendahl & Nielsen, 2015).

Tools enabling the use of parametric design by architects and designers usually rely on visual programming. Apart from it being more understandable to non-programmers, visual programming offers a direct link between the algorithm and generated or analyzed geometry, which makes the design more flexible (Negendahl & Nielsen, 2015).

2.5.1. Software Solutions for Parametric Performance-Based Design

In this context, architects and designers commonly employ Rhino 3D, in conjunction with the Grasshopper plugin, as the software of choice (Ahuja et al., 2015). This software package enables the creation of a multitude of variants in an easy-to-follow way with an easy-to-use interface resembling that of the 3D modeling software typically used by designers. The integration of Ladybug Tools, a comprehensive suite of tools for building performance and comfort assessment, enhances the analytical capabilities of the method. The objective of version comparison or optimization can be targeted in two major ways – by either saving all the generated versions (e.g. by utilizing the Colibri plugin in the TT Toolbox) or by finding optimal solutions with the use of genetic algorithms (for example Galapagos or Octopus plug-ins). The modifications of parameters can be made to both geometry, as well as non-geometric properties of the design, for example the thermal properties of windows (Rentfro & Gumpertz, 2020).

Examples of utilizing such tools in research include: reduction of energy demand thanks to energy-flow modeling and the choice of different building envelope surface orientations (Rhino 3D, Grasshopper, Ladybug Tools and a custom energy performance calculation toolkit)(Ahuja et al., 2015) and estimation of future performance of building retrofit (Rhino 3D, Grasshopper, Ladybug Tools and TTToolbox) (Gremmelspacher et al., 2020).

2.6. Building Performance Simulations

Building simulation is an approach allowing for an accurate emulation of reality in a form of system elements and complex equations (Clarke, 2001) by making a virtual experiment (Augenbroe, 2011). It is an interdisciplinary and problem-oriented approach to create and evaluate a realistic model of a complex system (Hensen & Lamberts, 2011). Building simulation is the best way to study future performance, since there are no measurements and collected data available yet (Crawley, 2008). Currently, there is a broad range of simulation tools that could be used for performance assessment (Crawley, 2008; Li, 2017), as well as decision support for the design (D. Robinson et al., 2007). The simulation tools aid in making well-informed choices, as well as help understand the influence of design decisions on buildings and the environment (Clarke, 2001; Flourentzou, 2012). They may also constitute an aid for policymakers in crafting urban programs (Crawley, 2008). Building performance simulation can be used for both naturally and mechanically ventilated buildings (Van Treeck, 2011). For the former, it can provide hourly temperatures inside, while for the latter – together with the input of HVAC setpoints, the simulation can provide the cooling energy demand.

The history of simulations is longer than that of digital tools and can be bound to the appearance of the first physical models (Crawley, 2008). The first building simulation programs were appearing already in the 1970s (Clarke, 2001; D. Robinson et al., 2012), although manual handbook-style calculation algorithms existed even earlier (Clarke, 2001). They did not have graphical interfaces and only enabled very simple calculations. Since then, the number of available solutions has increased and they have become more complex and intuitive for designers (D. Robinson et al., 2012). They started to include 3D models and to simulate physics, including energy flows and fluid dynamics, however, often ignoring crucial aspects, such as the urban heat island effect and more sophisticated radiation exchanges (D. Robinson et al., 2012). The role of building users and their behaviors was also studied (Mahdavi, 2011). Now, simulations are widely used, as it is apparent, that prediction of the future building performance and behavior is more efficient than making changes after its construction (Hensen & Lamberts, 2011).

Building performance simulations are limited in accuracy. The reasons for that include parameter uncertainty (Augenbroe, 2011; Clarke, 2001; Kotireddy, 2018), exclusion of significant parameters (Flores-Larsen et al., 2023) and lack of the "dynamic effects" of

a building, including especially user behavior (Kotireddy, 2018) or the accumulation of thermal energy in the building mass (Negendahl & Nielsen, 2015). Crawley, (2008) wrote: "*Every building design is based on assumptions about how the building will be used, but from its opening day, a building will be used differently than its designers assumed or planned.*" (Kotireddy, 2018), in his research addressed the assessment of the uncertainties in the building performance evaluation, through analysis of various scenarios and their sensitivity.

It is not possible to simulate the building performance entirely accurately over such a long period. However, an assumption can be made, that if for most of the criteria, one variant is much better than another one, this outcome assessment is likely to be resilient to such effects.

2.6.1. Energy Performance Simulation

One of the most common reasons for undergoing a simulation is to predict the future energy performance of the planned building. This approach analyzes the energy flow paths in the system, including mass and heat transfers in the building and can be performed either analytically or numerically (Clarke, 2001) and both with the use of simulations and manually (Spitler, 2011). The main purpose of such simulation is to predict the thermal loads for the building's systems sizing: the amounts of heat energy, which has to be either removed or provided to the building, thus the cooling and heating loads (Spitler, 2011).

2.6.2. Thermal Comfort Simulation

Thermal comfort simulation is a critical method in addressing climate change and overheating resilience. Several studies have already focused on this issue. In the work of Guarda et al., (2019), the influence of thermal insulation materials on indoor comfort in a small single-family house was studied. Escandón et al., (2019) built a model of a typical linear multi-family building stock in Spain to simulate indoor comfort for the year 2050 in A2 scenario. They defined the buildings parametrically, including 29 variables such as building orientation, window-to-wall ratios or physical properties of materials. The chosen evaluation method covered the number of discomfort hours in summer, winter and throughout the entire year, in comparison between the current weather and the weather generated for the year 2050. Their study demonstrates that the biggest

influence on thermal comfort was caused by the parameters associated with the operation, thus with user actions.

Alwi et al., (2022) simulated indoor environment of school classrooms in Malaysia with various retrofitting actions applied aiming at climate resilience. Their findings include the influence of window proportion and orientation, roof materials and overhang dimensions influence directly indoor thermal comfort(Alwi et al., 2022). Marx et al., (2023) analyzed the effect of using greenery on building facades in reducing the operative temperatures as a measure of climate change mitigation.

2.6.3. Weather Data

Traditionally in architectural design, no particular weather data was used to analyze the building's performance. The climate-related analyses were based on the choice of a climate zone. In the early 1900s, a division into four categories was established and they are as follows: polar/cold climates, temperate climates, hot dry climates and hot humid climates (Bougdah & Sharples, 2009).

The development of simulation tools enabled more accurate analyses, operating on very accurate weather data of high resolution, representing a precisely defined location. They are an essential part of every building performance simulation. Usually, one-hour step yearly data are used, which is an interval allowing fast, but still accurate simulation.

One of the commonly used climate data formats in simulation tools is EnergyPlus Weather File EPW (*EnergyPlus Weather File (EPW) Format*, n.d.). It contains weather data for a specific geographic location in a comma-separated text file, which can have a temporal resolution of up to one minute, though typically one-hour precision is chosen. Moreover, it can include additional information, such as typical and extreme periods, monthly average ground temperatures or special days and daylight saving times (*EnergyPlus Weather File (EPW) Format*, n.d.). The file can contain data for one year or another time range and is based on historical measurements (Dickinson & Brannon, 2016; Moazami et al., 2019).

Another weather data format used often is TMY, Typical Meteorological Year, which is a set of months being the most representative for a particular location (Barnaby & Crawley, 2011). Despite it being accurate for average and long-term building performance calculation, the format misses the extremes and therefore cannot serve in

prediction of peak demands (Barnaby & Crawley, 2011). Apart from EPW and TTM files, DDY files may play a major role in the simulation. They contain information about heating and cooling days and may be used to determine the year's extreme and typical weeks.

Weather data have their limitations building and energy simulations frequently involve their incorrect application (Zeng et al., 2023). Researchers argue that smaller intervals would be more appropriate and that there is no one representative year for a site. Additionally, they argue, that simulations should be run for a simulation period of 5-10 years to properly evaluate long-term performance (Barnaby & Crawley, 2011). Moreover, to assess the maximum cooling energy demand, exceptionally hot summer weather data should be analyzed instead of a typical summer weather data (Barnaby & Crawley, 2011).

2.6.4. Future Weather Data

In this study, though, the future building performance is analyzed. Thereby, the weather data should be also updated. According to the description of the thermal comfort criterion of the DGNB Criteria Set "*it is recommended that the climate data predicted for the future be taken into account from the outset so that the desired parameters in terms of thermal comfort of a building can still be achieved in the future. This measure for climate adaptation and increased building resilience is currently only addressed as a bonus, but will gain importance in future*" (*DGNB System. New Construction, Buildings, Criteria Set. Version 2023 International*, 2023).

As the topic of this master's thesis is climate resilience, the weather data input of the simulation will be a major focus. Updating the regular weather data file with the estimated future data would simulate climate change and could help assess the building performance in the future, thereby evaluating its climate resilience (Dickinson & Brannon, 2016).

There are two methods for producing design weather data for future, warmer climates: analogue scenarios and downscaling of global circulation models (Belcher et al., 2005). Analogue scenarios use present-day weather information from a location with a similar climate to the projected climate of the study site, while downscaling involves obtaining future climate data from global circulation models, reducing them to the particular location, and then using various methods to achieve a higher temporal resolution (Belcher et al., 2005). One of the most significant databases of such projections, filled

with data made by a multitude of organizations and climate research centers, is an effect of The Climate Model Intercomparison Project (CMIP), described in chapter 2.1.1 (Climate Change Projections and Future Climate Models).

In order to create a future weather file from such a model, it needs to be downscaled. Four common downscaling methods include morphing, regression, stochastic weather generators and weather pattern methods (Zeng et al., 2023).

The morphing method transforms present-day weather files in such a way as to match projected variables of a climate change scenario with data included in those models (Rodrigues et al., 2023). This method preserves the local climate characteristics and assumes that today's weather patterns will be the same in the future, making it ideal for estimating building energy performance over a long period (Rodrigues et al., 2023), but at the same time being less likely to accurately represent the future (Zeng et al., 2023).

Existing approaches to EPW data morphing include WeatherShift, CCWorldweatherGen Epwshift, and Future Weather Generator.

WeatherShift is a source of future EPW files used by the design and engineering group Arup (*WeatherShift*, n.d.), and is not free of charge. CCWorldweatherGen is a Microsoft Excel-based tool which can modify EPW files based on the HadCM3 A2 CMIP5 dataset files created by the Sustainable Energy Research Group at the University of Southampton and the Department of Mechanical Engineering at the University of Malaya in Kuala Lumpur (*Climate Change World Weather File Generator for World-Wide Weather Data - CCWorldWeatherGen - University of Southampton Blogs*, n.d.; Jentsch et al., 2013). Both tools use the CMIP5 dataset (Dickinson & Brannon, 2016; *WeatherShift*, n.d.). The current CMIP6 climate model data are however significantly more complex and accurate (Eyring et al., 2021). Tools using CMIP6 databases are, among others Epwshiftr and Future Weather Generator. The Epwshiftr is a package written in the R programming language (Jia & Chong, n.d.). Future Weather Generator is an open-source tool written in the Java language and first published in April 2023 (Rodrigues et al., 2023).

No examples of available EPW file creation tool for the regression method were found during the research. This method involves searching for relationships between large-scale climate data and regional-scale data (Zeng et al., 2023). This method might be a promising method of generating future weather data and should be developed further.

Stochastic weather generators use statistical resampling and distribution methods to efficiently simulate future weather conditions resembling the source data (Zeng et al., 2023). One example of such tools is Meteonorm, also capable of creating weather files for areas, for which there is no data available (Bougdah & Sharples, 2009). However, it bases its future projections on CMIP5 dataset (Meteonorm 8, 2023a). Meteonorm is a commercial software solution, which uses advanced interpolation algorithms, which merge ground and satellite data (Meteonorm 8, 2023b). Similar to most morphing tools, it uses the CMIP5 IPCC 2014 model for future weather morphing (Meteonorm 8, 2023a).

The weather pattern method relates a large collection of historical weather data to defined patterns, which makes it less usable for simulation of new weather conditions (Zeng et al., 2023).

2.6.5. Simulation with the Use of Estimated Future Weather Data

Approaches to using estimated future weather data for building performance simulations have currently become a focal point of scientific exploration in the field. The aforementioned studies of Guarda et al., (2019) and Escandón et al., (2019) both used EnergyPlus weather files morphed using CCWorldWeatherGen tool.

Various other studies also employed morphed weather files, including: an assessment of the climate change influence on various functions of buildings for all 7 climate zones of the US (Wang & Chen, 2014), a comparison of the risk of overheating and the energy consumption of buildings in Sweden dependent on the type of construction and chosen materials (Dodoo & Gustavsson, 2016) and an assessment of the impact of higher temperatures and evaluation of adaptation and mitigation strategies including window size and choice of materials (Hollý & Palková, 2019). Gremmelspacher et al., (2020) used TMY (typical metrological year) data in combination with extreme weather files (ECY – Extreme Cold Year and EWY – Extreme Warm Year). Parametric approaches including morphed weather files can be found in the study of Escandón et al., (2019), who made a sensitivity analysis of parameters influencing the future performance of buildings in Southern Spain.

Those studies, regardless of their methodology, consistently demonstrate that exchanging of the weather file significantly impacts the energy performance of buildings. This happens, among other reasons, because of changes in the number of days, during which heating or cooling energy is needed (Rodrigues et al., 2023)(Dodoo &

Gustavsson, 2016). As the research is still in progress, the simulation outcomes based on particular methods are different. The limitations include inaccuracies in data-resolution increasing methods or lack of attention to more complicated physical processes, including the diurnal cycle and climate variability, representing extreme events (Gesangyangji et al., 2022). The approaches to heatwave simulations are currently of interest to research (Flores-Larsen et al., 2023).

2.7. Section Summary

Architectural design is always future-oriented. It is based on certain assumptions including building usage and its exposure to external conditions – both including collected information and guidelines as well as predicted future changes (Kotireddy, 2018).

Climate change and the desire for new sustainable solutions will, however, cause the need for more flexibility in design decisions and thinking about the solutions to future problems. Those will include, among others, elevated temperatures and increased frequency and intensity of extreme events, such as heatwaves. Milder winters may decrease the european buildings' energy intensity, but hotter summers will increase the cooling energy demands and will make provision of internal comfort conditions even more challenging.

Modern simulation tools can target those issues and bring new opportunities to the design process, allowing design evaluation to take place already in the early stages. This way, particular design ideas can be compared and building designs improved. The utilization of a parametric approach can improve this process by variant generation and optimization techniques.

Even though there are successful methodologies for optimization of energy use, indoor and outdoor comfort, as well as methodologies including parametric approach or the use of future-updated weather data in the simulation, an approach for testing parameters for heatwave resilience has not been developed yet. This master thesis aims at filling this gap and proposes a methodology for evaluating the building design's response to the future event of a strong temperature increase.
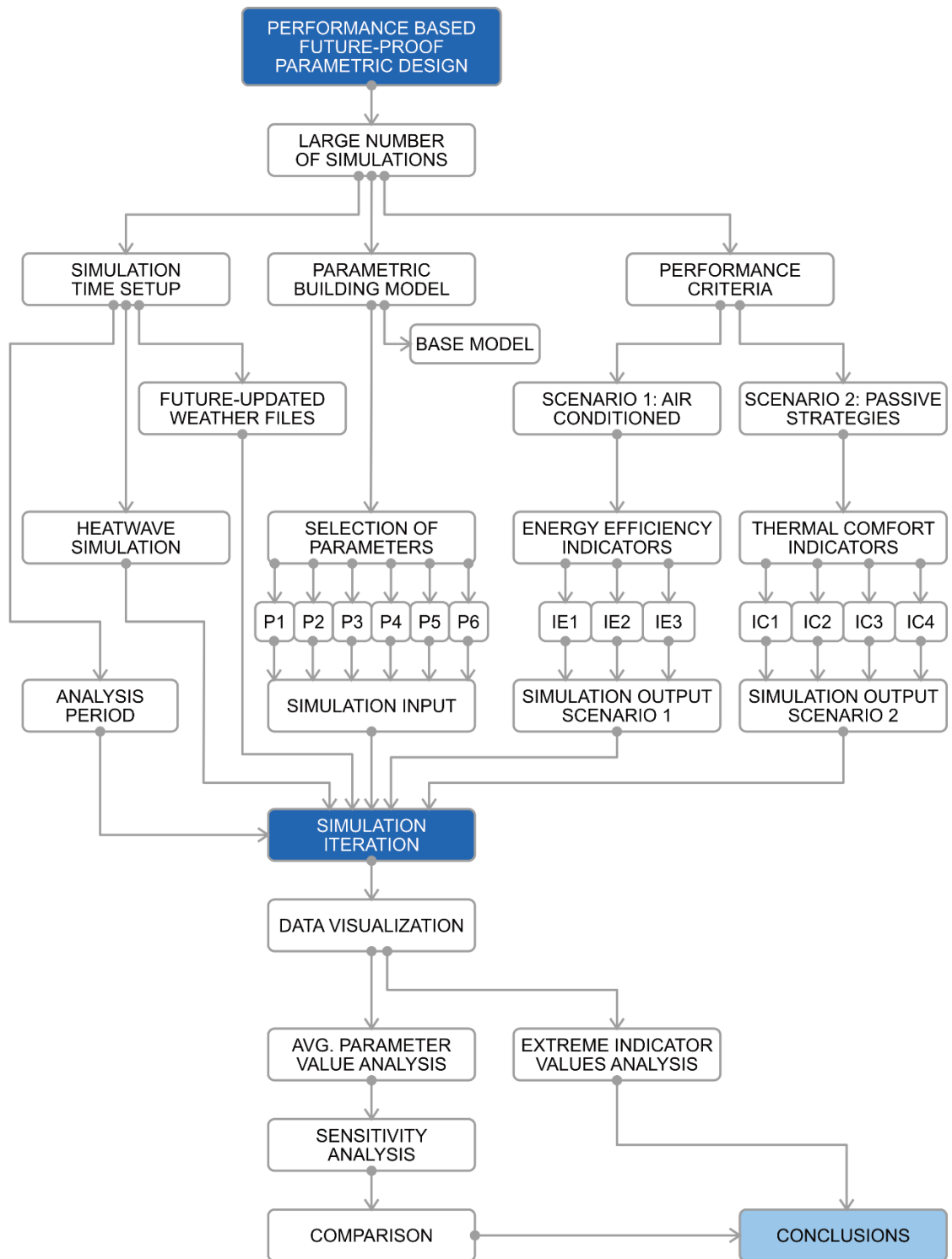
Figure 7 Flowchart of the Methodology

3. Methodology

The methodology of this master's thesis corresponds to that of the parametric approach and can be divided into three parts:

- input parameter definition,
- simulation settings and
- output information interpretation and evaluation.

The input data are parameters defining the geometry and selected characteristics, as well as weather files providing information about the external conditions. The simulation setup is mostly based on the possibilities of the selected simulation software and includes the information about the analysis period, which is the time range for which the simulation should run, the selection of building elements which should be analyzed, and other factors influencing the results. The simulation output includes numerical data, which can be saved, visualized, and compared. Considering a large number of possible outputs, a careful selection of performance indicators is crucial. The overview of the methodology is presented on Figure 7.

The parametric approach will enable the creation of building model variations, which have to be simulated separately, one after another. In order to avoid storing a large amount of data, only the selected information about each simulation result can be saved, such as particular values or graphical representations. This choice must be made before running all the simulations, as later retrieval of further data would require re-running the simulations. The number of simulation iterations will be directly dependent on the number of selected parameters and their analyzed values.

There are two main scenarios analyzed in this study:

1) The first scenario includes a building which is mechanically conditioned and whose energy demand, especially for cooling, is the main indicator defining heatwave resilience and climate adaptation.
2) The second scenario, contrarily, assumes that the building is naturally conditioned and the lack or cooling systems may worsen the interior conditions during extended heat periods – in this case the thermal comfort inside will be the main metric of the resilience and climate adaptation of the building.

Those two scenarios are analyzed separately, albeit with the same methodology and tools. This process is depicted in Figure 8. Along the aforementioned three parts of the process, the creation of buildings variants to compare was here introduced as additional workflow step. Therefore, the process is as follows:

1) Input data includes the guidelines and materials from the Eco+ project, described in Chapter 3.2.1 (P1 Construction Set) as well as future-updated weather files, detailed in Chapter 3.3 (Weather Data for the Simulation).
2) The simulation introduces creation and performance assessment of parametric building models (see Chapter 3.1.1 - Parametric Approach).
3) The simulation is iterated to evaluate a number of building variants.(Chapter 3.8).
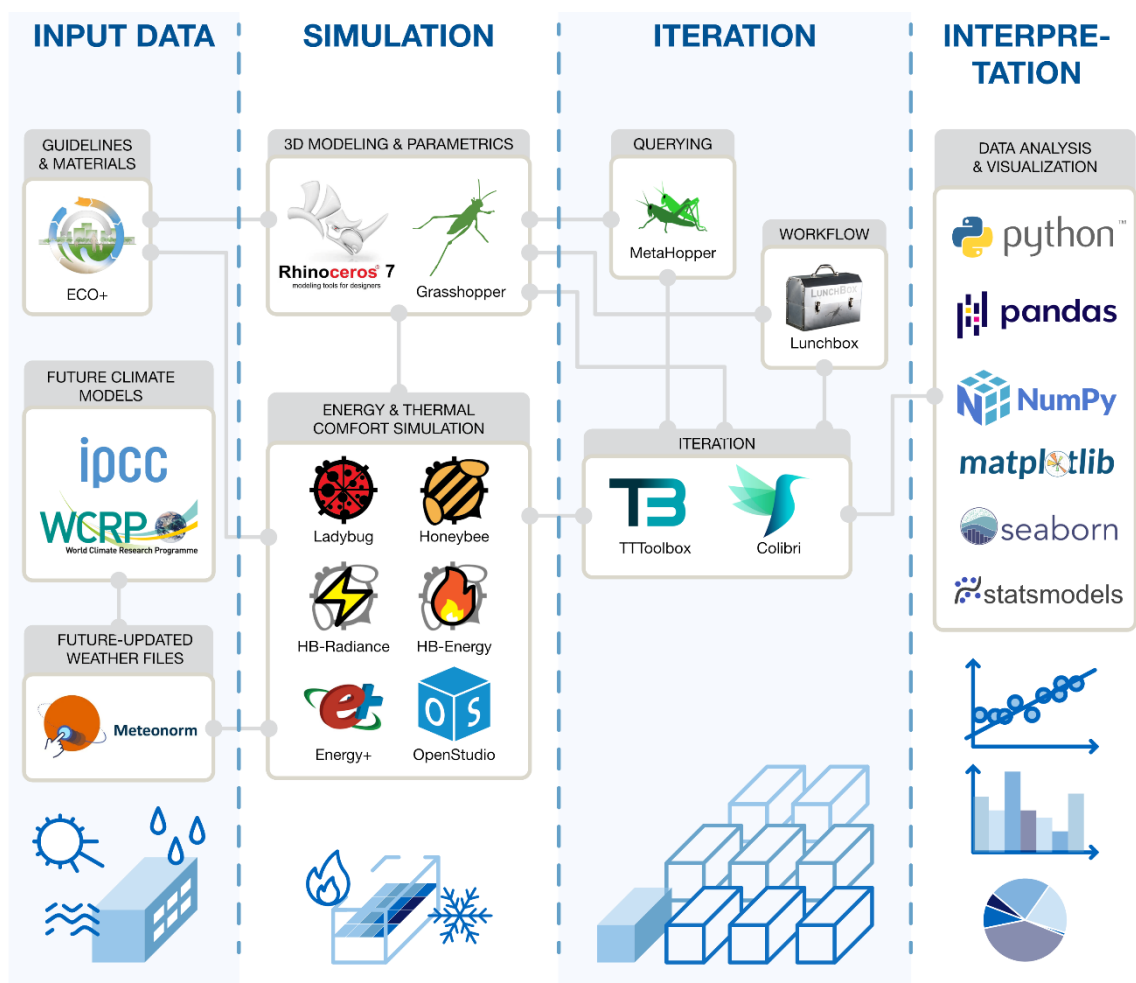4) Finally, the outcome data is interpreted, visualized and analyzed (Chapters 3.9-3.10).

Figure 8 Overview of the tools used in the workflow

3.1. Simulation

According to Augenbroe, (2011), the simulation process starts already before running the computation with selected software. The steps needed to be made before that are selection of performance criteria, methods of their measurement and the way to overcome possible conflicts and trade-offs between various targets (Augenbroe, 2011).

Building performance can be measured with the use of Performance Indicators, which measure and quantify Performance Requirements of the design in the Verification Method under given design conditions (Augenbroe, 2011). Moreover, Augenbroe, (2011) writes: "*one Performance Requirement can be measured by many Performance Indicators, whereas every Performance Indicator is related to exactly one Verification Method for its quantification*". For the two main scenarios presented in this thesis, the performance requirements are: energy efficiency during the hottest weeks of a year and indoor comfort. The indicators used to measure them are specified in further chapters.

All the tools used in the process are depicted in Figure 8.

3.1.1. Parametric Approach

For the purpose of this master's thesis, a parametric approach has been selected, utilizing Rhino and Grasshopper software. Performance simulations were conducted using the Ladybug Tools, including Ladybug, Honeybee, and Honeybee-Energy plug-ins for Grasshopper. Honeybee-Energy uses the EnergyPlus simulation engine through the OpenStudio environment to evaluate the energy performance of a building (*Honeybee Energy's Documentation*, n.d.) EnergyPlus is an open-source solution usually used by architects and engineers via user-friendly graphical interfaces, such as Ladybug Tools (*EnergyPlus*, n.d.). Additionally, the Colibri plug-in was utilized to automate the generation of simulation outputs. Other Grasshopper plug-ins used within this study, especially for workflow querying and automation, were Lunchbox and Metahopper.

With the use of multiple design variants and future weather files (for various scenarios and years), it is crucial to design the simulation in such a way that the outputs are accurate and comparable. As every iteration may be time-consuming (Ahuja et al., 2015), a reduction of parameters will also be necessary to enable proper focus on the

topic of resilience. There are many parameters influencing the simulation output, such as the air exchange with the use of natural ventilation (Candido, 2021) or mutual overshadowing of buildings (Okeil, 2010) as well as the building form-related and structural parameters, including windows-to-wall-ratio, ceiling height and the presence of systems like photovoltaic panels (Ahuja et al., 2015). A sensibility analysis may help determine which parameters influence in the simulation output to the biggest extent.

3.1.2. Performance Criteria

Based on the method described by Augenbroe, (2011), the Aspect System has been defined. The Aspect System is a selection of design elements which play a role in the simulation and are relevant for the desired function (Augenbroe, 2011). In this system, a virtual experiment takes place.

Table 2 Preliminary selection of building performance criteria

Performance Criteria	PI #	PI Name/Description	Quantitative Method
Area Efficiency	1	Location of buildings	Geometric measurements
Energy Performance	2	Cooling energy demand	Honeybee calculation
	3	Total energy demand	Honeybee calculation
Indoor Comfort	4	Median/minimum thermal comfort	PMV, PPD etc. Adaptive models
Environmental Impact	5	Lifecycle assessment	LCA Tools, Ökobaudat
Overheating Risk	6	Probability of overheating	DIN categories 15251 Number of hot hours

Table 2 presents the preliminary choice of performance criteria, which may be used to compare design options. The criteria marked with blue were selected for the scope of this master's thesis.

3.1.3. Building Model

In order to make running a large number of simulations feasible and the results comparable, a simplified "shoebox" model was used. It is depicted in Figure 9 was created. It is a simplified representation of a 3-floor high residential building, 12 meters wide and 36 meters long. In order to make the results of particular iterations comparable,

throughout the entire simulation, the building size and proportions remained the same, and the windows were placed on all 4 elevations uniformly.
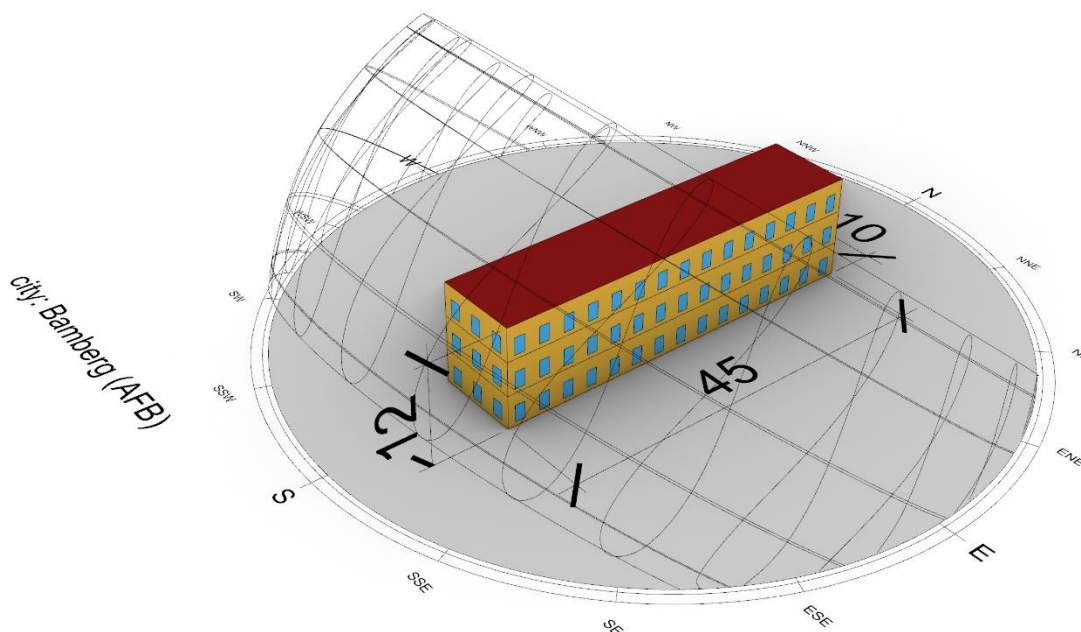

Figure 9 Basic model for an early simulation set-up

3.2. Input Parameters

Parametric design enables a seamless workflow of sensitivity analysis. Sensitivity analysis is a process of analysis and comparison of various parameters, their importance and interdependencies, recognition of irrelevant data and search for sources of uncertainty in a simulation (Razavi & Gupta, 2015). To make the sensitivity analysis, enough simulation runs has to be made (Razavi & Gupta, 2015).

As it was described in Chapter 2.5 (Parametric Design), a building, even at an early stage of the design may be described by a broad number of parameters, all of which may have numerous values. Considering the desire to run a simulation for every possible combination of parameters, the final number of iterations explodes combinatorically with every new parameter value. Depending on the number of parameters and their selected values with which to test the model, the total number of iterations can be described as:

$$N = \prod_{i=1}^{n_P} v_i$$

Where:

- N is the total number of simulation iterations,
- n_P is the total number of selected parameters,
- v_i is the number of selected values of the ith parameter P1 Construction Sets.

The parameters and their tested values used in the study of this master thesis have been collected in Table 3:

Table 3 Set of the selected and tested simulation parameters

#	Parameter name	No.	Values
P1	Construction Set	4	[0] V01_Sandlime, [1] V02_Brick, [2] V03_WoodMassive, [3] V04_WoodLight
P2	Building Rotation	5	[0] 0°, [1] 30°, [2] 60°, [3] 120°, [4] 150°
P3	Window Shading Style	4	[0] nothing, [1] louvers, [2] overhang [3] external rolls
P4	Window U-Factor	2	[0] 0.6, [1] 1.2
P5	Window SHGC	3	[0] 0.4, [1] 0.6, [2] 0.8
P6	Window-To-Wall-Ratio	3	[0] 0.2, [1] 0.3, [2] 0.4
	In total N=	1440	Model variants to be simulated

3.2.1. P1 Construction Set

In the Honeybee-Energy simulation, the information about selected building materials is provided in the form of a construction set. It is then divided into exterior, ground, interior and subface subsets (*HB-Energy Primer*, n.d.). The preset construction sets are grouped into 4 construction types: "SteelFramed", "WoodFramed", "Mass" and "Metal Building", the choice of which, together with the information about the "Building Vintage" (defining built period) and the Climate Zone, can help automatically assign a

corresponding set of materials. In total, 257 predefined construction sets are available to use as of Ladybug Tools version 1.6.77.
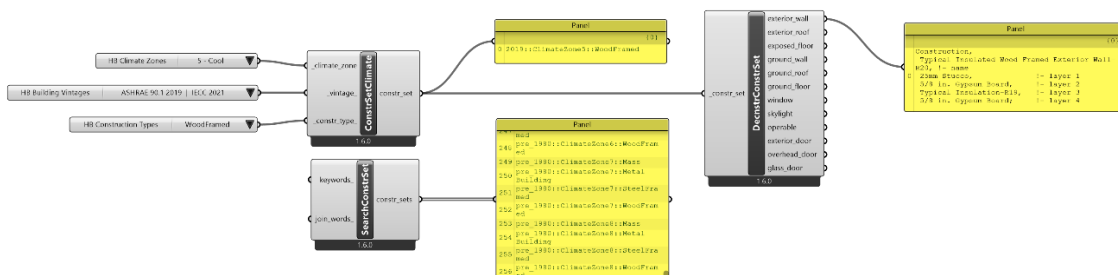

Figure 10 Simple way of creating climate-based construction sets with Honeybee

As this thesis is a part of the Eco+ project, the default Honeybee-Energy construction sets were replaced with custom ones. Accordingly, 4 construction sets were proposed:

- V01 KS (*Kalksandstein*) – a construction set with the use of sand-lime brick and expanded polystyrene for external walls, drywall interior walls and reinforced concrete floor slabs,

- V02 Brick – a construction set similar to V02 KS, with external walls made of insulation-filled bricks,

- V03 Wood massive – a construction set with external walls made of solid structural timber and wood fiber insulation, internal walls with clay panels and floor slabs from glued laminated timber,

- V04 Wood light – a construction set with wood-frame construction of solid wood or glued laminated timber filled with wood fiber insulation.

For an accurate recreation of those materials in Honeybee Energy simulation, each material had to be prepared manually, by providing information about its heat conductivity [W/m*K], density [kg/m^3], specific heat capacity [J/kg*K], as well as the layer thickness. The Eco+ material lists provided layer thickness information, as well as links to the materials in the service Ökobaudat (*ÖKOBAUDAT*, n.d.)(see Annex 3 - Original material list of the ECO+ Project), from which material density could be acquired. Information about specific heat capacity of some materials was found in the norm *DIN 4108-4*, (n.d.) The missing information about conductivity and specific heat capacity were found online and taken from the available, commercial product declarations, information sheets and generic webpages. They were additionally compared with similar

materials already available in the Honeybee database. All of those was summarized in Annex 4.

The creation of the construction sets, in order to avoid unnecessary repetitions in the parametric code, had to be structured in such a way, that each change would not require multiple actions. For this reason, firstly the materials were prepared, then particular building elements compounds were defined, and finally the construction sets were established. This piece of the Grasshopper definition was then grouped in a single *"cluster"* component with the construction sets definitions as its outputs.
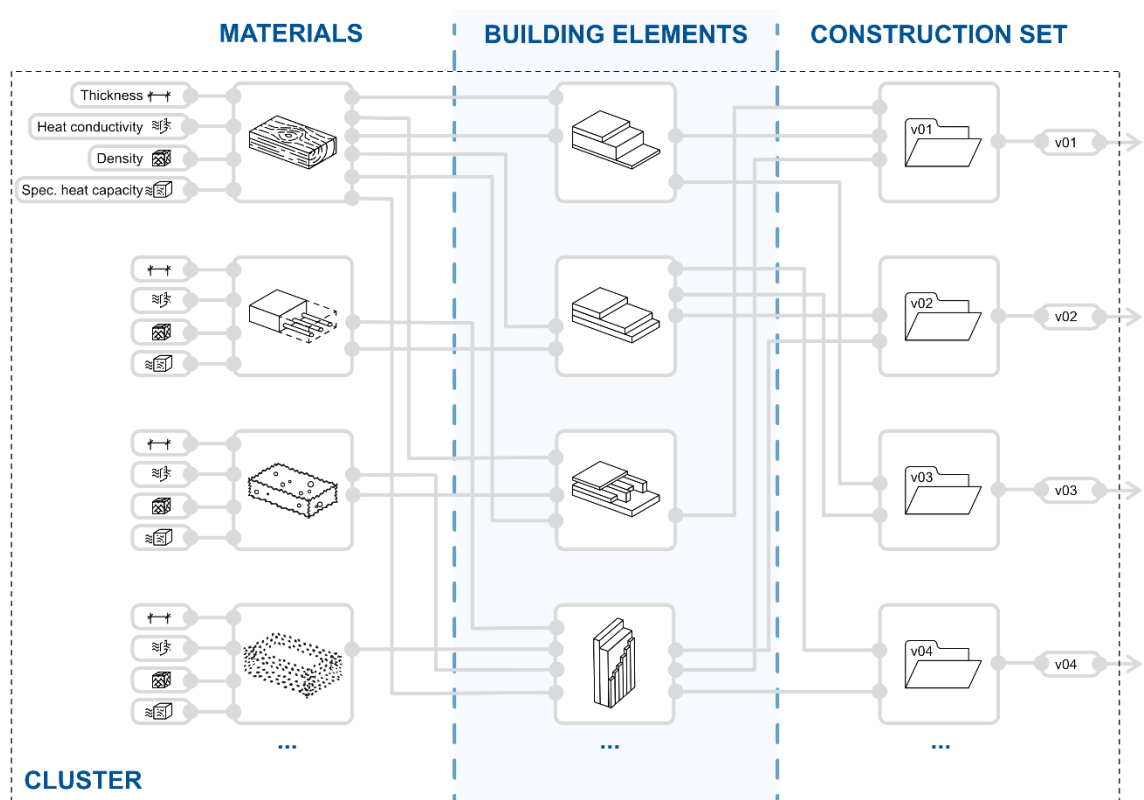
Figure 11 Structure of the cluster containing construction sets - schematic graph

3.2.2. P2 Building Rotation

Building rotation is a parameter defining the orientation of a building. It is typically dependent on the building plot and usually cannot be influenced. The values selected to be simulated were: 0°, 30°, 60°, 120° and 150° to the north direction. This way, a representative range of various building configurations can be evaluated.

The significance of this design characteristic relies on its high influence on the interior access to the solar radiation, without affecting the building size or proportions.

3.2.3. P3 Window Shading Style

This parameter considers the window shading possibilities offered by components HB Window Construction Shade with *HB Apply Window Construction* and *HB Louver Shades*.
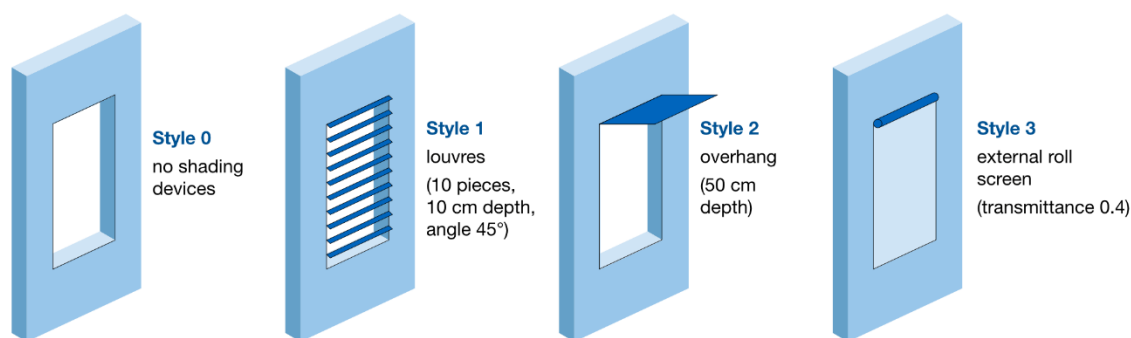

Style 0
no shading devices

Style 1
louvres
(10 pieces, 10 cm depth, angle 45°)

Style 2
overhang
(50 cm depth)

Style 3
external roll screen
(transmittance 0.4)

Figure 12 Window shading configurations - from left: [0] to [3],

As depicted in Figure 12, the selected parameter values are:

- [0] no window shading,
- [1] louver shading – where tested were 10 horizontal opaque louvers, 10 cm deep, with the angle of 45 degrees, without schedule applied,
- [2] overhang shade – a single horizontal opaque shade whose depth is 0,5 meters,
- [3] external roller shade – a full-window-covering material, using semi-transparent (transmittance of 0.4) with *ShadeMaterial* component's default values, apart from the thickness set to 0.05 m.

The aforementioned components allow for many more possible configurations, but due to the combinatorial growth of the number of simulation iterations with each parameter and its possible value, the choice had to be limited.

Moreover, during the simulations, it was observed, that the building shading style was the most critical parameter influencing the simulation time. The parameter set with the

parameter P4 value set to 1 (so the louver shade), took significantly more time to compute due to a multitude of additional surfaces and the resulting reflections.

3.2.4. P4 Window U-Factor

The U-Value, expressed in W/m²K, is a unit of measurement for thermal transmittance of a material and defines the heat flow that passes through it. In the case of windows, the U-Value is composed of thermal transmittance of the glass and the frame. For triple-layered glass the U-Value can reach up to 0.3 W/m²K (Hegger & Institut für internationale Architektur-Dokumentation, 2008). This parameter, as it defines the heat losses, has the highest relevance for the thermal insulation in winter, though evaluating its influence in the case of a heatwave has brought additional insights to this study. Considering the lower importance of this parameter, only the extreme values of 0.6 and 1.2 W/m²K were simulated.

In the used software, the U-Value is called U-Factor, and is calculated as an rea-weighted average of all the window components (Rentfro & Gumpertz, 2020). For nomenclature consistency, in this thesis, the U-Factor term is used.

3.2.5. P5 Window SHGC

Solar Heat Gain Coefficient is another parameter, which describes thermal quality of a material. Following American norms, it is a ratio of solar radiation transmitted through the element relative to the total radiation hitting the element (Rentfro & Gumpertz, 2020). The European equivalent is the g-value (German: *g-Wert*), which describes the same property of a material. The g-value considers both the energy transmitted directly through the material, as well as the energy absorbed and radiated to the interior (Hegger & Institut für internationale Architektur-Dokumentation, 2008). It is the key parameter defining the performance of a window in the summer, influencing both the cooling energy demand, as well as the thermal comfort of the building users.

SHGC values of 0.4, 0.6 and 0.8 were tested in the simulation. These three values correspond to best-performing, standard and non-coated types of glass respectively.

3.2.6. P6 Window-To-Wall-Ratio

Apart from the material properties of the windows, the influence of window geometry should also be tested. Even though analyzing various proportions and placement of

windows are crucial in the design, especially in terms of daylighting, the most significant and easily comparable input will come from the window-to-wall ratio, as it defines the total proportion of glazing to the façade. The selected ratios tested in this study were: 0.2, 0.3 and 0.4, as those are typical for residential architecture.

3.3. Weather Data for the Simulation

In Chapter 2.6.3 (Weather Data) of the Literature Review, the critical role of weather files in building performance simulation was emphasized. This chapter specifically focuses on the selection of the optimal EPW file source and the most suitable weather file morphing tool, as discussed in the Chapter 2.6.4 (Future Weather Data).

A convenient method for obtaining a weather file for simulation with Ladybug Tools involves the use of the "EPWMap" component. This component directs users to a map-based selection interface at https://www.ladybug.tools/epwmap/. This website provides links to multiple data sources, including EnergyPlus and Climate.OneBuilding.Org servers. For the location nearest to the study area, Bamberg, the data can be obtained from the latter. These files, according to Climate.OneBuilding.Org, adhere to the TMY/ISO 15927-4:2005 methodologies (Climate.OneBuilding.Org, n.d.). The nearest dataset to the site from the official EnergyPlus database is Frankfurt am Main, approximately 160 km away, which dataset originated in 2001 from the American Society of Heating, Refrigerating and Air-Conditioning Engineers (ASHRAE), Inc. Another potential source of weather files is the Meteonorm application, which combines weather station and satellite data utilizing advanced computational methods to generate the required weather files.
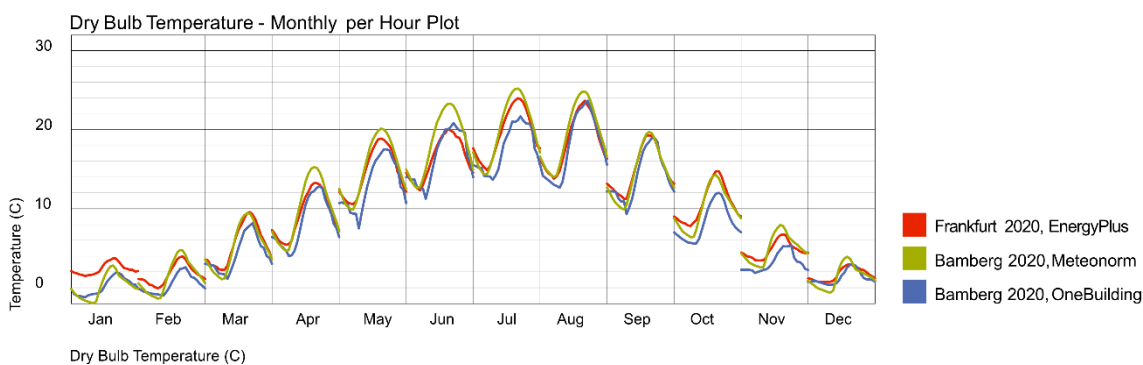

Figure 13 Comparison of Dry Bulb Temperature for three contemporary weather data sources

Figure 13 illustrates a comparison of the aforementioned contemporary EPW files for Bamberg and Frankfurt am Main in terms of Dry Bulb Temperature, as a representative parameter for the entire weather data. The plot presents temperature information in the "Monthly per hour" manner, depicting temperature variations throughout an average day for each month. This format is more informative than average daily temperatures for each month, as it provides data crucial for understanding diurnal cooling effects.

This plot, as well as other parameter plots, reveal a high degree of consistency across different data sources. This consistency indicates that regardless of the chosen data source, simulations using contemporary weather data are likely to yield similar results. However, the focus of this study is on future weather files, where the level of consistency might vary. This variation is attributed to the use of different interpolation methods, future scenarios, and degrees of uncertainty inherent in these updated files.

3.3.1. Comparison of Future-Updated Weather Files

Figures Figure 14 to Figure 17 demonstrate how different morphing methods impact the data in weather files, comparing contemporary sources with their future-updated versions for the 2080 "fossil-fuels" scenario. These comparisons involve data from Meteonorm and the Future Weather Generator. Selecting the appropriate morphing tool was challenging due to the distinct advantages and drawbacks of each.

Future Weather Generator (v1.0.1) utilizes the CMIP6 database, offering a choice among 9 CMIP6 models or a combination thereof. In this study, the EPW data from OneBuilding (*DEU_BY_Bamberg.106750_TMYx.zip*) was used to receive future climate based on SSP585 scenario for the year 2080. Meteonorm, on the other hand, employs the CMIP5 data, which may be less accurate, though it extends up to the year 2100. Despite reviewing other tools discussed in Chapter 2.6.4 (Future Weather Data) they were excluded early in the process for various reasons. The decision was informed by thorough analysis and comparison of the files.

For consistency, Meteonorm's files were chosen for further processing. They more accurately reflect the actual climate data for Bamberg, particularly in aspects like global radiation patterns and wind rose plots, compared to sources like Meteoblue – see Annex 2 (*Simulated Historical Climate & Weather Data for Bamberg - Meteoblue*, n.d.). This choice, however, should be revisited in future studies, acknowledging that no tool perfectly captures the evolving climate models and studies.
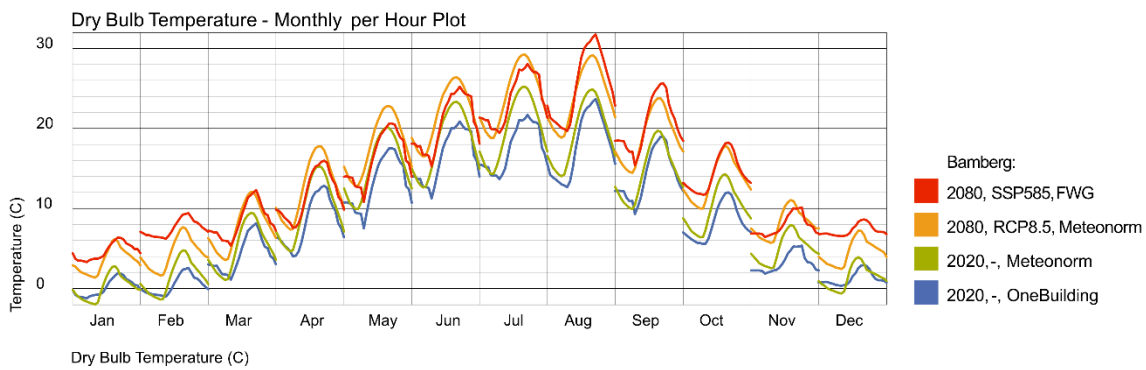
Figure 14 Comparison of contemporary and future-updated weather files – Dry Bulb Temperature
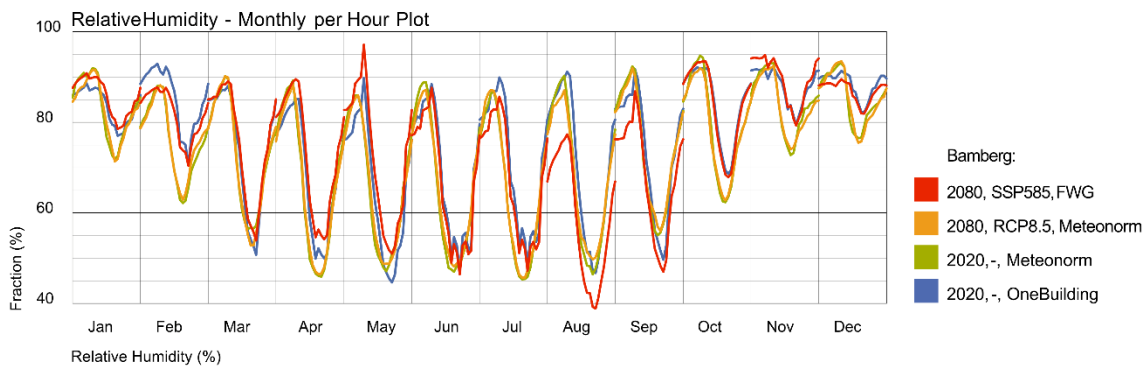

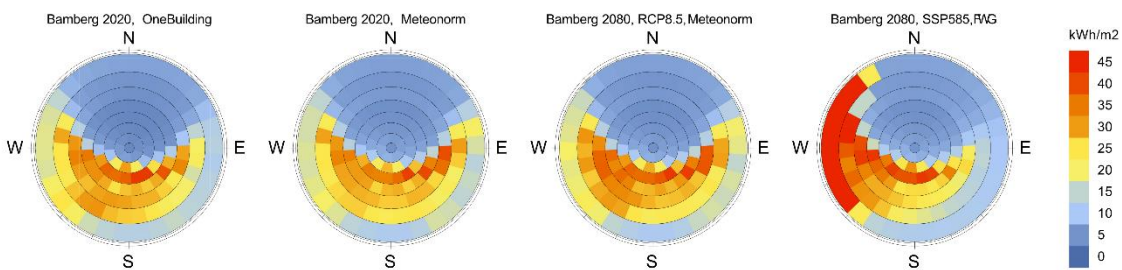**Figure 15 Comparison of contemporary and future-updated weather files - relative humidity**

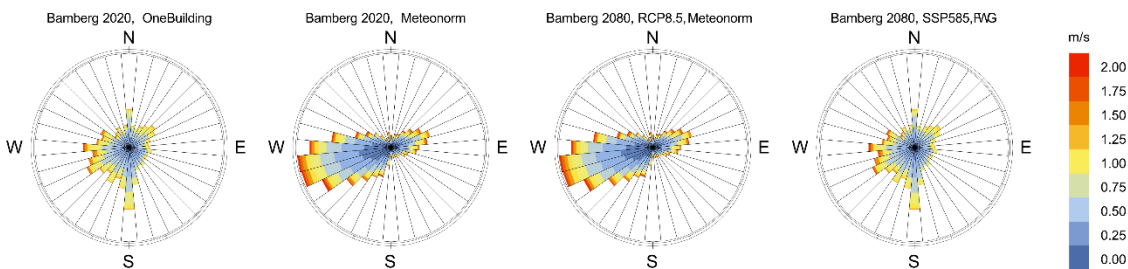**Figure 16 Comparison of contemporary and future-updated weather files - total global radiation**

Figure 17 Comparison of contemporary and future-updated weather files – wind

3.3.2. Comparison of Future Scenarios

Finally, the differences between various future scenarios could be studied. Figure 18 explores the variations in dry bulb temperature under different future scenarios, as described in Chapter 2.1.1 (Climate Change Projections and Future Climate Models).

It can be noticed that there are large discrepancies between various future scenarios for the same year (2100). The RCP8.5 scenario assumes that, for instance, average daily temperatures will be exceeding 30 °C in summer days. On the other hand, the most positive scenario RCP2.6 shows only slight temperature elevations compared with the base year (2020).
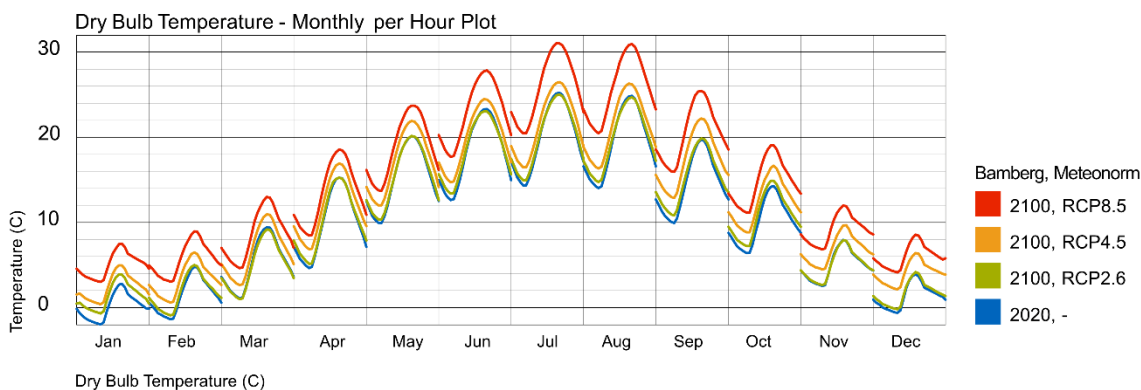

Figure 18 Comparison of the contemporary and future-updated weather files from Meteonorm for three various future scenarios - Dry Bulb Temperature

In order to focus on the "worst case scenario" the scenario RCP8.5 for the year 2100 was selected. It may correspond to an extremely hot summer, or the threat of a heatwave. In this scenario, July and August are particularly challenging for building performance, with midday temperatures potentially reaching 32 degrees Celsius. While nighttime cooling might mitigate these peaks, only performance simulations can confirm its effectiveness.

Other weather file properties, such as wind velocity, solar radiation, and precipitation, showed less variation than dry bulb temperature in future scenarios compared to contemporary data.

3.4. Analysis Period

Within Honeybee-Energy, two components significantly impact every iteration's computing time: *Model To OSM* and *Read Room Energy Result*. *Model To OSM* is responsible for converting the Ladybug model into an OpenStudio file, while *Read Room Energy Result* reads and categorizes simulation results. The computation time is heavily influenced by the selection of simulation parameters provided by the Simulation Parameter component. This component allows for the specification of various time-related details, such as the inclusion of daylight-saving time, holidays, and the option to restrict the simulation to a specific period defined in the Analysis Period component. Reducing the analysis time can greatly decrease the simulation time. However, omitting periods not directly analyzed could lead to inaccurate simulation results, due to missing data such as the energy stored in the thermal mass of building elements.

The hypothesis tested in this chapter is: running the simulation for the simulation period of two months and evaluating only the second one, would provide the results sufficiently similar to those obtained from a full-year simulation, potentially replacing the need for the more resource-intensive annual simulation.

To assess the validity of a time-limited simulation, five different set-ups were tested, each using the simple building model, described in the chapter 3.1.3, but varying in the EPW file selection and building construction set. Three simulation types were run for each set-up: a full-year simulation later cropped to July, a month-long simulation for July, and a two-month simulation for June and July, later cropped to July. The outcomes were evaluated based on two metrics: thermal load balance (from the *Load Balance* component's balance output) and cooling energy demand (from the *Read Room Energy Result* component's cooling output).

Figure 19 illustrates a comparison of the July-cropped yearly simulation with the outputs from the July-only simulation, showing notable differences, in some cases exceeding 8%. This suggests that simulations limited only to the period under analysis can yield inaccurate results. However, simulations spanning two months and cropped to the second month have output results very close to the full-year simulation, with deviations ranging between approximately -0.06% to 0.06%. Limiting the Analysis Period to two months could thus significantly accelerate the simulation process.
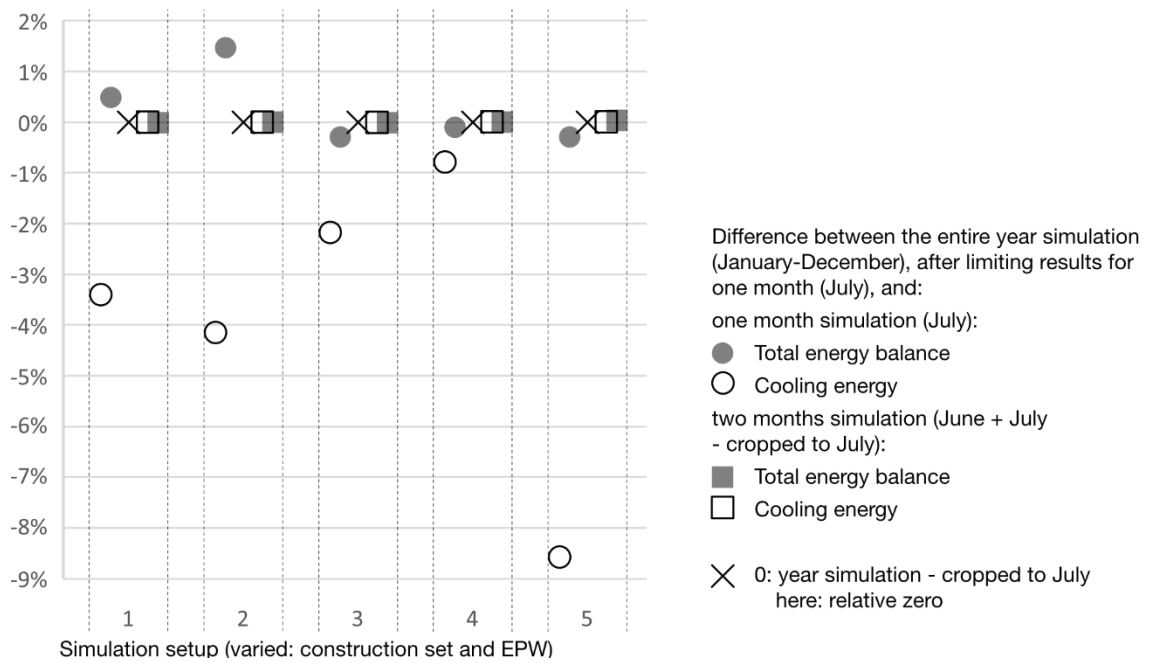
Figure 19 Comparison of cropped analysis-period to only-simulated analysis period for the month of July and 5 simulation setups

In further development of this study, the simulation period was extended to three months (June to August), with subsequent data limitation extended to the July-August period. Given the frequent repetition of this operation, a set of components was assembled into a cluster named "Cut June out", depicted in Figure 20, which was then duplicated and applied to various data sets.
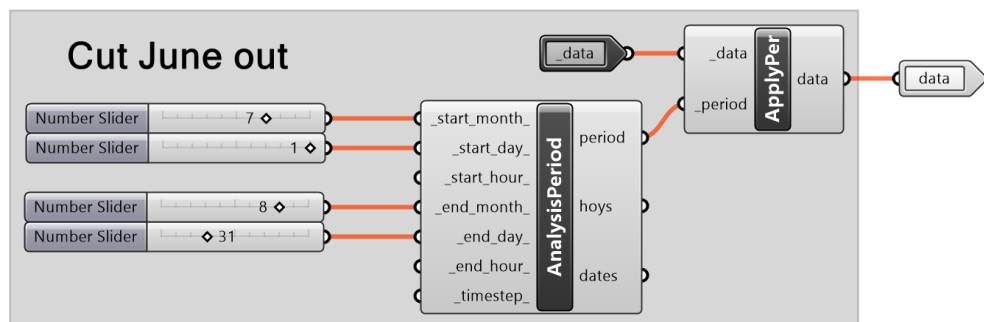

Figure 20 A cluster removing the first month (June) from the results

3.5. Simulating a Heatwave

In the initial phase of this study, it was planned for the simulation to utilize the "Hottest week" output from Ladybug's "Import STAT" component. This output was described as *"A Ladybug AnalysisPeriod object representing the hottest week within the corresponding EPW."* (*Ladybug Primer*, n.d.). However, this approach may not effectively represent a heatwave, as it focuses on a very short period. Longer duration should be considered to account for the heat accumulation in building materials' thermal mass (Flores-Larsen et al., 2023) and the effects of user's longer exposure to the heat (D. Robinson & Haldi, 2008).

Subsequently, it was decided to use the various future-updated EPW, interpreting them as various future summers, ranging from milder to extremely hot ones. This change was made to better prepare for extreme conditions by using the generated weather data for the year 2100 and scenario 8.5. As presented in Figure 21, a very hot summer might be expected, with very few milder days. Although cooler nights may provide some relief, the frequent occurrence of consecutive daily temperatures exceeding 40°C creates a challenge for building design. This scenario effectively simulates the impact of a severe heatwave.
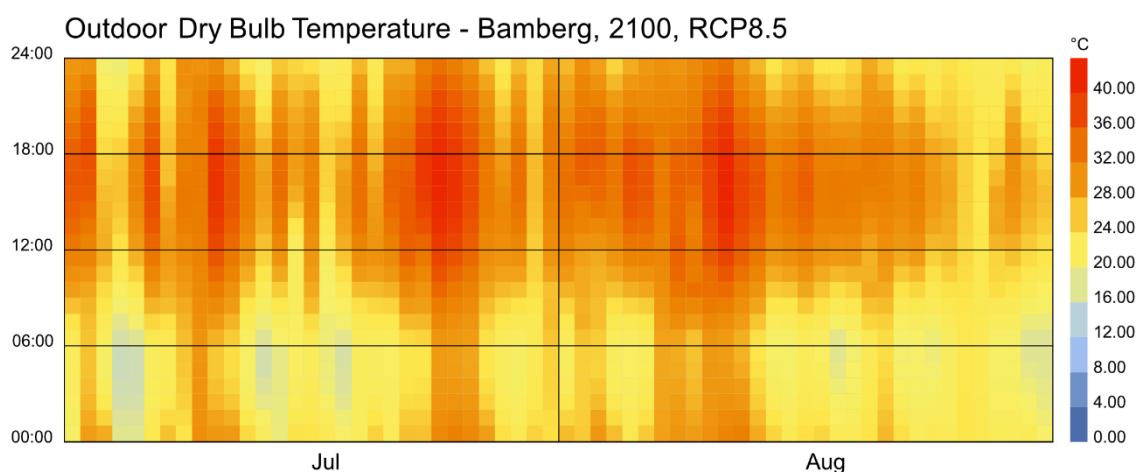

Figure 21 Hourly temperatures for the scenario RCP8.5 of the year 2100 in Bamberg

3.6. Output Indicators: Energy Performance

Energy performance is a critical metric for assessing building sustainability and can vary significantly when projected onto different future scenarios. Initial approaches to the topic, though, revealed that the annual energy demand in the analyzed location is expected to decrease. This is primarily due to a more pronounced reduction of the heating energy demand comparing to the increase in cooling energy demand. This study focuses therefore on the cooling energy demand, though not disregarding the meaning of other types of energy loads.

The Ladybug Tools energy simulation workflow can be divided into two parts: preparing the model with Honeybee (*Honeybee Primer*, n.d.) and adjusting its properties with Honeybee-Energy plugin (*HB-Energy Primer*, n.d.). This includes building programs, constructions, schedules, HVAC components, as well as the simulation settings. A Honeybee model can be then translated to an OpenStudio Model, and then simulated using the EnergyPlus engine. In Ladybug Tools, once the model is exported to OpenStudio for simulation, the simulation outputs can be accessed with *Read Room Energy Result*. This component lists all the energy loads making it possible to calculate the average and the totals, as well as to identify the peak values. Prior to analysis, these values are normalized by the building's floor area, in order to express energy per square meter.

Ladybug Tools additionally include a wide range of components that can be used to read and visualize the data, as well as to make various numerical operations on them. Each dataset in Ladybug Tools' structure consists of a header, explaining the meaning of the data, and a list of values at a given temporal resolution, typically hourly.

3.6.1. Selection of Indicators

The energy simulation outputs a comprehensive numerical model, which can be assessed using various measures and performance indicators. For this study, the following energy performance indicators were selected:

3.6.2. IE1 Peak Hour Cooling Energy Intensity [kWh/m^2]

This indicator reflects the highest hourly energy demand for cooling over the entire analysis period of the two months (July-August – see Chapter 3.4). It is particularly

useful for comparing the sizing of cooling systems, originally designed for less severe summers.

3.6.3. IE2 Total Cooling Energy Intensity [kWh/m²]

The second selected indicator captures the building's total cooling energy demand, during the entire two months of a heatwave period. This is computed by aggregating all partial results with the *LB Mass Arithmetic Operation* component (see Figure 22).
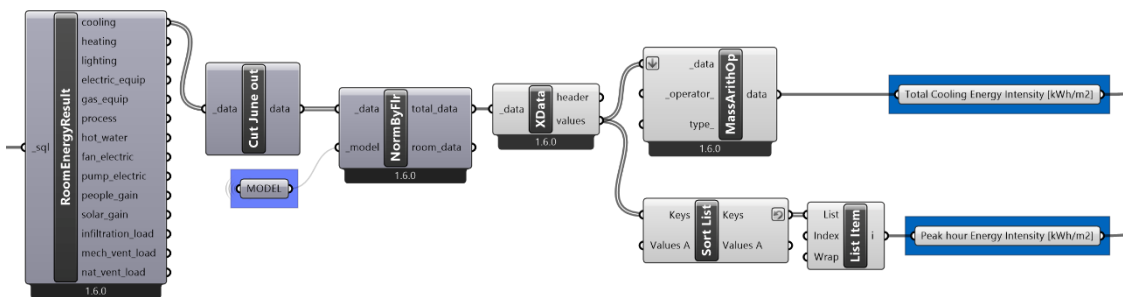

Figure 22 Part of the script responsible to read the Total and Peak Hour Cooling Energy Intensity as two of the Energy Performance Indicators

3.6.4. IE3 Total End Use Energy Intensity [kWh/m²]

This indicator measures the total energy demand for all the significant energy loads throughout the entire two-month heatwave period. Apart from cooling, also heating and electrical energy was considered, in order to find out if the design decisions can influence different aspects than cooling. It provides a holistic view of the building's energy performance, considering not just cooling, but also heating and electrical energy. This helps in understanding how design decisions might impact various aspects of energy use beyond cooling (see Figure 23).
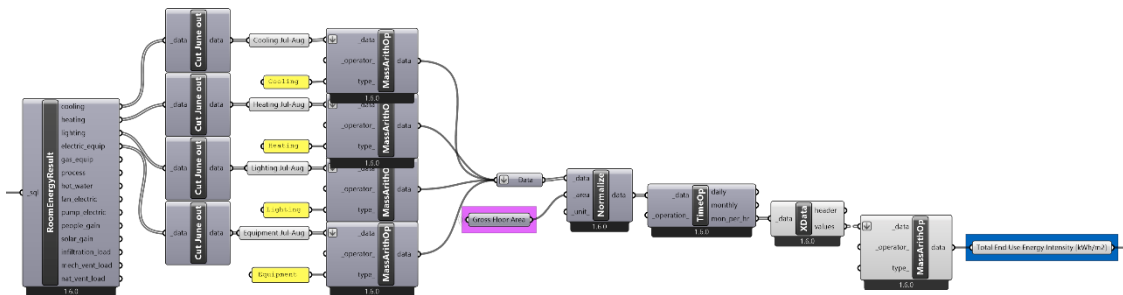

Figure 23 Fragment of the Grasshopper definition responsible for aggregating the four major elements of the building energy balance

3.7. Output Indicators: Thermal Comfort

Buildings ventilated naturally (employing passive air circulation through windows and leaks), are and will be a large portion of the building stock. Apart from old and not unmodernized houses, modern objects may also opt out from using such systems, utilizing passive strategies instead. Without a mechanical ventilation unit, the energy demand, and thus the operation prices, will not increase. However, such objects often encounter a distinct challenge: the potential decline in occupants' thermal comfort, particularly during hot summers and heatwaves. This section of the thesis outlines the methodology for simulating these conditions and introduces criteria for evaluating and comparing the outcomes of various simulations. Due to high computation intensity, only the top floor of each design variant was included in the model.

3.7.1. Selection of Indicators

Bringing long-term data to single quantities, can be done in multiple ways. Van Treeck, (2011) analyzed the long-term indicators described by the norms ISO 7730 (2005) and EN 15251 (2007). According to his work, the three possibilities are: a number of hours or percentage of time when the thermal comfort is satisfactory, the degree hours, where this number is weighted by the level of the deviation from the comfortable temperature, as well as the weighted PPD (see Chapter 2.3.3 PMV / PPD Thermal Comfort).

The Norm EN ISO 7730:2005 outlines several approaches for estimating long-term thermal comfort (*DIN EN ISO 7730*, 2006). It includes methods for calculating the proportion of time when the Predicted Mean Vote (PMV) or operative temperature exceeds desired values, adjustments using a weighting factor that considers the degree of deviation from desired temperature levels, and variations in this factor based on seasonal changes. Additionally, the norm provides methods for calculating the median and cumulative PPD over the usage period of a space.

3.7.2. Ladybug Tools Components

For adaptive models selected for this topic, the choice of indicators was based on the data offered by the chosen software. Ladybug Tools include several possibilities to estimate the thermal comfort of the user within the model, both indoors and outdoors. To calculate the previously described indicators, such as PMV and PDD, as well as

adaptive comfort indicators, it uses the official method according to the 2015 ASHRAE 55 thermal comfort standard, which corresponds to the European Norms EN-15251 and EN-16798 (*Ladybug Primer*, n.d.).

In the Ladybug Tab, the indoor thermal comfort can be measured with LB Adaptive Comfort and LB PMV Comfort components. The former should be used for buildings without, and the latter with air conditioning systems (*Ladybug Primer*, n.d.). Outdoor thermal comfort can be measured with LB UTCI Comfort component, which measures "feels-like" perception-related temperatures based on outdoor conditions. Additionally, LB PET Comfort component calculates Physiological Equivalent Temperature based on the Munich Energy Balance Model (MEMI) of the human body (*Ladybug Primer*, n.d.).

Those parameters consider the provided conditions, such as air temperatures, mean radiant temperatures (calculated with the use of either LB Indoor Solar MRT or LT Outdoor Solar MRT), air humidity and speed, as well as the information about the affected human body – the clothing rate, metabolic rate, posture or even the shortwave absorption. The calculations accept hourly condition data as arguments and in return output the information about the estimated user comfort under the provided conditions. They do not consider the building geometry or materials. To compare various building variants using those components, the indoor temperature, as well as the relationship between the human body and the geometry in which it is enclosed needs= to be calculated. That can be done with the use of the LB Human to Sky Relation component. This approach, however, would require a different model than the ones created with the Honeybee components.

Another possibility to calculate the thermal comfort within a building is to use components from the Honeybee tab. Two similar components to the previously described can be found: HB PMV Comfort Map and HB Adaptive Comfort Map for indoor thermal comfort, as well as HB UTCI Comfort Map for outside thermal comfort. Those components utilize EnergyPlus simulation engine for the model analysis together with Radiance sensor grids (*HB-Energy Primer*, n.d.). Moreover, the components additionally consider the building occupancy scheduled within the Honeybee model.

The Honeybee component "Adaptive Comfort Map" includes, among others, calculated Radiance's view factors, shades and MRT (Mean Radiant Temperature). The outputs for this component are Thermal Comfort Percent (TCP), Heat Sensation Percent (HSP)

and Cold Sensation Percent (CSP) measured on a scale of 0 to 100, as well as the inside conditions, including MRT, operative temperature and "condition" represented on a ternary scale, indicating a range of thermal sensations (-1: unacceptably cold, 0: neutral, 1: unacceptably hot). Those outputs may be used for the formulation of thermal comfort indicators.

3.7.3. IC1 Number of Hot Hours

Apart from the intensity of a heatwave, the length of its occurrence is a critical factor in resilience strategies. Therefore, the first indicator for analysis is the overall number of hours classified as "hot". The Honeybee Energy component "Adaptive Comfort Map" provides the output "condition", where for each cell of the sensor grid, one of the following values can be displayed: -1 (unacceptably cold), 0 (neutral) or +1 (unacceptably hot), according to the norm EN 15251 function (see chapter 2.3.4 Adaptive Thermal Comfort). For this indicator, all the +1's were summed. The maximum value of this indicator is 1488 (24 hours * 31 days * 2 months), which would indicate the "worst case scenario" in which the internal thermal conditions were hostile for the designed building's users for during the entire analysis period.

Considering the sensor grid within the top floor of a building, the decision had to be made as to when the indicator should be increased: when all the sensors output the condition +1, when at least one of them does, or when the average value is above a certain value. For this study, the indicator contains those hours of the analysis period, in which at least 20% of the building sensors exceeded the temperature defined as comfortable.
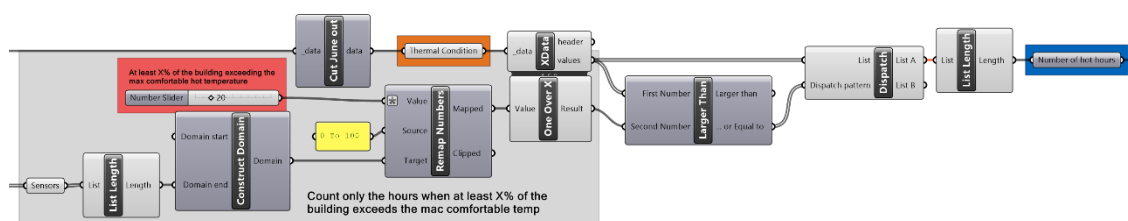
3.7.4. IC2 Average Temperature Difference Outdoor-Indoor

Probably a simpler measure of the building performance during the heatwave can be the difference between the outdoor and indoor temperatures. Even though it does not

directly inform about the thermal comfort of the building users, it is a measure, which can be further analyzed and included in numerous comfort calculations.

3.7.5. IC3 Maximum Average Operative Temperature

Operative Temperature can be referred to as "perceived temperature" (Hegger & Institut für internationale Architektur-Dokumentation, 2008) and it considers air temperature and velocity as well as mean radiant temperature (MRT). The norm DIN EN 15251 defines, that it should be measured at a height of 60 cm in a room's occupancy area and defines the guidelines of its values, depending on average outdoor air temperature, with variations allowed up to ±2K for maximum thermal comfort, though it can be adapted by appropriate clothing (*DIN EN 15251*, 2012). According to the norm, the comfortable operative temperature is 22C for outdoor temperature below 16 °C, 26 °C for above 32 °C, and the range between is defined by the formula 18 °C+0.24 * outdoor air temperature (see Chapter 2.3.4 - Adaptive Thermal Comfort).

This temperature is averaged from all the sensors on the sensor grid sampled once an hour. Among such values, the highest hourly value is selected as the maximum (see Figure 24).
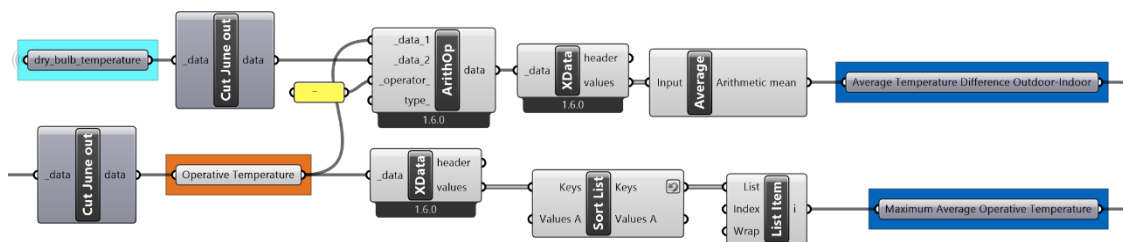

Figure 24 Fragment of the Grasshopper definition that includes two further comfort indicators

3.7.6. IC4 Average HSP

Heat Sensation Percent is one of the indicators of thermal comfort provided by the "Adaptive Comfort Map" component of the Honeybee Energy plugin from Ladybug Tools. According to the HB-Energy Primer, "*HSP is the percentage of occupied time where thermal conditions are hotter than what is considered acceptable/comfortable*" (*HB-Energy Primer*, n.d.).

As the value is also provided for each cell of the sensor grid, this value is averaged. It is also averaged for the duration of the analysis period.

3.8. Iterative Process and Data Preparation

Due to the large number of simulations to be made, the simulation process had to be divided into smaller segments and often repeated after the input of new knowledge. This required an introduction of a structured workflow and specific data management strategies. To distinguish the new datasets from the previous iterations, a fragment of the Grasshopper definition was responsible for creating custom file paths for each newly generated data set, based on the current date with the precision of up to one hour. With the use of the MetaHopper plugin, the paths could be relative to the Grasshopper definition file. The manual trigger, which had to be clicked before every iteration, assured that during a long process the data will not be divided into multiple folders.
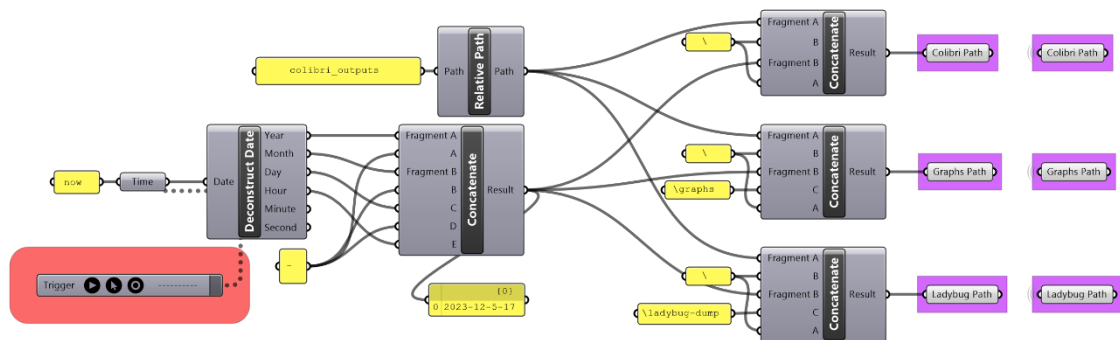

Figure 25 Fragment of the Grasshopper definition responsible for file path generation

The dataset collected with *Colibri Aggregator* was each time saved in a file named data.csv. The CSV tables had to be combined and post-processed, the latter of which included removing invalid data (outputs: 0 or -999) and duplicates. Moreover, unreliable data had to be re-stimulated in order to check for simulation mistakes (see Figure 26).

Figure 26 Example of a potential simulation mistake to be re-simulated and compared

3.9. Data Visualization

The parametric approach to sensitivity analysis had to be tested on a simple model before applying it to data which is difficult to comprehend, and which potentially requires a lot of time to compute. A simple and easy to understand idea was to calculate how various geometric parameters may affect the building's total area and its area to volume ratio (A/V Ratio).

3.9.1. Test Model Description

A simple Grasshopper definition, utilizing the Colibri plugin was created to test this method. As input parameters building width, length and the height of a floor were selected, while the number of floors remained constant. The area and volume were calculated after combining the geometry by means of a Boolean union operation. To avoid situations in which the generated files may be overwritten, a new directory with the current date and time was being created, in the way described in Chapter 3.8. The Grasshopper definition, generated a simple 3-floor high building (see Figure 28) with following test parameters and their values:

Table 4 Selection of test parameters and their values for the methodology formulation

	Parameter Name	Tested Values
TP1	Floor Height	3; 3.4; 4.7; 4
TP2	Building Width	10; 11; 12; 13; 14
TP3	Building Length	30; 38; 45; 52; 60

The Grasshopper definition would output values of the following test indicators:

TI1:   A/V Ratio = building hull area / building volume

$$TI1 = \frac{A}{V} Ratio = \frac{\left(2 * P2(v) * P3(v) + 2 * 3 * P1(v) * P2(v) + 2 * 3 * P1(v) * P3(v)\right)}{P2(v) * P3(v) * P1(v) * 3}$$

TI2:   Gross Floor Area

$$TI2 = GFA = P2(v) * P3(v) * 3$$

Those indicators were computed graphically, considering the graphical character of a typical Rhino+Grasshopper workflow. They were selected in such a way as to be interesting from an architectural point of view, but to still provide an intuitive way of evaluation of the methodology and coding correctness.
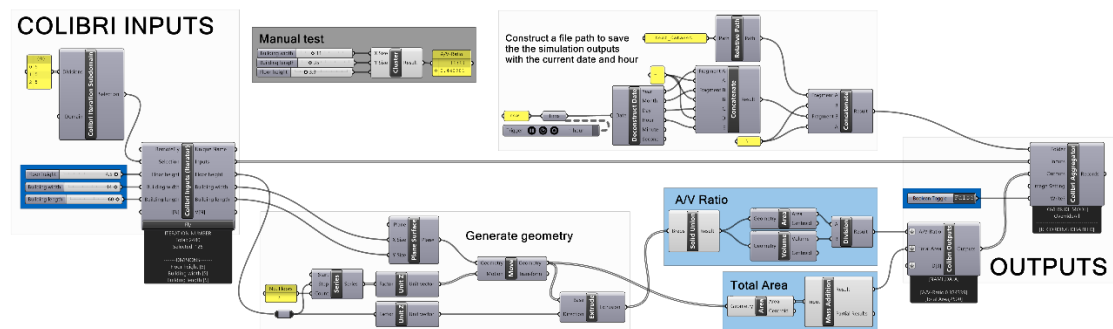
Figure 27 Grasshopper definition aggregating model variations with Colibri plugin

An excerpt of the database containing the simulation results is presented in Table 5

Table 5 CSV Table generated by the Colibri plugin - fragment

Figure 28 Test model for methodology

in:Floor Height	in:Building Width	in:Building Length	out:A/V-Ratio	out:Total Area
3	10	30	0.488889	900
3.4	10	30	0.462745	900
3.7	10	30	0.446847	900
4	10	30	0.433333	900
4.5	10	30	0.414815	900
3	11	30	0.470707	990
…	…	…	…	…
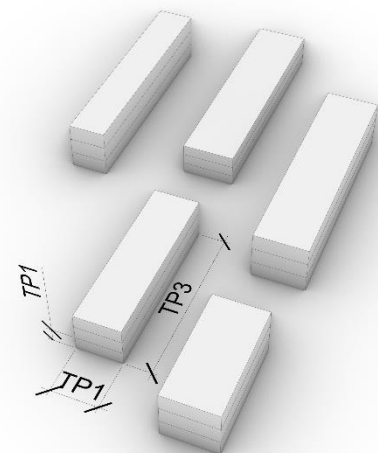
3.9.2. Visualization of Individual Results

Data visualization and evaluation was performed further with the use of charts. Because of the iterative character of this study, it was decided, that in order to minimize the number of repetitive tasks (such as opening spreadsheets with data), the charts should be created in an automatic way wherever possible. To achieve this, a series of Python scripts was written, utilizing Pandas, Matplotlib and Seaborn libraries. The written

programs open and use as an input the "data.csv" file (created by the Colibri plug-in), located in the same directory.

The first script, called "scatter", selects two of the output indicators and places the particular values on a chart with those two indicators as axes. Utilizing the Seaborn's jointplot() and regplot() functions, it draws a scattered plot, and for selected plots (used later in this study) fits a regression line, additionally plotting marginal histograms with regression lines for both plot axes (Figure 29) (*Seaborn: Statistical Data Visualization — Seaborn 0.13.0 Documentation*, n.d.).
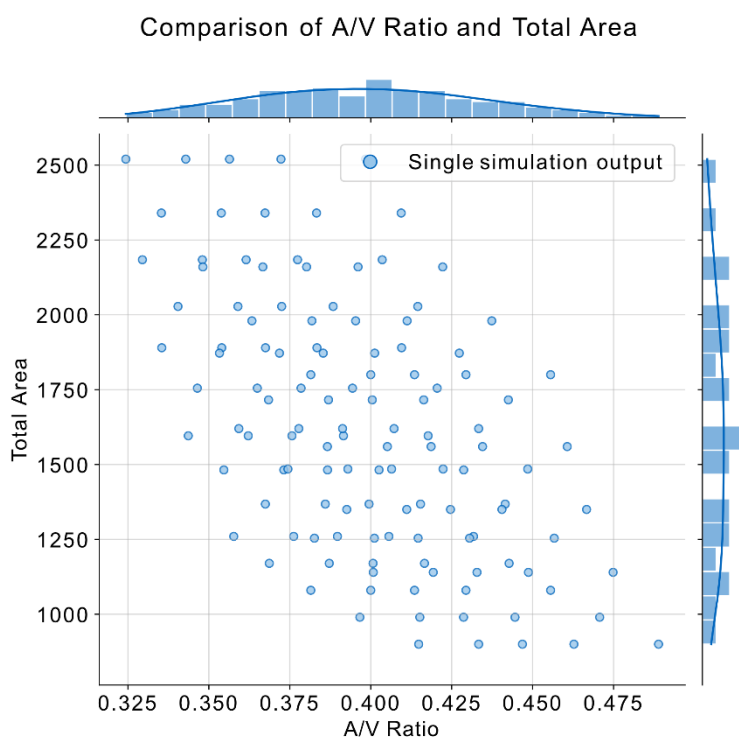
Figure 29 Scattered plot of the output values for a pair of indicators

3.9.3. Visualization of Average Results for Unique Parameter Values

The analysis of individual simulation outputs brings great insights to the topic, however in order to compare the influence of selecting particular input parameter values on the indicator value, a different approach to the data analysis has to be utilized. Next scripts prepared for this study, therefore, calculate an average of all the selected indicator values when the model was defined by this parameter value. As all the combinations of parameters have been simulated, the overall mean value of each indicator is at the same time the average of all the indicator values grouped by parameter values, as presented

in Table 6. Moreover, if only for example, two values of a selected parameter were analysed, this average will be made of half of all the building variants.

Table 6 Fragment of the generated CSV file listing the average indicator values for every unique parameter value and the list of indicator values from which it is averaged (fragment)

out:A/V Ratio			
Parameter	Value	Average	Values List
in:Floor height	3	0.438367	[0.488889, 0.470707, 0.455556, 0.442735, 0.431746…
in:Floor height	3.4	0.412224	[0.462745, 0.444563, 0.429412, 0.416591, 0.405602…
in:Floor height	3.7	0.396325	[0.446847, 0.428665, 0.413514, 0.400693, 0.389704…
in:Floor height	4	0.382812	[0.433333, 0.415152, 0.4, 0.387179, 0.37619…
in:Floor height	4.5	0.364293	[0.414815, 0.396633, 0.381481, 0.368661, 0.357672…
in:Building width	10	0.429767	[0.488889, 0.462745, 0.446847, 0.433333, 0.414815…
…	…	…	…

In the example of the analyzed test model:

P = {p1, p2, ..., pn} – parameters, for example P = {Floor height, Building width, Building height}
I = output indicator, for example I = A/V Ratio

The values are grouped by the unique parameter value and then averaged:

$$\bar{I}_{P_i}(v) = \frac{\sum_{i \in G_{P_i}(v)} i}{\left| G_{P_i}(v) \right|}$$

Assumption: $\left| G_{P_i}(v) \right| > 0$

$\bar{I}_{P_i}(v)$ – the mean value of the indicator I for a specific value v of the parameter P_i

$G_{P_i}(v)$ – the subset (group) of the dataset, where the parameter P_i has the value v

$\left| G_{P_i}(v) \right|$ – the number of occurrences of the value v ot the parameter P_i = the size of this subset

$\sum_{i \in G_{P_i}(v)} i$ – the sum of the values of the indicator I for the dataset subset where P_i has the value v

Those averages were then plotted together on one bar chart per indicator.
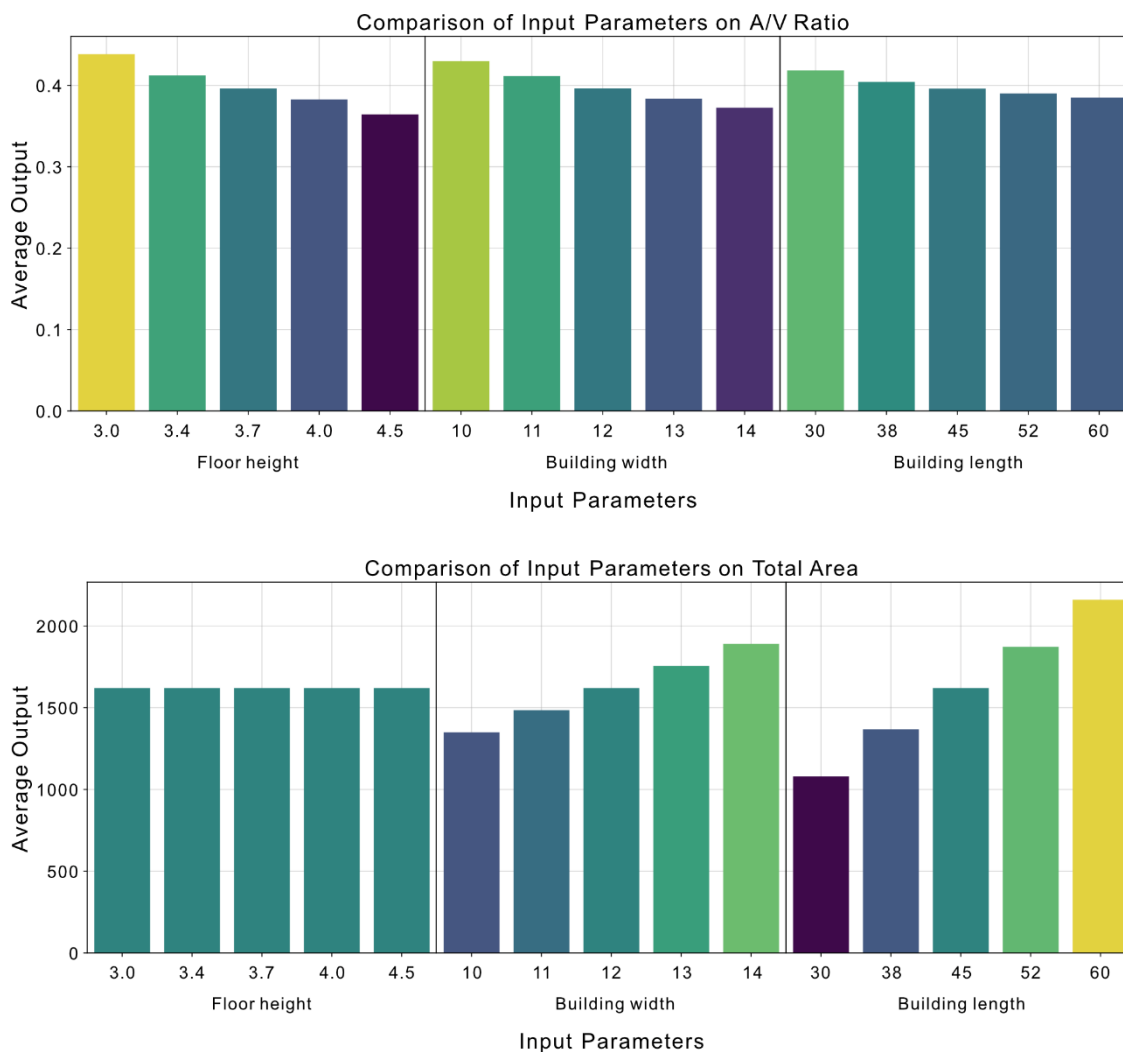
Figure 30 Comparison of unique parameter values averaged in form of a bar plot per indicator a) A/V Ratio, b) Total Area.

The graphs above correctly present the averaged data. Increasing all three parameters will increase the A/V Ratio, while the floor height has no influence on the total floor area of the analyzed building.

The differences between average indicator values of various parameter inputs were also plotted together on one axis per parameter for comparison:
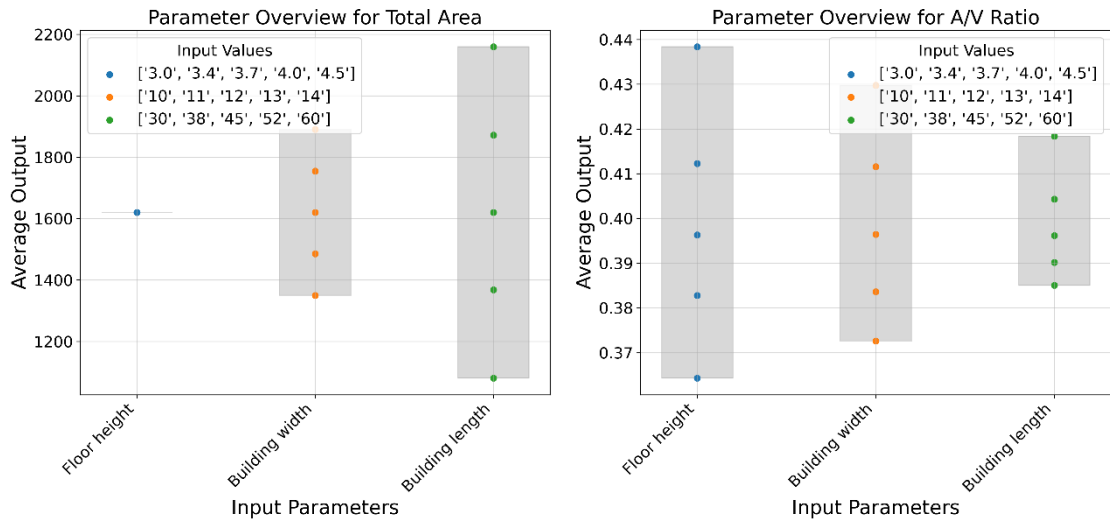
Figure 31 Average parameter values plotted together for easier visual comparison

Finally, the last average parameter value visualization included interposing two selected parameters at a time in the form of a heatmap. This could be especially useful in cases where one parameter value is constant (e.g. it has already been decided for the project) and other parameters should balance its impact. If, for example, it were critical to set one parameter to a value earlier defined as disadvantageous, the performance could be potentially balanced by making correspondingly good decisions in the other aspects of the design.
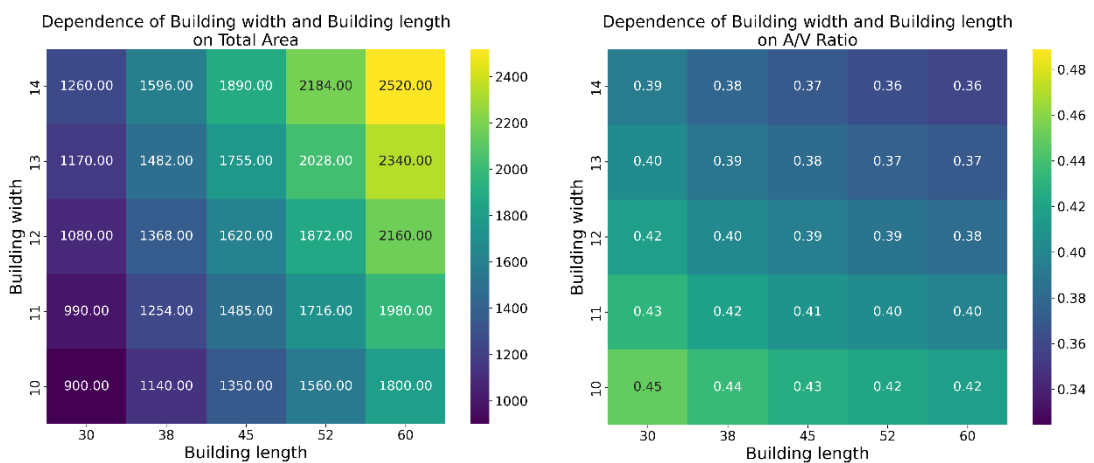
Figure 32 Examples of 2 generated heatmaps showing dependencies between the influence of two parameters (Building Width and Length) on the output values a) Total Area, b) A/V Ratio

3.10. Sensitivity Analysis

One-at-a-time (OAT) local sensitivity analysis is a method which is comparably easy to compute, as it measures changes of one output value when only one parameter at a time is being changed. In case of the study's simulation data, this method has to be adjusted, as there is no single "baseline" model. Moreover, the parameter values in the final model are not usually linearly distributed and appear in varied ranges and scales, or are even nonnumerical, like the selection of the construction set or the type of the shading devices.

Instead of this, two consecutive average indicator values of each unique parameter value can be compared, for example the A/V Ratio of the average building with floor height of 3 m with these of the building with floor height of 3.4 m and 3.4 m with 3.7 m and so on.

$$\Delta_{P_i}(v_j) = |\bar{I}_{P_i}(v_{j+i}) - \bar{I}_{P_i}(v_j)|$$

$\Delta_{P_i}(v_j)$ – is the absolute difference between the mean values of the indicator I for the two consecutive values of the parameter P_i. The value is absolute to ensure it is always nonnegative.

For example, for P_i = Floor height, v_j = 3 and v_j= 3.5 for the indicator I = A/V Ratio.

$$\Delta_{Floorheight}(3) = |\bar{I}_{Floorheight}(3.4) - \bar{I}_{Floorheight}(3)| = |0.44 - 0.46| = 0.02$$

The value 0.02 represents the sensitivity of the change of the parameter value from 3 to 3.4 for the A/V Ratio indicator.

Finally, the sensitivity of each parameter can be calculated as the mean of all the sensitivities for all parameter value pairs:

$$S_{P_i} = \frac{1}{|V_{P_i}| - 1} \sum_{j=1}^{|V_{P_i}|-1} \Delta_{P_i}(v_j)$$

S_{P_i} is the sensitivity of the indicator I to the parameter P_i

$\left|V_{P_i}\right|$ is the number of unique value pairs of the parameter P_i. As the number of consecutive pairs $(\left|V_{P_i}\right| - 1)$ is considered, it is one less than the number of unique values.

$\Delta_{P_i}(v_j)$ is the absolute difference between two consecutive values (see above)

The results of those calculations are:

Table 7 Test results of the sensitivity analysis of the selected parameters

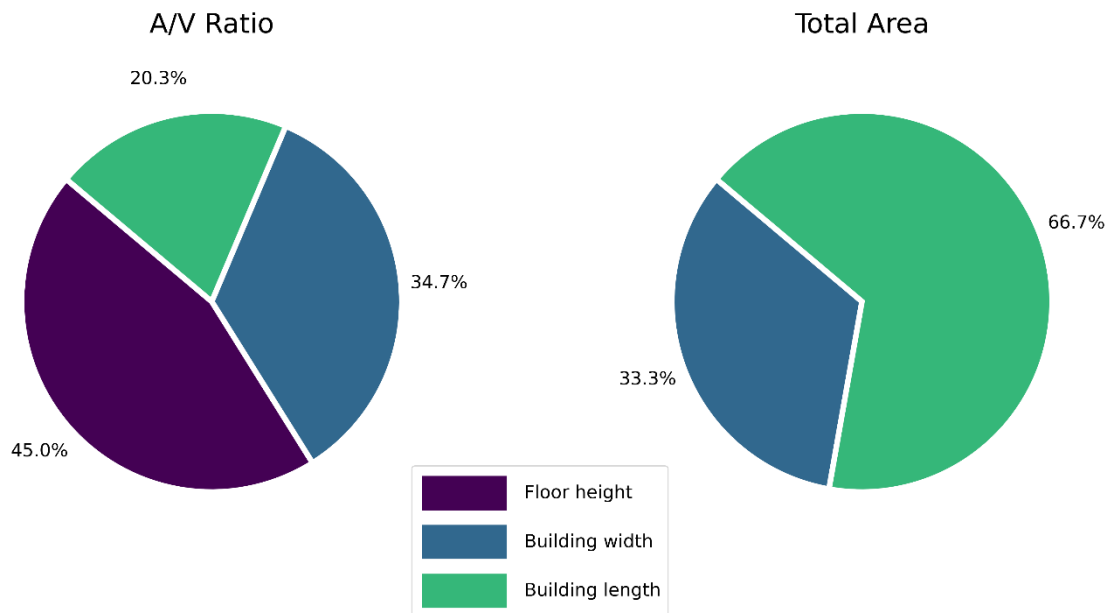|	A/V Ratio			Total Area		
	Mean	Sensitivity	Normalized	Mean	Sensitivity	Normalized
Floor Height	0.398804	0.018519	0.450160	1620	0	0
Building Width	0.398804	0.014286	0.347268	1620	135	0.333333
Building Length	0.398804	0.008333	0.202572	1620	270	0.666667

Figure 33 Pie charts displaying graphically the sensitivity analysis' results

The sensitivities were calculated with the use of a simple Python script presented below and then visualized with the Matplotlib library. This way, every time the data was updated, it was possible to immediately generate the new plots and charts.

```python
for idx, output_col in enumerate(output_columns):
    output_col_clean = output_col.replace('out:', '')
    sensitivities = []
    for input_col in input_columns:
        input_col_clean = input_col.replace('in:', '')
        grouped = data.groupby(input_col_clean)[output_col_clean].mean()
        differences = grouped.diff().abs().dropna()
        avg_sensitivity = differences.mean()
        sensitivities.append(avg_sensitivity)
        results_df.loc[input_col_clean, f'{output_col_clean}_Mean'] = grouped.mean()
        results_df.loc[input_col_clean, f'{output_col_clean}_Sensitivity'] = avg_sensitivity
    normalized_sensitivities = [s / sum(sensitivities) for s in sensitivities]
    results_df[f'{output_col_clean}_Normalized_Sensitivities'] = normalized_sensitivities
```

3.11. Section Summary

The selected methodology includes using a parametric model and future-updated weather data to analyze climate adaptation and heatwave resilience of the building design.

To model an effect of a heatwave, the most negative future scenario was selected, representing a very severe summer. The simulation was limited to three summer months (June-August) and cropped to the last two. This way, computation intensity of the large number of simulations could be limited, while keeping the accuracy of outputs for the time affected by potential heatwaves.

A selection of parameters and their values, as well as energy performance and thermal comfort indicators, enables the evaluation of various design strategies and can aid in making decisions that are usually made in the early stages of the design. The sensitivity analysis uncovers which parameters influence the simulation output to the biggest extent.

4. Results

The execution of thousands of simulations, a fundamental part of this study, required multiple repetitions due to frequent updates to the Grasshopper definition throughout the iterative process. After each iteration, a precise verification of the database was undertaken to identify duplicates or missing values, thereby ensuring the highest accuracy of the results.

One of the advantages of the selected tools was their ability to automatically generate charts for each iteration of the dataset. The Python scripts were designed to produce these graphs efficiently, regardless of the number of parameters, their respective values, and the diversity of indicators involved. This automation significantly reduced the need for time-intensive data processing and minimal graphic post-processing was only occasionally required. The resultant charts and tables facilitated straightforward manual interpretation of the data, allowing for an in-depth analysis of the most influential parameters in terms of climate adaptation and building resilience against heatwaves.

Having all the datasets in a single CSV file per topic, the next step involved data presentation, comparison, and analysis. The findings from this chapter will be a valuable contribution to the field of sustainability, as well as a valid input to the ECO+ Project, providing unique insights into the impact of climate change on building energy performance and user comfort.

4.1. Difference in Energy Performance Between Simulations for Present-Day and Future Weather Files

An initial exploration, prior to conducting large numbers of simulations, involved assessing how outputs might vary across selected future-updated weather files (see Chapter 3.3, Weather Data for the Simulation). The intent was to simulate the energy performance for all design variants multiple times, each with a different weather file. Considering this was a preliminary analysis and taking into account the extensive nature of the simulations required, a decision was made to limit the scope to the least-intensive simulation setup.

Early tests revealed that most parameter configurations had negligible impact on computation time, except for the P3 Window Shading Style parameter. The addition of extra surfaces in the louvers style significantly increased the number of surfaces to be processed by EnergyPlus and Radiance calculations. Consequently, the simulations described in this subchapter included all defined parameter variations, but with the P3 (window shading style) parameter set to 0, indicating no shading devices. This approach reduced the number of iterations per weather file to 361, facilitating faster initial comparisons before delving deeper into parameter sensitivity analysis.

Regarding future weather files, Meteonorm files representing the years 2020, 2080 (in RCP2.6 and RCP8.5 scenarios), and 2100 (in RCP2.6 and RCP8.5 scenarios) were selected for this part. Table 8 presents the average outcomes of these simulations for all three energy performance indicators described in Chapters 3.6.2-3.6.4.

Table 8 Average values of indicators across years and scenarios

Year	2020	2080		2100	
Scenario		2.6	8.5	2.6	8.5
IE1 Peak Hour Cooling Energy Intensity [kWh/m^2]	0.040	0.046	0.055	0.041	0.090
IE2 Total Cooling Energy Intensity [kWh/m^2]	9.158	11.660	23.704	9.000	44.202
IE3 Total End Use Energy Intensity [kWh/m^2]	16.695	19.133	31.053	16.428	51.551

For the indicators IE2 and IE3, Figure 34 was plotted, presenting the worst-case scenario RPC8.5 as the upper boundary, and the sustainability scenario RCP2.6 as the lower boundary, with the area between those curves filled in, showing the spread of various possible values in between. As can be noticed, this visualization resembles that in the Figure 3 from the page 21, a graph cited from the IPCC Report, which illustrates the projected temperature developments in various future scenarios.

Both Table 8 and Figure 34 indicate that the energy required for building operation, particularly for cooling, is likely to increase, either significantly or slightly by 2080. However, the trends beyond 2080 vary drastically between scenarios: either a slight increase to levels seen in 2020 or a near tripling of the 2020 values can be seen. This suggests that designing with only the year 2080 in mind might seem a safer option, as

the scenarios do not diverge significantly until then. This approach could be considered choosing the path of least resistance.
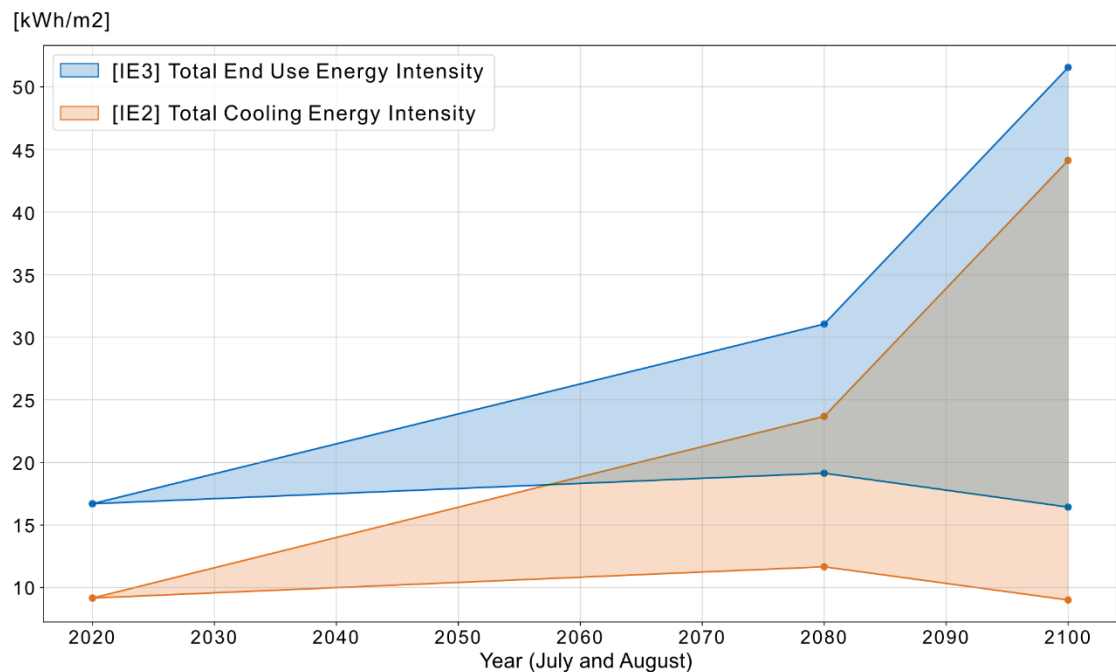
Figure 34 Indicator IE2 and IE3 values across years and scenarios

However, the data from the statistics portal of the German Federal states reveal that a third (34.5%) of residential buildings in Germany, in Bavaria 40.4%, were built in the year 1980 or later (*Wohngebäude Nach Baujahr | Statistikportal.De*, n.d.). Despite a significant proportion (38.9 %) of buildings built in years 1950-79, 26,5% of German buildings and 25% in Bavaria are at least 75 years old. This durability of buildings emphasizes the relevance of designing for longevity, making the year 2100 a valid target for designs aimed at resilience and climate adaptability.

Additional insights emerged from examining the values of selected parameters. For most parameters, the ranking from best to worst remained consistent and usually proportional. The only parameter which influenced the results in a disproportionate way was the building rotation for the peak hour cooling energy intensity indicator, as illustrated in Figure 35.

Building rotation Across Years and Scenarios for Peak Hour CoolingEnergy Intensity [kWh/m2]
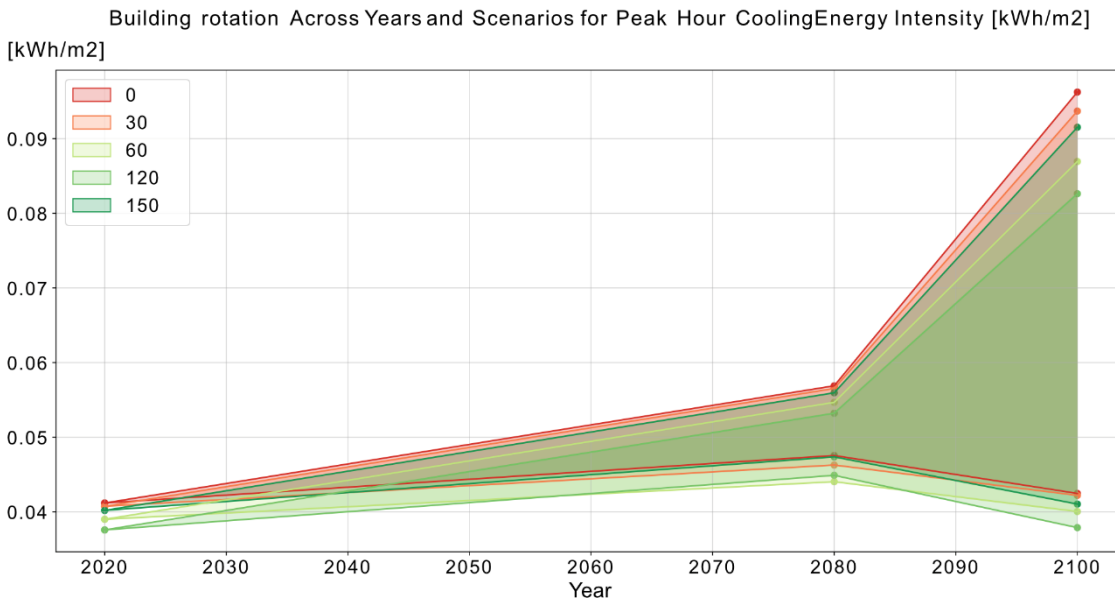
Figure 35 Influence of the building rotation on the peak hour cooling energy intensity across years and scenarios

Apart from that, it is crucial to recognize that climate variability can influence extreme events, such as heatwaves (Seneviratne et al., 2021). Therefore, a truly future-proof design cannot focus solely on one version of the future, particularly not the 'average' one. Each summer and winter will differ from the preceding and succeeding ones, making it critical to consider both milder and more extreme periods in the decision-making process.

The conclusions drawn from these simulations indicate that even in the most sustainable scenarios, buildings may face increased cooling energy demands during summers for at least the next 50 years. Post-2080, there is a possibility of a temperature drop, but in most scenarios, the trend is likely to escalate further, leading to significantly higher cooling energy demands. This topic will be explored in greater depth in Chapter 4.2.

4.2. Energy Performance Simulation Results

To analyze climate adaptation in terms of energy demand of mechanically conditioned buildings, 1440 simulations were conducted. The analysis of the simulation data followed the previously described methodology, with a list of selected parameters presented in Table 3 the Methodology section of the thesis, encompassing 6 parameters with their 21 unique values in total. The three selected performance indicators were described in Chapters 3.6.2-3.6.4.

4.2.1. Analysis of Individual Variants

Even at first glance, looking at the data, one can observe that the selected indicators appear to have a linear dependency, with only the extreme iterations deviating from this trend. The plots for both Total Cooling- and Total End Use Energy Intensity indicators when comparing with Peak Hour Energy Intensity, look very similar, and the former is presented in Figure 36.
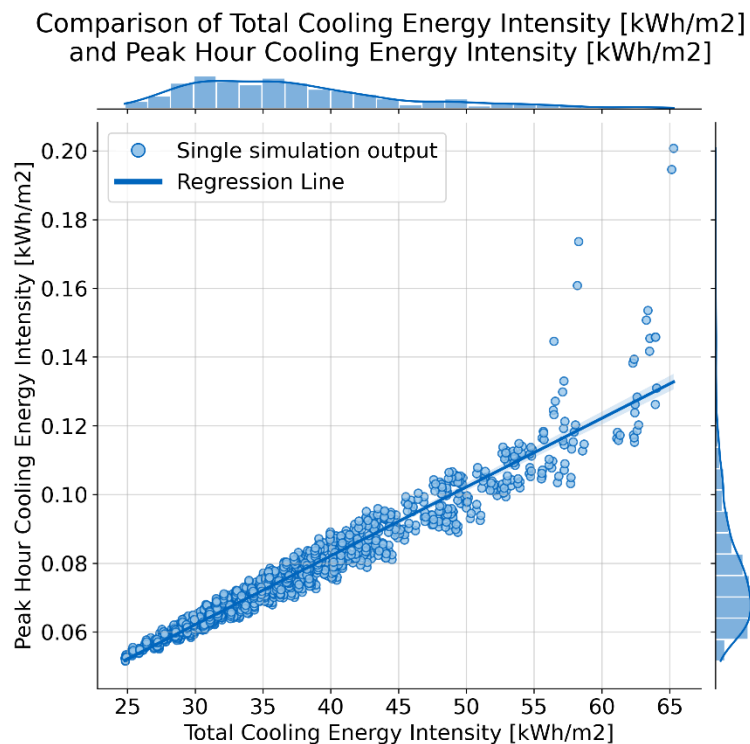
Figure 36 Scattered plot and linear regression for the dataset for indicators IE1 and IE2

With the use of statsmodels library the regression parameters can be read, including the regression line function, the coefficient of determination (R^2) and the standard error of the regression (S) (Seabold & Perktold, 2010; *Statsmodels 0.15.0 (+180)*, n.d.).

The regression line y(x) = a*x + b is here modeled as:

- x is Total Cooling Energy Intensity,
- y is Peak Hour Cooling Energy Intensity,
- a (the slope parameter) equals 0.002003162067,
- b (the intercept parameter) equals 0.001993205315,
- R^2 (the coefficient of determination) equals 0.921917434339,
- S (the standard error of the regression) equals 0.000589911665.

This can be understood as: there is proportionality between those indicators, which can suggest further similarities between them in parameter sensitivities.

Figure 37 Scattered plot of the results of the simulation and a linear regression model

The relationship between the Total Cooling Energy Intensity and Total End Use Energy Intensity in Figure 37, however, presents a direct relationship and can best be described with a simple linear regression model of y(x) = a*x + b, where:

- x is Total End Use Energy Intensity
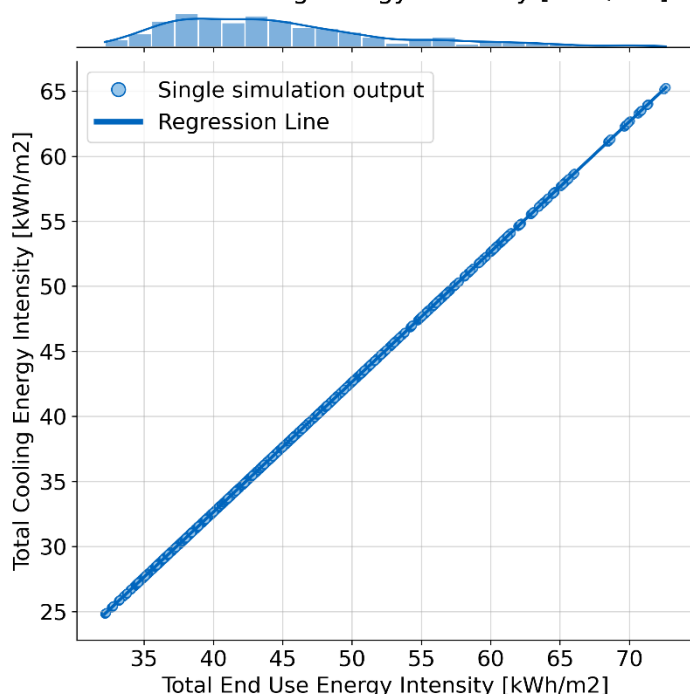- y is Total Cooling Energy Intensity
- a equals 1.000000000473
- b equals -7.348895287208

With the simulation data, in the linear regression model presented above, the R^2 (the coefficient of determination) equals 1.000000000000 indicating direct proportionality of the variables. S (the standard error of the regression) equals 0.000000065609, indicating high precision of the model's predictions.

This directly linear relationship suggests that other forms of energy demand, aside from cooling, do not significantly fluctuate with the variation of the selected parameters. This pattern implies that the energy demand for lighting and other electrical appliances may not increase significantly enough to impact the energy performance calculations in the context of climate adaptation.

In Table 9, the highest and lowest value of each parameter is presented, along with the corresponding parameter values configuration:

Table 9 Extreme values of indicators

	Value	P1	P2	P3	P4	P5	P6
out:Total End Use Energy Intensity [kWh/m²]							
Lowest	32.167571	1	60	1	0.6	0.4	0.2
Highest	72.628797	4	0	0	0.6	0.8	0.4
out:Total Cooling Energy Intensity [kWh/m²]							
Lowest	24.81868	1	60	1	0.6	0.4	0.2
Highest	65.2799	4	0	0	0.6	0.8	0.4
out:Peak Hour Cooling Energy Intensity [kWh/m²]							
Lowest	0.051542	1	120	1	0.6	0.4	0.2
Highest	0.200778	4	0	0	0.6	0.8	0.4

The analysis of extreme values in the simulation data reveals that a building of the same size can double its cooling energy demand during the hottest months or a heatwave,

assuming all design choices were nonoptimal, compared to a well-planned one. Considering that for all three indicators almost all parameters of maximum values present the same parameter configurations, it could be already possible to suggest, that those design decisions are the worse. Further analyses evaluate this and confirm or invalidate, as well as provide better insights on which parameters, among the analyzed ones, have the greatest influence on heatwave resilience and climate adaptation of the planned building.

Ladybug Tools additionally offer data visualization components, including various plots. The comparison of the extreme variants – the best and the worst performing one might be a good insight regarding the influence of the resilience-aimed decisions on the future-energy performance. A visual representation of those differences makes it easier to analyze their character. Knowing the hourly values and the distribution of local peaks in energy demands will provide an insight for HVAC system sizing. During this study such plots were saved for each iteration, complementing the dataset with valuable information for possible further processing.

The hourly plots in Figure 39 and Figure 39, on the other hand, may provide a better overview on the peculiarities of the performance of each design. In this figure, the best and worst performing designs, according to Table 9, were presented as an excerpt from the saved pictures. The difference in energy efficiency for those two variants is significant, displaying that selecting the right parameter values is crucial in terms of heatwave resilience of the design.
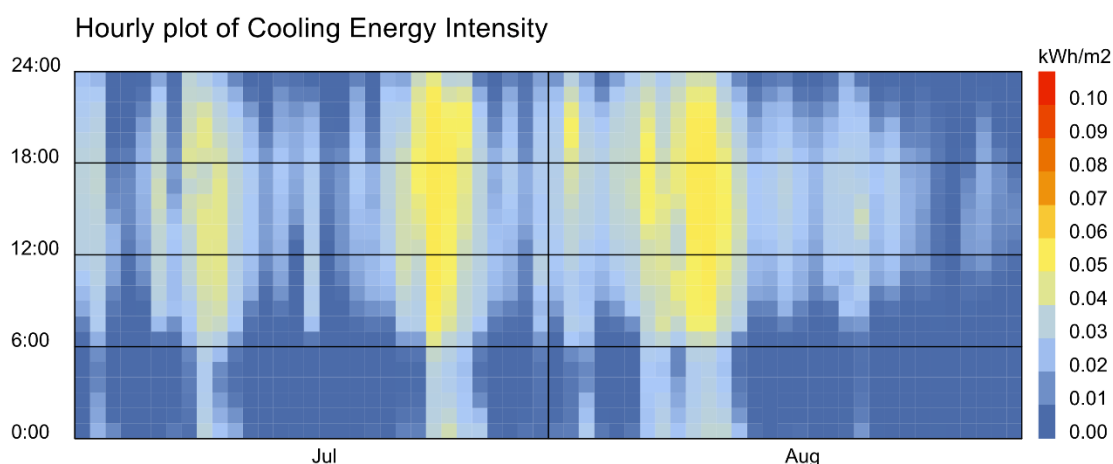
Figure 38 Hourly plot of the best performing variant
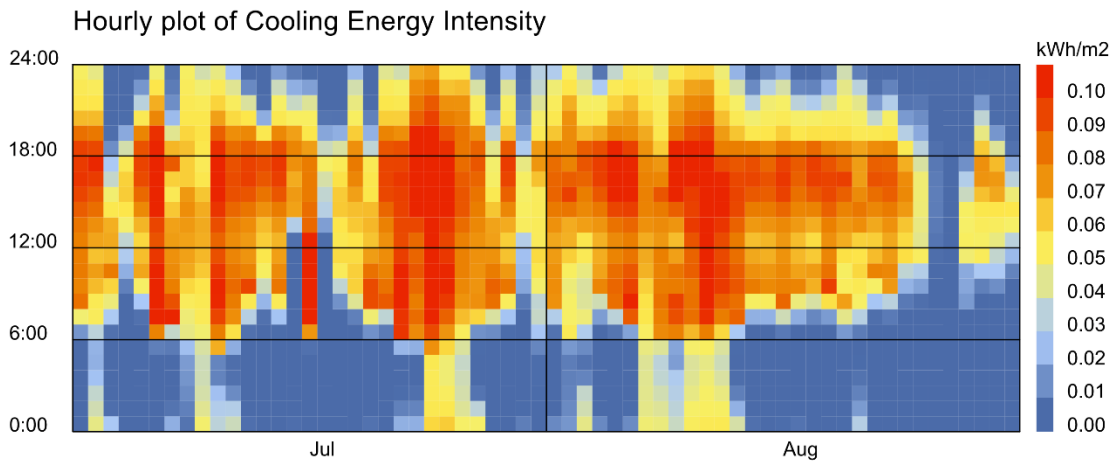
Figure 39 Hourly plot of the worst performing variant

When comparing those values in the form of daily totals (Figure 40) or hourly averages (Figure 41), the differences appear to have even greater consequences for the cooling system sizing. The periods requiring extensive cooling are much longer, which in turn decreases the efficiency of the complimentary passive solutions. Moreover, the difference between the daily totals is even more meaningful, as most of the increase in cooling demand occurs during the daytime, with night-time energy intensities remaining relatively similar. This pattern, when analyzed alongside comparable data for other variants, implies that even only slightly worse designs in terms of total or average energy demands, can lead to substantially higher peak energy demands. Consequently, these peaks have a more profound effect on the HVAC system sizing than the aggregate totals might indicate.
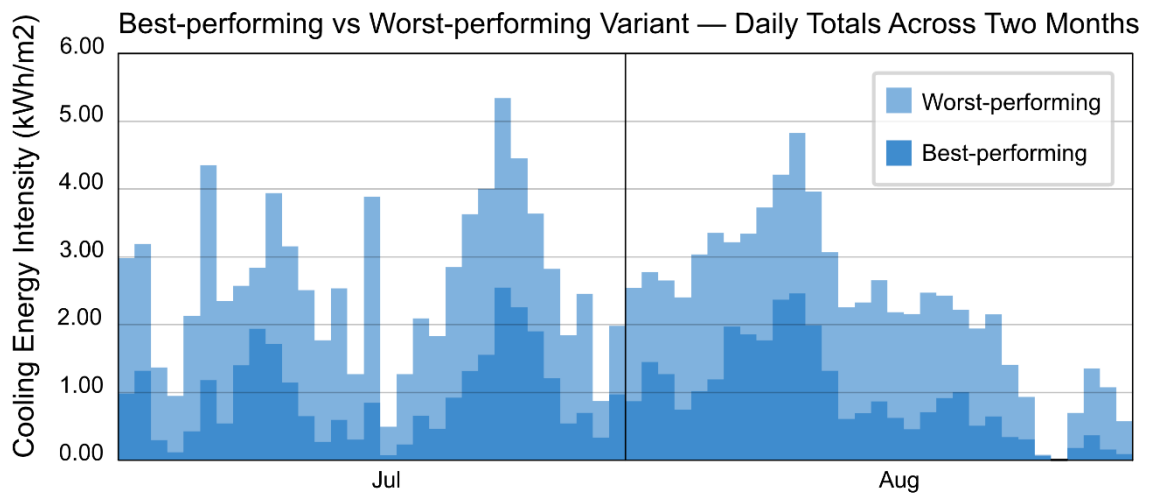
Figure 40 Comparison of the best- and worst-performing variants - daily totals
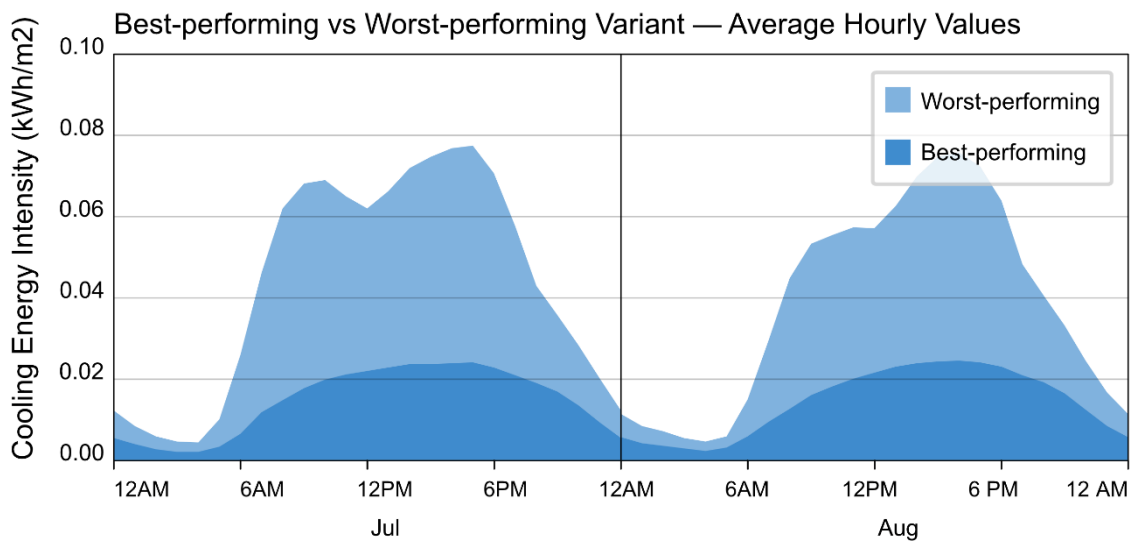
Figure 41 Comparison of the best- and worst-performing variant - average hourly values for cooling energy intensity

In summary, this subchapter highlighted the importance of making well- informed design decisions. Employing parametric design and performance simulations already at the early stages of design can be instrumental in preventing choices that could result in the unnecessary over-sizing of cooling systems. This approach applied in the initial design phase is essential in optimizing system efficiency and ensuring sustainable design solutions, especially aiming at heatwave resilience and climate adaptability.

4.2.2. Dataset Evaluation and Sensitivity Analysis

The analysis of extreme values within the dataset cannot be directly generalized across the entire database. It is important to recognize that specific parameter configurations should not limit the design process. Central to this thesis was the task of analyzing the sensitivity of these parameters, therefore, following the chosen methodology, the next task of the study was to calculate average values of each indicator for every unique parameter value. These averages are detailed in Annex 5. The mean for each parameter, as well as the overall mean, is the same, as its iteration covers the entire spectrum of model variations.

The average values of the indicator IE2 were represented on the bar plot in Figure 42 and compared parameter-wise on Figure 43. It is evident, that the P3 (Window shading style) parameter has the greatest influence on the design performance, ranging from the average value of 31.96 kWh/m^2 for value 1 (louver shading) up to 44.20 kWh/m^2 for the value 0 (no shading). Other influential parameters are P6 (Windows-To-Wall-Ratio), where the average indicator output ranged from 32.34 kWh/m^2 for [0]=0.2 to 42.56 kWh/m^2 for [2]=0.4 and P5 (SHGC) from 32.59kWh/m^2 for [0]=0.4 to [2]=42.28 kWh/m^2.
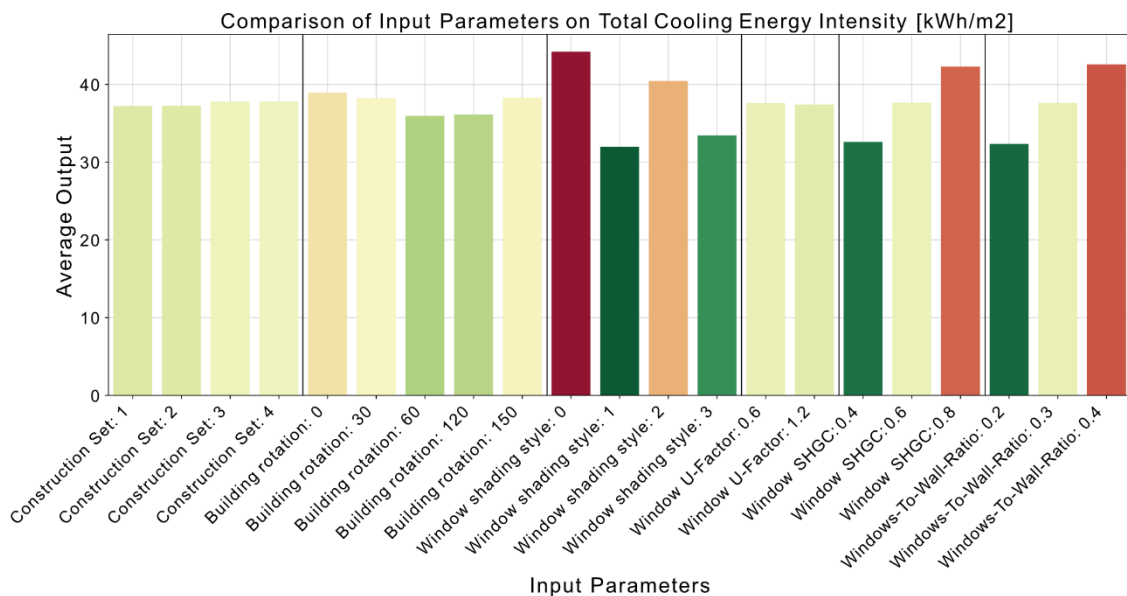
Figure 42 Average indicator values of unique parameter values - Total Cooling Energy Demand
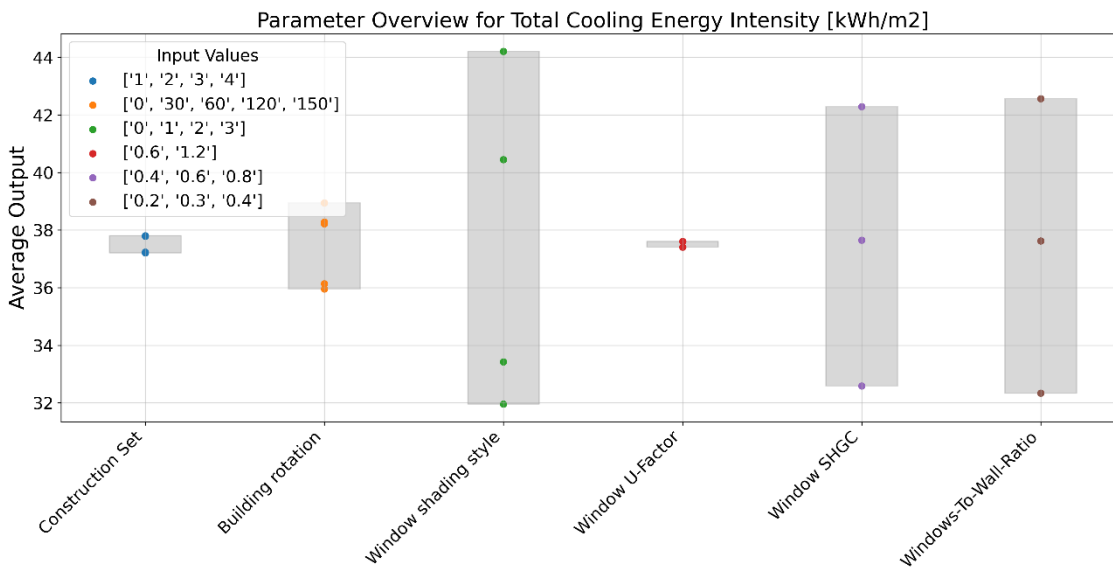
Figure 43 Overview of differences between average indicator values for parameter values - example plot

The sensitivity analysis of both IE1 and IE3 indicators has confirmed that the most influential parameter is the window shading style, followed by windows-to-wall-ratio and the selection of solar heat gain coefficient of the glass. The relative influence of each parameter is depicted in a pie chart (Figure 44), with specific values detailed in Annex 9. The sensitivities were calculated according to the previously described method and confirm the predictions inferred from of the bar charts.
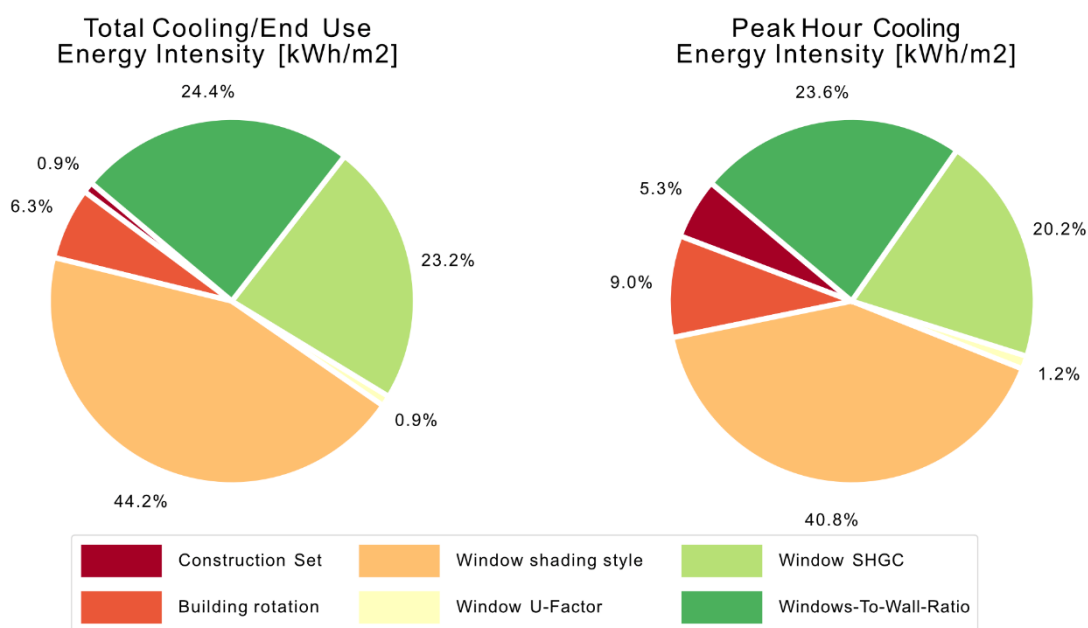
Figure 44 Ratio of sensitivity of indicators on the change of selected parameter values

4.2.3. Heatmaps as Decision-Making Aid

Last but not least, heatmaps were plotted to aid design decisions, particularly when one of the selected parameters is predetermined. The heatmaps, as depicted in Figure 45 present the optimal selection of other parameters to minimize the total cooling energy intensity in the two hottest months for selected building rotations. This is only an example of the method for highlighting effective parameter combinations, thereby providing a valuable tool for designers aiming to optimize the building performance under specific constraints.
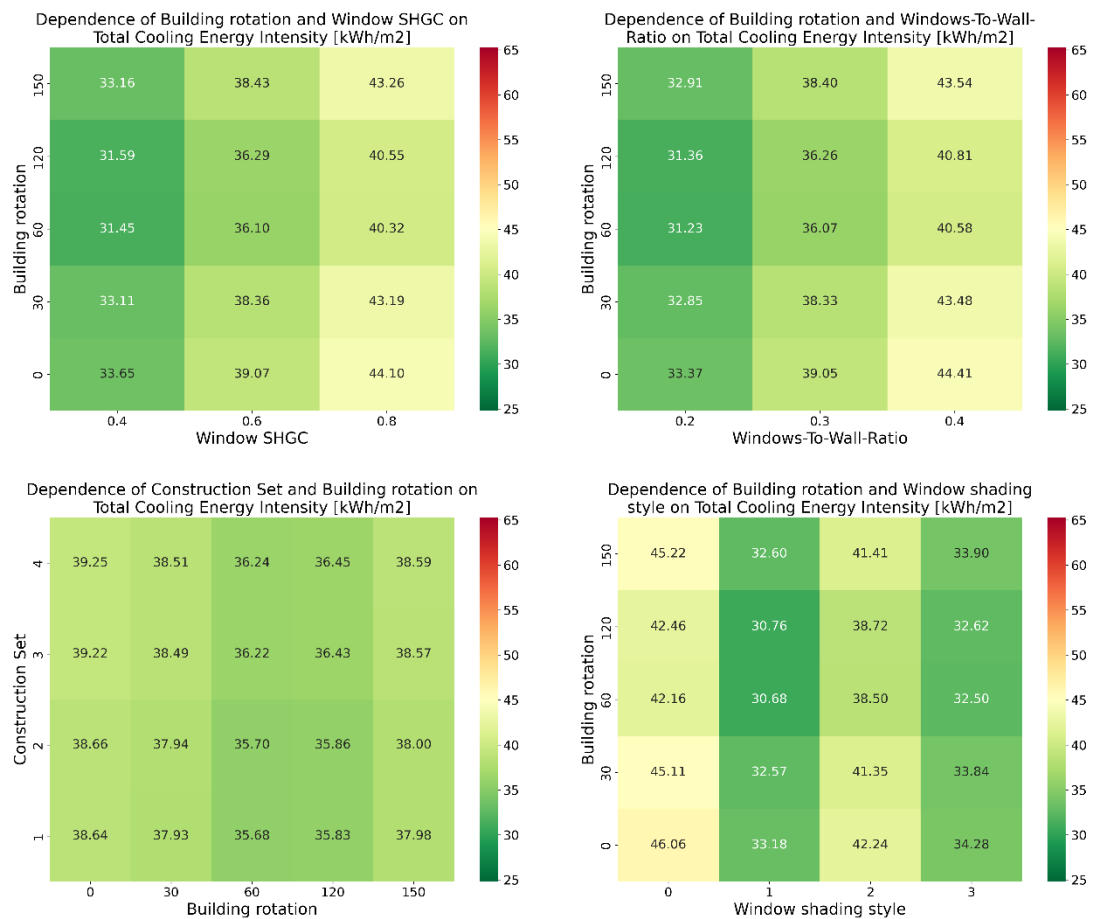
Figure 45 Heatmaps presenting dependencies between pairs of parameters: example of total cooling energy demand dependent on building rotation and a) window SHGC, b) window U-Factor, c) window-to-wall-ratio and d) window shading style.

4.3. Thermal Comfort Simulation Results

Similarly, the results from all 1440 simulations focusing on thermal comfort in scenarios involving natural ventilation were examined. The visualizations generated by Ladybug Plots indicate that under extreme heatwave conditions, none of the building variants could achieve a level of thermal comfort that would qualify them as fully resilient to a heatwave. However, these simulations do reveal varying degrees of performance among the building designs. This suggests that in the case of providing them with air conditioning systems, some designs can be better at maintaining a less hostile environment for occupants during power outages, when those systems are not operational.

4.3.1. Analysis of Individual Variants

The scattered plots revealed interesting insights about the distribution of indicator values across the building variants. The selected indicators of thermal comfort did not typically exhibit a linear dependency, leading to more diverse results and challenging comparisons thereof. The most linear relationship was noted between IC2 (Average Temperature Difference Outdoor-Indoor) and IC3 (Maximum Average Operative Temperature), as depicted in Figure 46.

Other indicator relations, however, resembled various forms of power functions. The relationship between average temperature difference outdoor-indoor (IC2) and heat sensation percent (IC4) plot (see Figure 47) and the correlation between Number of hot hours (IC1) and Maximum Average Operative Temperature (IC3) (Figure 48) are examples of those.

The marginal histograms of the former plot, in particular, reveal that for a significant portion of the dataset (85%) experienced indoor conditions are hotter than comfortable for 90% of the time or more (1222 out of 1440 variants).

The latter plot illustrates, that that in scenarios where every hour was hot, interior temperatures, in the worst cases, could exceed 50°C in peaks, making it impossible for humans not only to feel comfortable but to live inside. This was the case for 940 parameter configurations. Conversely, only 8 configurations could provide comfortable temperatures for at least 10% of the time.

Comparison of Average Temperature Difference Outdoor-Indoor and Maximum Average Operative Temperature
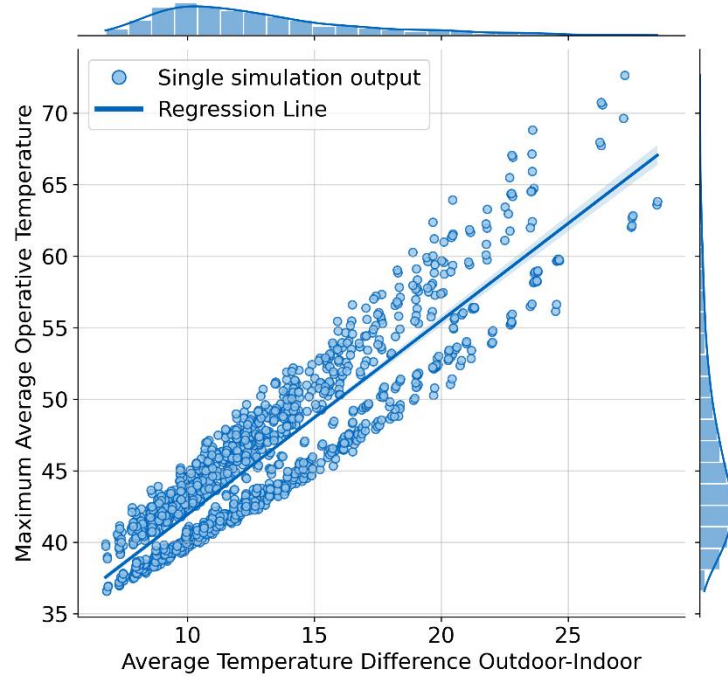
Figure 46 Scattered plot and linear regression for the IE2 and IE3

Comparison of Average Temperature Difference Outdoor-Indoor and Average HSP
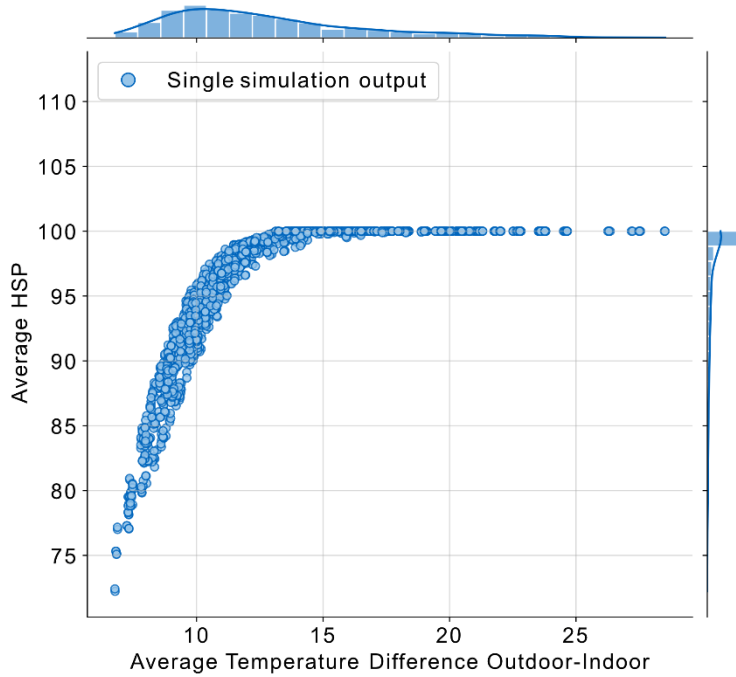
Figure 47 Scattered plot for the relation between IC2 and IC4
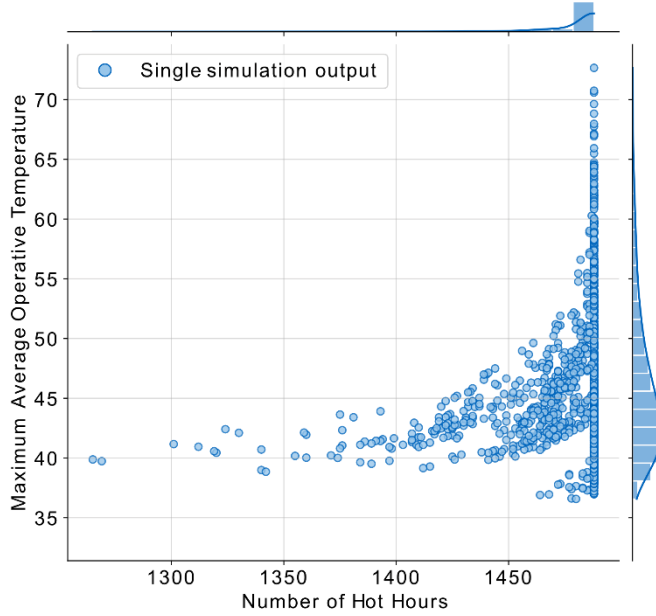
Figure 48 Scattered plot for the relation between IC1 and IC3

The extreme values have been presented in Table 10, while the average indicator values for each parameter's unique value can be found in the Annex 6 to this thesis.

Table 10 Extreme values for the thermal comfort indicators and corresponding parameter sets

	Value	P1	P2	P3	P4	P5	P6
out:Number of hot hours							
Lowest	1265	4	60	1	1.2	0.4	0.2
Highest	1488 (max)	Many					
out:Average Temperature Difference Outdoor-Indoor							
Lowest	6.768822	4	120	1	1.2	0.4	0.2
Highest	28.518329	2	0	0	0.6	0.8	0.4
out:Maximum Average Operative Temperature							
Lowest	36.57319	1	120	1	1.2	0.4	0.2
Highest	72.656529	4	0	0	0.6	0.8	0.4
out:Average HSP							
Lowest	72.231411	4	60	1	1.2	0.4	0.2
Highest	100	Many					

A deeper examination of the best-performing variants revealed that their designs facilitated heat storage within the thermal mass and enabled effective nighttime cooling, thereby balancing indoor temperatures. Figure 49 presents an hourly plot of the average operative temperature inside the best-performing variant for IC3. The temperatures fluctuate between 28 and 36°C without exceeding 40°C. Comparing these values with the data previously presented in Figure 21 on page 66 (Hourly temperatures for the scenario RCP8.5 of the year 2100 in Bamberg), the differences can be calculated. Those were plotted on the chart in Figure 50.
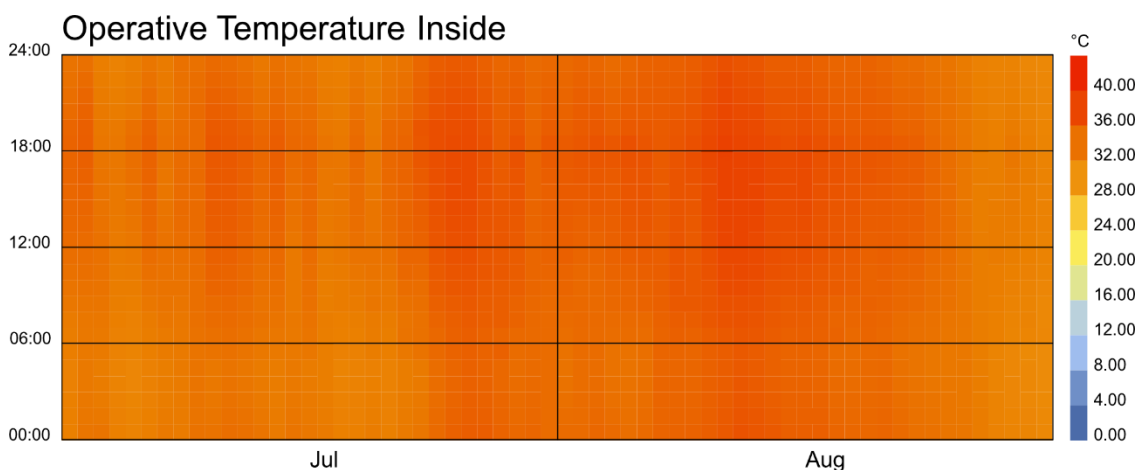
Figure 49 Operative temperature inside the best-performing variant of the building in IC3 indicator
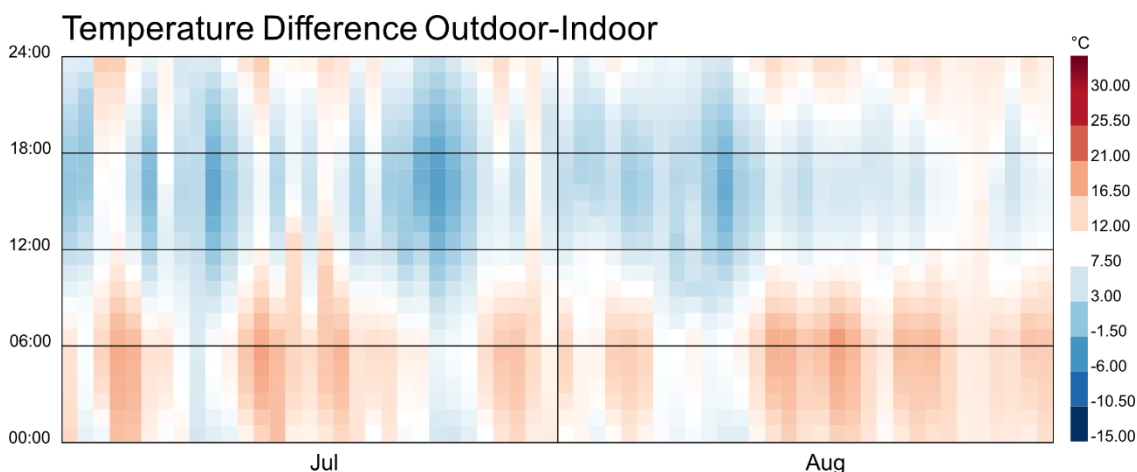
Figure 50 Temperature difference between indoor and outdoor conditions in the best-performing variant of the building in IC3 indicator

4.3.2. Dataset Evaluation and Sensitivity Analysis

After calculating the average indicator values for each unique parameter value, further insights could be found in this set of simulations. These averages are listed in the Annex 6 to this thesis. As every indicator presented different outcomes, the IC3 Maximum Average Operative Temperature indicator was chosen as the most representative for this section of the chapter.

The bar plot presented in Figure 51 and composite bar plots in Figure 52, provided concrete information for evaluating the impact of various parameters on this indicator. As expected, the variant with no shading devices performed much worse than any other variant, independent on the building rotation, construction, and other properties, reaching an average value of 50.29°C as the highest whole-floor average. Additionally, the louver shades (average 42.44°C) and the external roll screen (average 42.55°C) were markedly more effective than the overhang option (average 47.97°C). The Window Solar Heat Gain Coefficient (SHGC) and the Window-to-Wall Ratio also appeared to have significant impact, while the Construction Set, though relevant, had a somewhat lesser impact, with the set-ups P1=[1] and [2] performing the best and [4] the worst. The building rotation and the window U-factor were the least significant parameters.
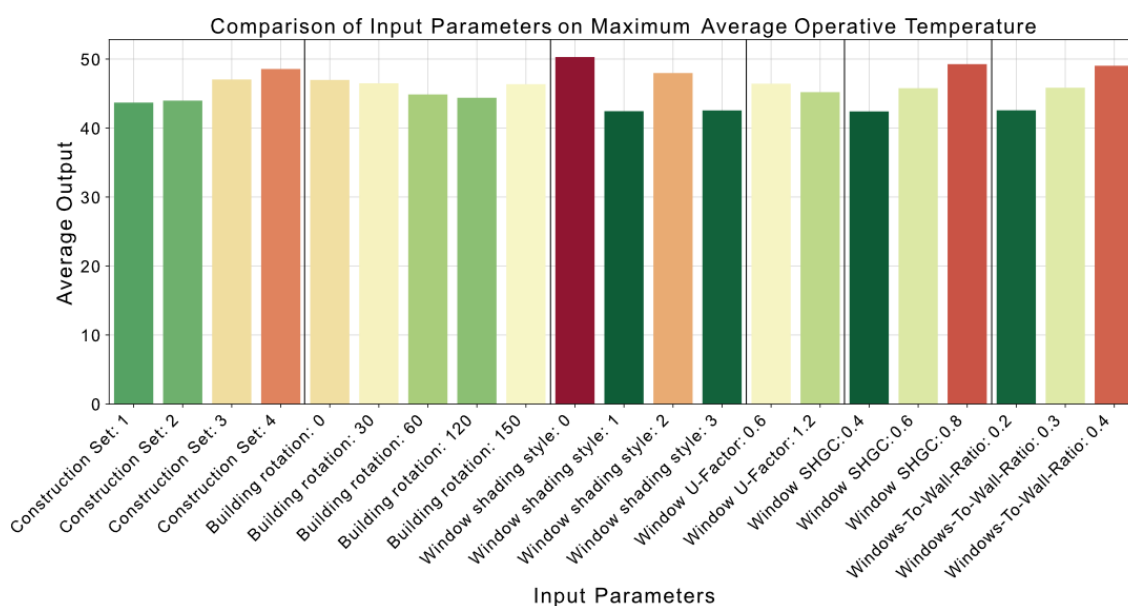
Figure 51 Bar plot of all unique parameter value averages for one indicator - example of Average Operative Temperature
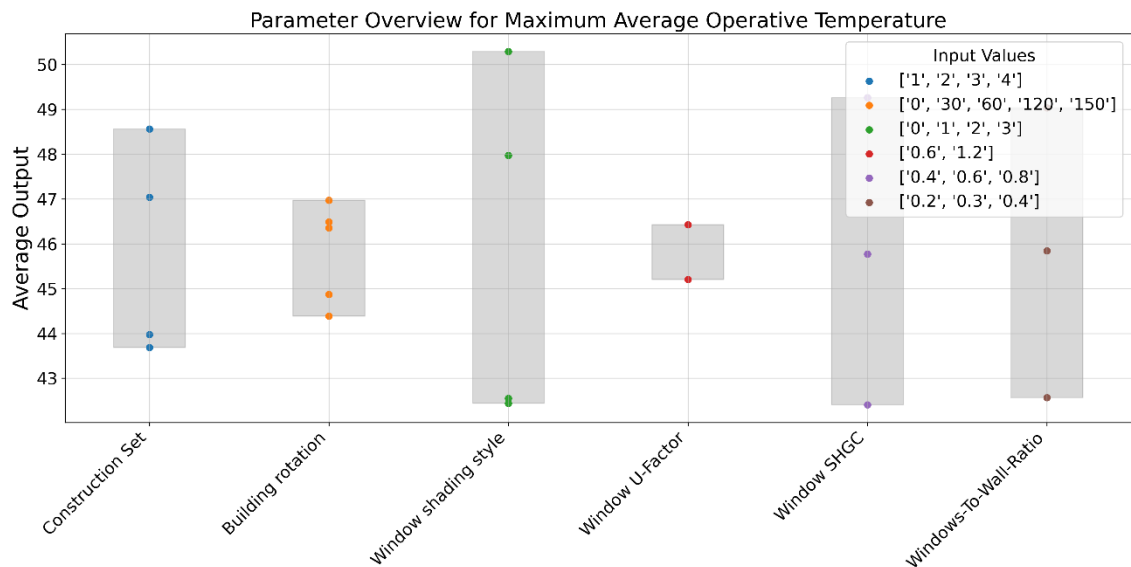
Figure 52 Composite bar plot presenting average unique parameter values grouped by parameters

The sensitivity analysis, represented in the pie charts in Figure 53, and detailed in Annex 10, reveals that while the relative importance of parameters fluctuates across different indicators, their general order of influence remains fairly consistent. The significance of the Construction Set becomes more evident in relation to the Number of Hot Hours, possibly due to its effect on the building's thermal mass and insulation properties.

Nevertheless, it is crucial to acknowledge that none of the variants analyzed can be called future-proof. The inevitable conclusion drawn from this chapter is that under the future climate scenario RCP8.5, all buildings will require mechanical conditioning to provide adequate protection against heatwaves.

Number of hot hours

17.2%
8.5%
19.2%
4.3%
31.9%
18.8%

Average Temperature Difference Outdoor-Indoor

18.1%
1.4%
6.1%
21.7%
12.1%
40.6%

Maximum Average Operative Temperature

19.1%
20.3%
9.6%
6.7%
7.2%
37.1%

Average HSP

16.9%
20.3%
4.0%
6.3%
13.5%
39.1%

Construction Set	Window shading style	Window SHGC
Building rotation	Window U-Factor	Windows-To-Wall-Ratio
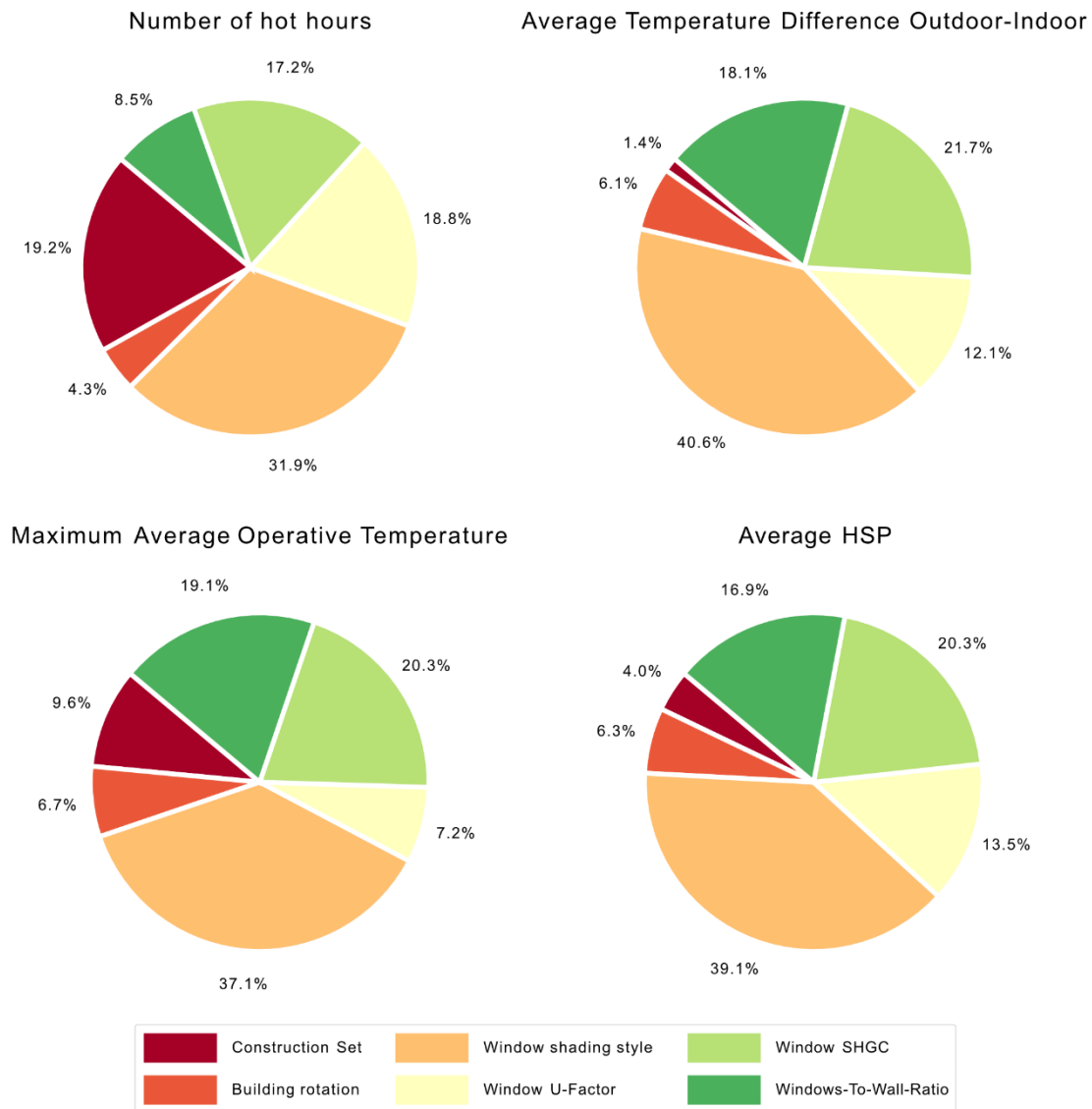
Figure 53 Sensitivity of parameters influencing thermal comfort

4.4. Thermal Comfort Simulation Results for Sustainability Scenario

Following the conclusion that none of the building variants would be able to provide comfortable conditions in the worst-case future scenarios for the year 2100, the focus shifted to evaluating performance under a more optimistic 'sustainability' scenario. The EPW value in the RCP scenario 8.5 was exchanged with 2.6, and the same simulations and analyses were repeated.

As can be seen in Figure 54, the outdoor temperatures in this scenario are much lower, and the extreme hot days are less frequent and interwoven with milder days with outdoor temperatures not exceeding 25°C. These conditions potentially give building elements sufficient time to cool down.
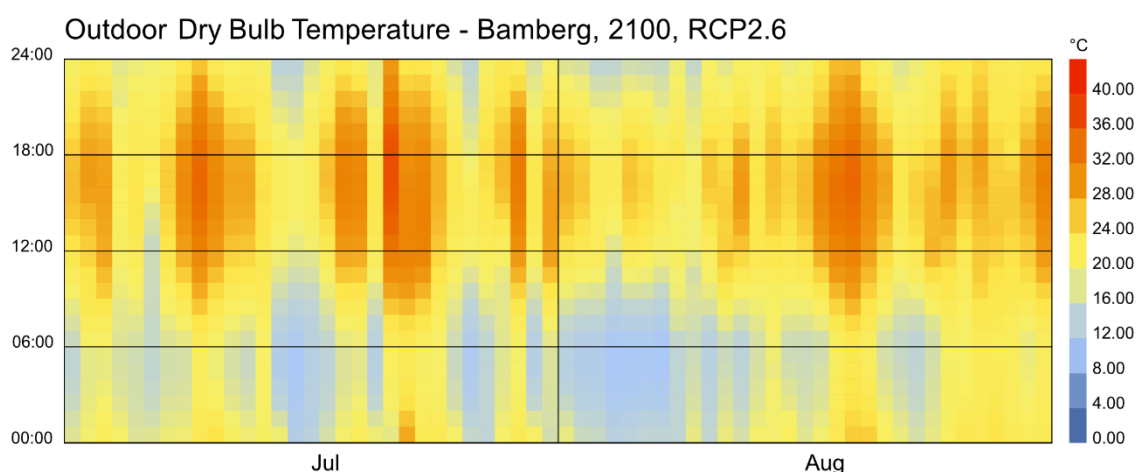
Figure 54 Hourly dry bulb temperatures in the sustainability scenario

4.4.1. Analysis of Individual Variants

As expected, in the more positive future scenario, in some of the variants it was possible to provide enough protection against overheating (see Figure 55). The average indicator values for each unique parameter setting are detailed in Annex 7, while the extremes are listed in Table 10. Although these values differ from those in Chapter 4.3 (Thermal Comfort Simulation Results), the configuration of the best and worst-performing variants largely remains consistent (compare to Annex 6 and Table 10).
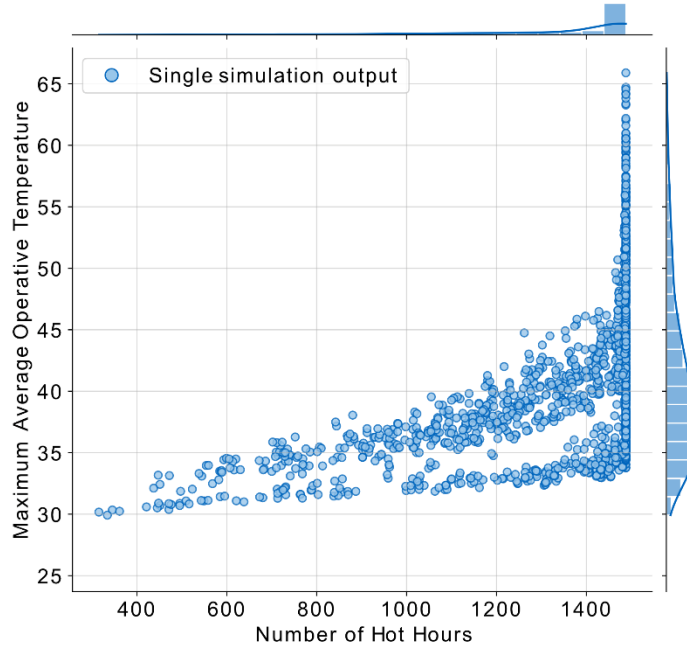
Figure 55 Scattered plot for the comparison of the construction sets for the Maximum Average Operative Temperature and the Number of Hot Hours indicators

Table 11 Extreme values for the thermal comfort indicators and corresponding parameter sets

	Value	P1	P2	P3	P4	P5	P6
out:Number of hot hours							
Lowest	315	1	60	1	1.2	0.4	0.2
Highest	1488 (max)	Many					
out:Average Temperature Difference Outdoor-Indoor							
Lowest	6.893	1	60	1	1.2	0.4	0.2
Highest	27.303	2	0	0	0.6	0.8	0.4
out:Maximum Average Operative Temperature							
Lowest	29.92	1	120	1	1.2	0.4	0.2
Highest	65.894	4	0	0	0.6	0.8	0.4
out:Average HSP							
Lowest	5.52	1	60	1	1.2	0.4	0.2
Highest	100	Many					

In this scenario, the maximum interior temperatures were, on average, over 5°C lower than in scenario 8.5. The average number of uncomfortably hot hours decreased in this scenario by about 150. While for 572 variants it was still not possible to provide any comfortable hours, 496 configurations offered more than 10% of comfortable hours, with 80 configurations in which half of the time was marked as comfortable. The Heat Sensation Percent decreased by almost 14 percentage points.
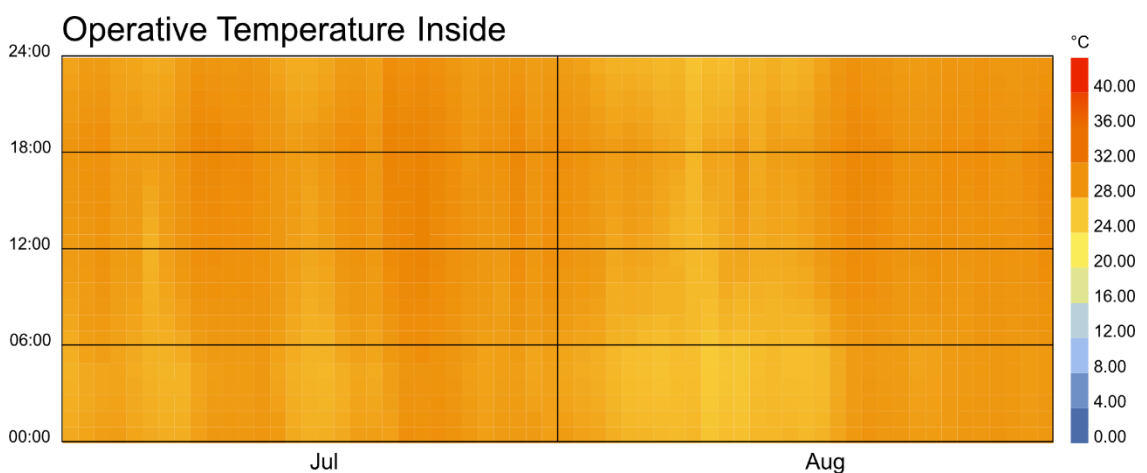
Figure 56 Operative temperature hourly plot for the best performing wariant in IC3

Figure 56 illustrates the conditions on the top floor of the best-performing variant in terms of the IC3 (Maximum Average Operative Temperature) indicator. The parameters defining this variant are: P1[1]=0, P2[3]=120, P3[3]=3, P4[1]=1.2, P5[0]=0.4, P6[0]=0.2. The temperature outside as presented in Figure 54, fluctuates between 16 and 40 degrees Celsius during the day and drops to as low as 8 degrees Celsius during the night. Inside the building however, as depicted in Figure 56, the values remain between 24 and 32 degrees Celsius. For 62,5% of the analysis period of July and August most of the building provided comfortable, neutral thermal conditions, while during 37,5% of the hours made at least 20% of the top floor area was uncomfortably hot.

4.4.2. Dataset Evaluation and Sensitivity Analysis – Comparison with the RCP8.5 Scenario

The analysis of parameter influence shows similarities to the previous set of simulations (compare Figure 51 and Figure 57, as well as Figure 53 with Figure 60). As described previously, the choice of shading devices had the greatest influence on the design's

thermal comfort performance, meaning that variants not equipped with shading devices rendered the worst outcomes, and using a 0.5 m long overhang was still not sufficient to provide enough shade and protection from the sun. The versions with louvers and external rolls appeared to be the best performing ones. The window properties, specifically SHGC and window-to-wall-ratio, remained more influential than building rotation or material selection.
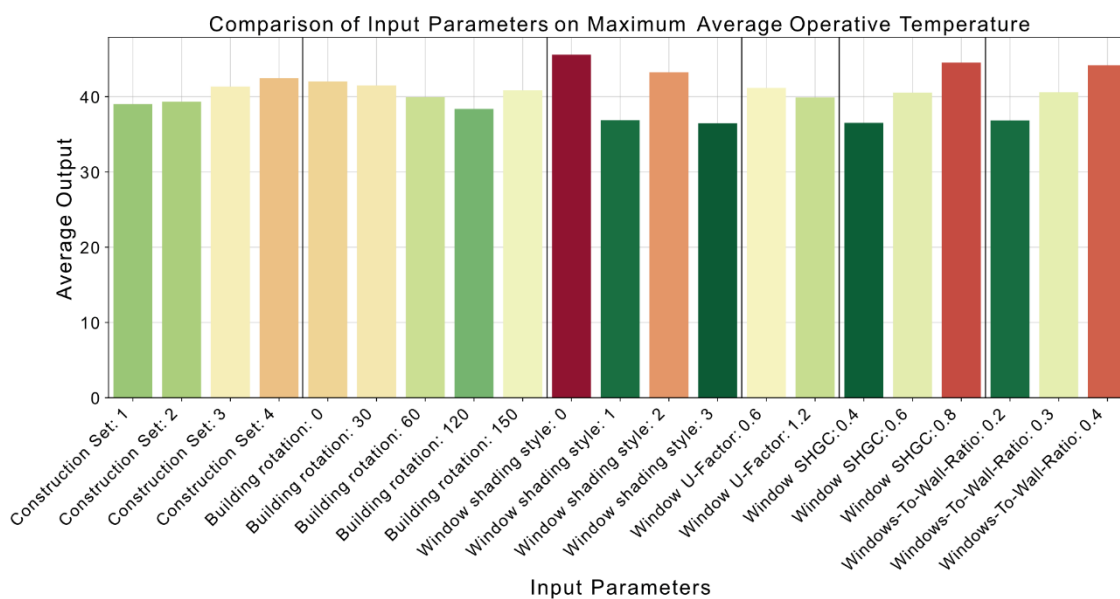
Figure 57 Average values of the Maximum Average Operative Temperature indicator for particular parameter values

Despite slight variations in sensitivity, the ranking from worst to best choice remains constant across scenarios, as illustrated in Figure 58 and Figure 59. These figures juxtapose the changes in average IC3 and IC1 values across parameter values between RCP8.5 and RCP2.6, with connecting lines emphasizing the consistency in ranking order. This finding suggests that similar design decisions are applicable across both future scenarios and potentially other "moderate" scenarios not yet analyzed.
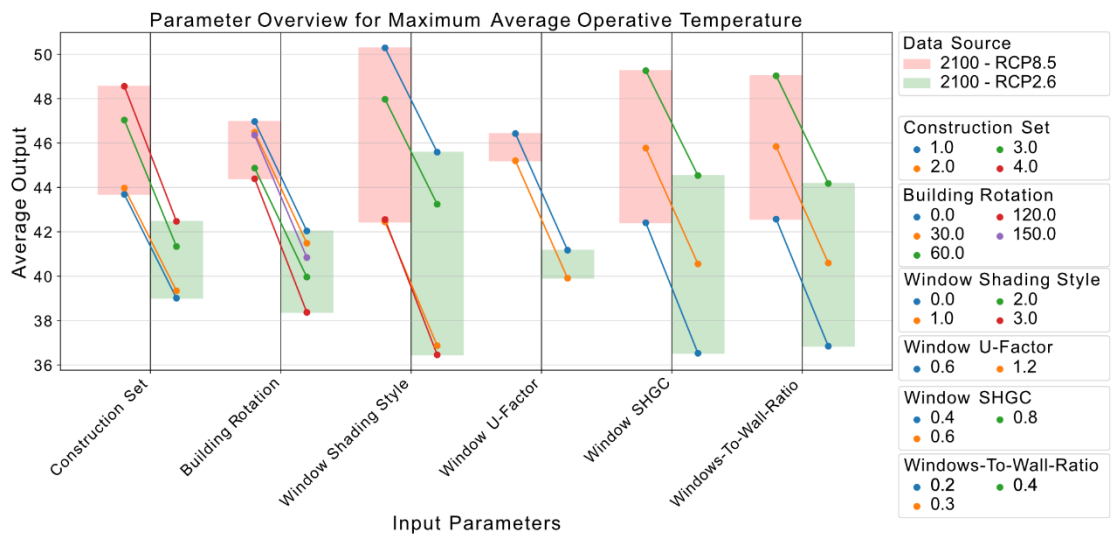
Figure 58 Change of the average IC3 value across the parameter values between scenarios RCP8.5 and RCP2.6
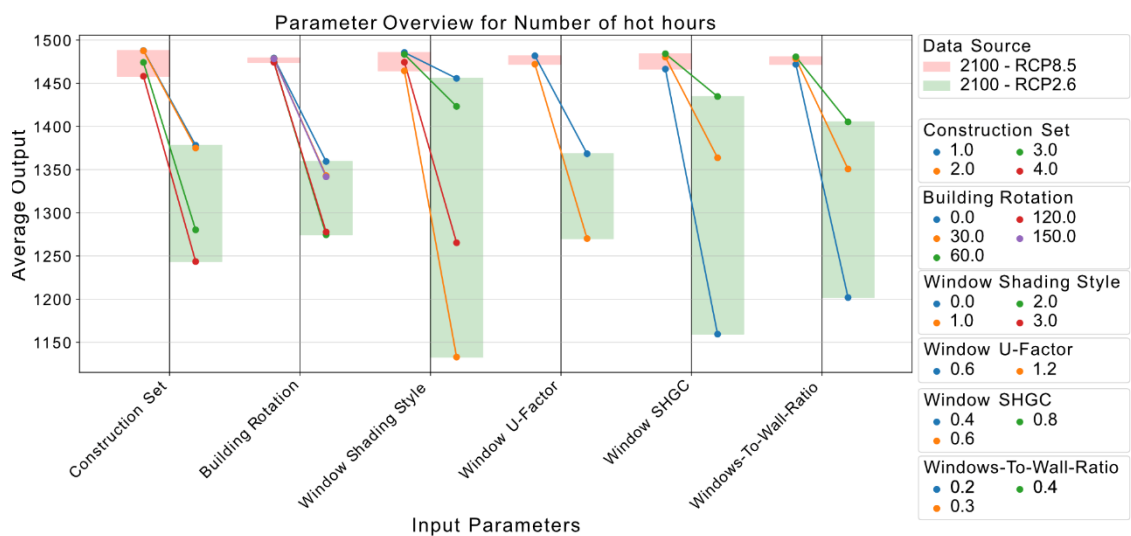
Figure 59 Change of the average IC1 value across the parameter values between scenarios RCP8.5 and RCP2.6

Comparing normalized sensitivities, visible in Figure 48, with the same representation of the previous simulation results (Figure 53 on page 102, also Annex 10 and Annex 11 - Summary of sensitivities Thermal Comfort simulation results), it is evident that sensitivities are more consistent across indicators in the RCP2.6 scenario. Unlike in RCP8.5, where the Construction Set (P1) parameter had a significant impact (19.2%) on IC1 (Number of Hot Hours), in RCP2.6, it only accounted for 6.6% of the influence

on this indicator. This observation underlines the importance of considering different climate scenarios in designing for thermal comfort.

Nevertheless, the main finding from this analysis remains the prevalent consistency of parameter unique values ranking among the scenarios. This consistency is a notably positive outcome, suggesting that a design optimized for one future scenario is likely to be well-suited for alternative future projections, considering the analyzed parameters and their respective values.
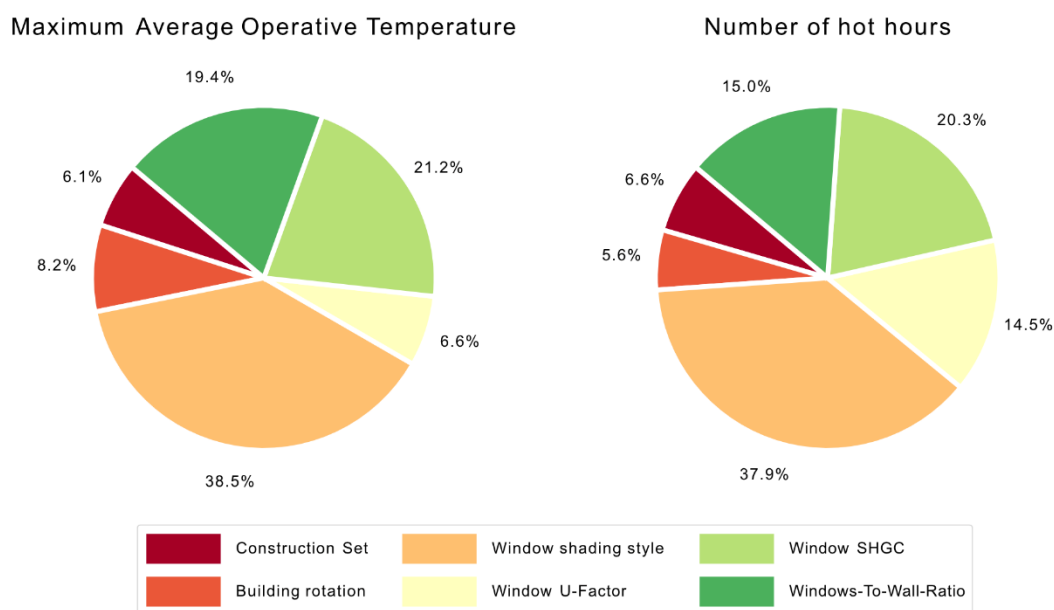
Figure 60 Sensitivity of parameters influencing thermal comfort in sustainability scenario RCP2.6

4.5. Comparison Between two Ventilation Scenarios

The assessment of parameter sensitivities in building design, particularly under various future scenarios and diverse indicators, is dependent on whether the building will be mechanically conditioned. The comparison of indicator values would require assigning appropriate weights to particular indicators, so as to "normalize" them with respect to their outcomes. However, what can be effectively compared are the sensitivities calculated according to the methodology defined in this study.

Figure 61 accumulates the results from chapters 4.2-4.4, encompassing both energy performance and thermal comfort outcomes, with the latter considering both RCP2.6 and RCP8.5 scenarios. This figure compounds the sensitivities previously illustrated as pie charts into bar plots, facilitating an easier visual comparison. A notable observation from this visualization is the relative consistency in the influence level of parameter values across all indicators. The choice of Window Shading Style (P3) emerges as a critical design decision for enhancing heatwave resilience and climate adaptability. In contrast, the Building Rotation (P2) and, especially, the Construction Set (P1) parameter demonstrate less impact compared to factors like the Window-to-Wall Ratio (P6) or the Solar Heat Gain Coefficient (SHGC) of the glazing (P5).

Understanding these nuances is instrumental in prioritizing early-design decisions. Focusing on the most impactful aspects of the design allows for a more efficient allocation of resources, freeing designers from the constraints imposed by parameters that have less influence on resilience. Parameters such as building rotation or predefined material sets, while important from the design perspective, may not significantly contribute to the building's resilience and thus can be selected more freely in the early stages of design development.
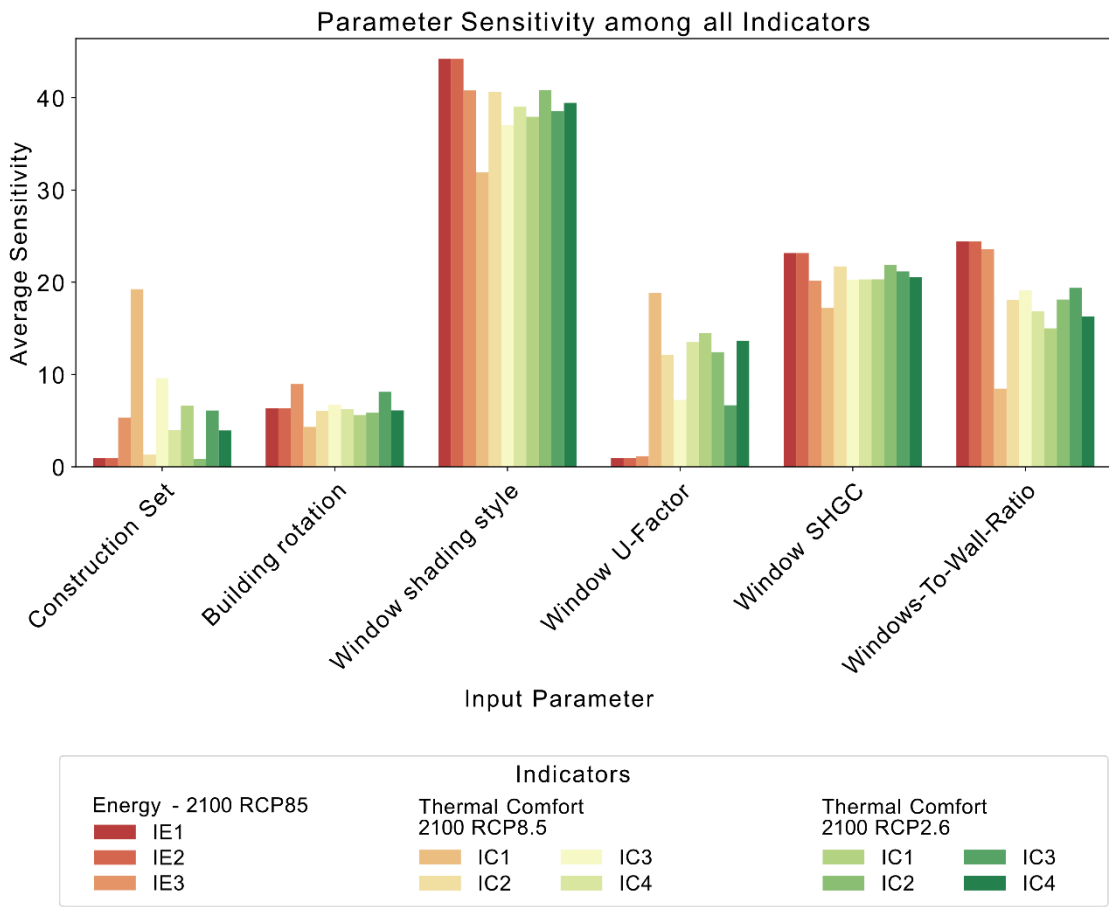
Figure 61 Comparison of sensitivities for all the indicators

4.6. Influence of the Natural Ventilation Through Windows

Chapters 4.3 (Thermal Comfort Simulation Results) and 4.4 (Thermal Comfort Simulation Results for Sustainability Scenario) demonstrated that buildings without mechanical conditioning may not be able to provide adequate thermal comfort during heatwaves or exceptionally hot summers. The worst-case scenario for the year 2100, represented by RCP8.5, rendered all design variants insufficiently protective. In contrast, in the more optimistic RCP2.6 scenario for the year 2100, some designs showed improved performance, though not consistently achieving desired comfort levels.

This chapter employs the same methodology as the preceding ones but is focused on parameters related to ventilation control, thereby integrating passive cooling into the model. To assess the impact of natural ventilation and analyze various ventilation strategies during heatwaves, a new series of simulations was conducted. These simulations incorporated the previously described model and selected the worst-performing parameter values from both scenarios, specifically in terms of maximum average operative temperature on the building's top floor. These parameters included:

- P1 Construction Set: 4
- P2 Building Rotation: 0
- P3 Window Shading Style: 0 (no shading)
- P4 Window U-Factor: 0.6
- P5 Window SHGC: 0.8
- P6 Window-to-Wall Ratio: 0.4

The output indicators for the natural ventilation simulations remained consistent with prior settings.

A "moderate" future scenario, RCP4.5 for the year 2100 (as provided by the Meteonorm tool), was selected for these simulations. Given the similar sensitivity of parameters in both scenarios, this scenario served as a moderate case study. Figure 62. illustrates the Dry Bulb Temperature for this year, highlighting the variability between milder days and extreme heat periods, where temperatures can exceed 36°C. Nighttime temperatures typically fall below 20°C, although they remain higher following exceptionally hot days. These observations suggest that nighttime cooling may prove to be effective. This

chapter aims to analyze this hypothesis and identify the most efficient strategies among the simulation set-ups.
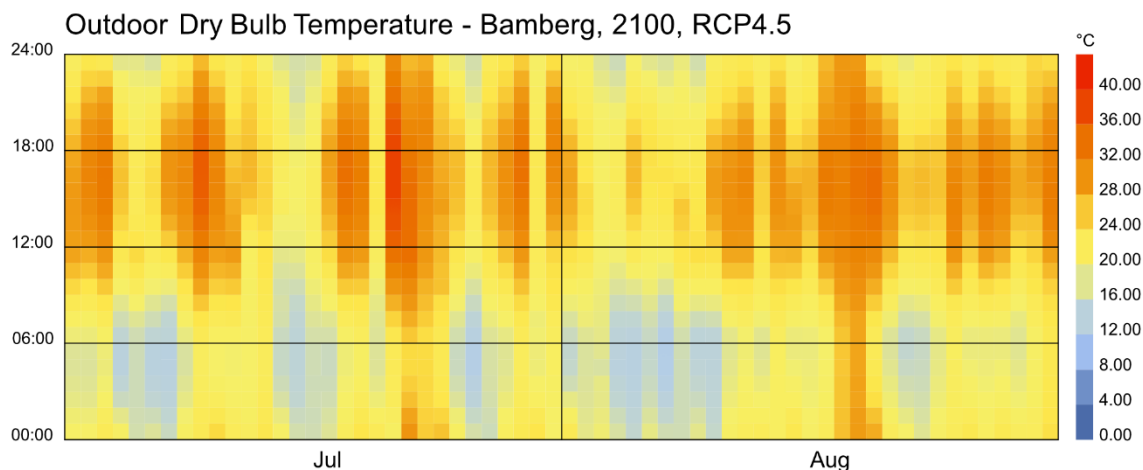
Figure 62 Outdoor Dry Bulb Temperature in Scenario RCP 4.5 for the Year 2100

4.6.1. Selection of Natural Ventilation Parameters

Modifications to natural ventilation through window openings were primarily adjusted using the 'HB Window Opening' component in Honeybee-Energy. This component introduces 'ZoneVentilation' to the model, accounting for both single-sided ventilation (mainly buoyancy-driven stack ventilation from temperature differentials) and cross-ventilation (wind-driven ventilation).

The new set of parameters, with their values (including default values used previously), evaluated for this simulation is presented in the Table 12. The values -100 and 100 were used to represent no temperature limit.

Table 12 Parameters and their tested values influencing the simulation with Ladybug Tools (NVP = Natural Ventilation Parameter)

Component	No	Parameter Name	Values	Description
HB Ventilation Control	NVP1	Min Indoor Temp	[0] -100[def], [1] 20, [2] 25	Minimum and maximum **indoor** temperature when windows can be open
	NVP2	Max Indoor Temp	[0] 30, [1] 100[def] [2] 35	
	NVP3	Min Outdoor Temp	[0] -100[def], [1] 15, [2] 20	Minimum and maximum **outdoor** temperature when windows can be open

	NVP4	Max Outdoor Temp	[2] 25 [0] 30, [1] 100[def]	
	NVP5	Delta Temperature	[0] -100[def], [1] 0, [2] 5	Windows are closed, when reached
HB Constant Schedule	NVP6	Schedule Number	[0] S0(24h), [1] S1(20-6), [2] S2(1h+1h)	Series of true-false hourly data if opening is possible
HB Window Opening	NVP7	Cross-ventilation	[0] True [1] False	True if cross-ventilation is possible
	NVP8	Window Obstructions	[0] 0.40, [1] 0.65 (unobstructed)	Insect screens (0.45=def) and other obstructions
		In total N=	2916	Model variants to be simulated

The selection of these parameters was based on four constraints:

Temperature: NVP1-NVP5 – These parameters involve internal and external temperatures and the difference between them. The natural ventilation and air exchange through windows may be constrained by temperature, encompassing both manual window operations and automated window opening based on temperature sensor value readouts. The aim is to determine which temperature-based strategies are most effective, as well as their actual influence. Selected values include software defaults and realistic temperature constraints for this scenario.

Schedule: NVP6 – This parameter concerns natural ventilation according to a predefined schedule. Although Ladybug Tools' schedules can be influenced by various factors, including temperature, activity level, or power (*HB-Energy Primer*, n.d.), this study opted for a simple On-Off limitation. Three schedules were evaluated to distinguish different window opening patterns:

- S0 – when there is no window opening possible,
- S1 – in which the windows can be open throughout the night, from 20:00 till 5:00,
- S2 – where the windows can be open for one hour in the evening (at 22:00) and for one hour in the morning (at 6:00).

Cross-ventilation: NVP7 defines if cross ventilation is possible. The relevance of this parameter is, however, questionable in case of the shoebox model.

Obstructions: NVP8 defines the obstructions of air movement. By default, it is set to 0.45, representing a window with an insect net. For testing, two parameter values were chosen: a slightly more "obstructing" parameter 0.4, as well as a value of 0.65, representing no obstruction to the air flow (*HB-Energy Primer*, n.d.).

The Grasshopper definition could be easily updated with the new set of parameters, introduced with the second instance of Colibri Iterator (see Figure 63). The previous parameters were then "hard-coded" using Grasshopper Panels to ensure the correct values were applied.
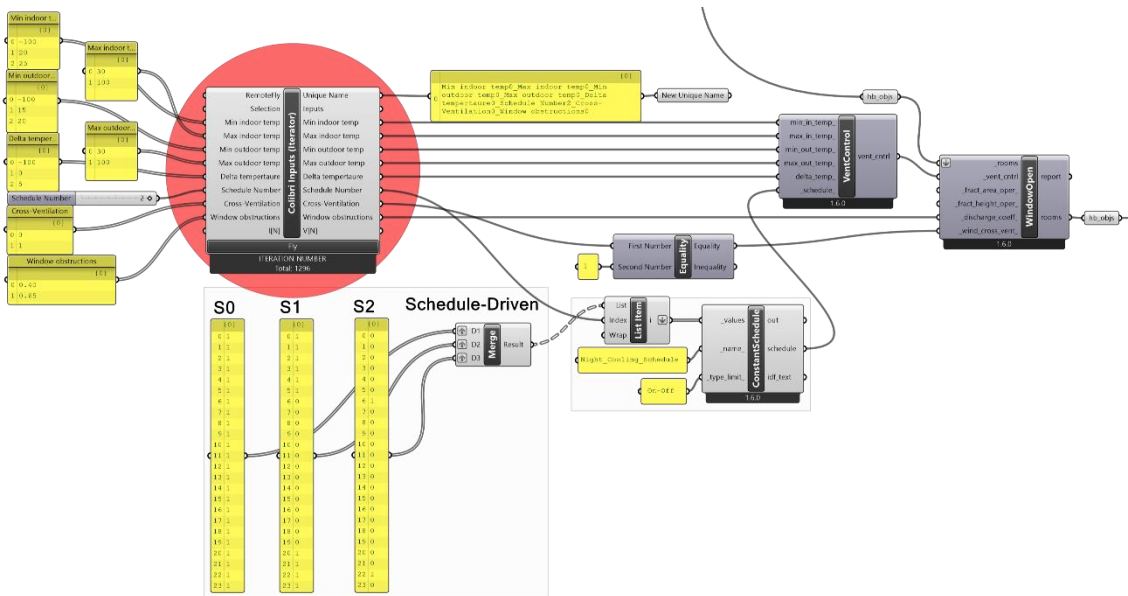
Figure 63 Changes introduced to the original Grasshopper definition to test the natural ventilation strategies

4.6.2. Dataset Evaluation and Sensitivity Analysis – Natural Ventilation Strategies Simulation

After running 2916 simulations, the data was visualized and analyzed in the way described in the Methodology chapter of the thesis. As expected, the results showed a high variance in all the indicator values, suggesting significant influence of natural ventilation strategies. Figure 64 displays this variety on an example scattered plot.

Figure 64 Scattered plot of the simulation outcomes for the Number of Hot Hours and maximum Average Operative Temperature

As was done previously, the average indicator values for every unique parameter value were calculated and presented on bar plots, including the one in Figure 65. Those averages for all indicators can be found in Annex 8.
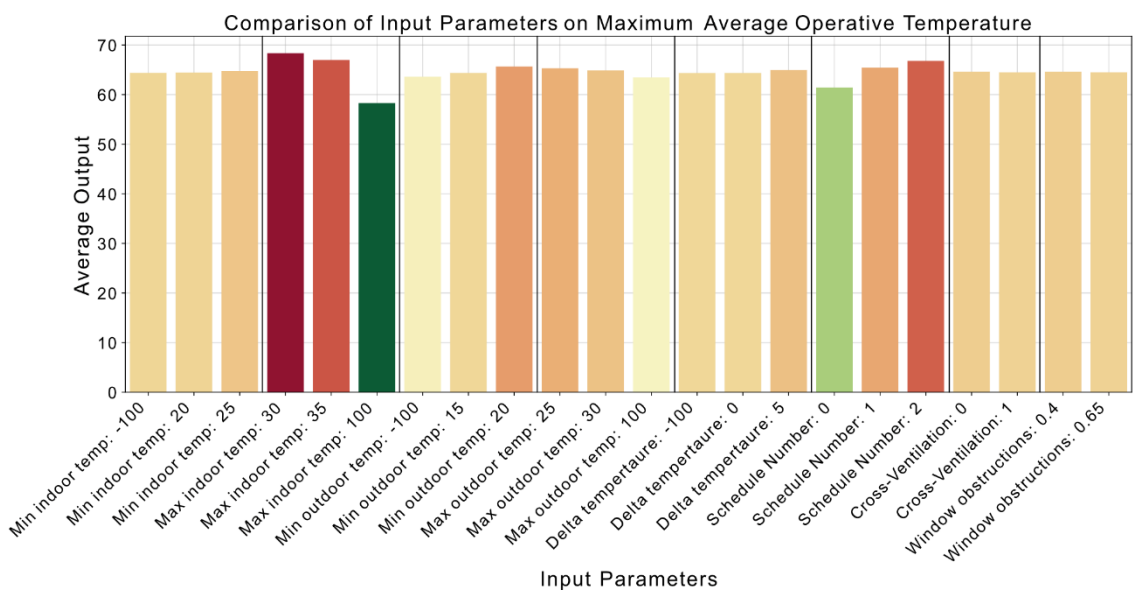
Figure 65 Average IC3 values for unique parameters in the natural ventilation scenario

The analysis of the plots provided several insightful observations. These findings are detailed below one by one for clarity.

Selecting a minimal value of the indoor temperature at which the windows can be open (NVP1) is important in colder periods. It was decided to test this regardless, in order to analyze the potential influence of a building user, who does not want to open windows when temperatures outside are too cool. The default value of -100°C (indicating no limit) showed slightly better outcomes compared to a 25°C limit, with a negligible difference when the limit was set to 20°C. This suggests that extensive nighttime cooling, even to the point of discomfort for some, does not significantly impact overall thermal comfort across the range of results.

Conversely, the strategy of determining a maximum indoor temperature for window operation (NVP2) emerged as a critical parameter, being either the most or second most influential variable depending on the selected analyzed indicator and implying that there should ideally be no upper temperature limit for opening windows.

When considering outdoor temperatures, the findings vary. Setting a minimum outdoor temperature for window operation (NVP3) significantly affects the number of hot hours and the average HSP yet does not substantially influence the maximum average operative temperature indoors.

In contrast, the maximum outdoor temperature (NVP4) had minimal impact on the indicators, meaning that window operability based on outdoor temperatures might extend periods of excessive indoor heat without significantly affecting the peak indoor temperatures reached.

The Delta temperature parameter (NV5), which defines the indoor-outdoor temperature difference for closing windows, surprisingly showed minimal influence across all indicators. A setting of 0°C did not notably differ from the default value of -100°C, suggesting that these settings are functionally equivalent. The value of 5°C only marginally affected certain indicators, such as the average HSP.

Schedule-driven natural ventilation (NV6) was found to be highly influential, either the most or second most, depending on the indicator. Allowing windows to be operational throughout the day proved significantly more effective than restricting their use to specific times, such as between 20:00-06:00 and for an hour each in the evening and

morning. Surprisingly, the second scenario was closer to the third in terms of the outcome.

Parameters NV7 (Cross-ventilation) and NV8 (Window Obstructions), however, demonstrated a negligible impact on cooling effectiveness. This might be due to the limitations of the simulation model, which was a simplified 'shoebox' model without interior walls.
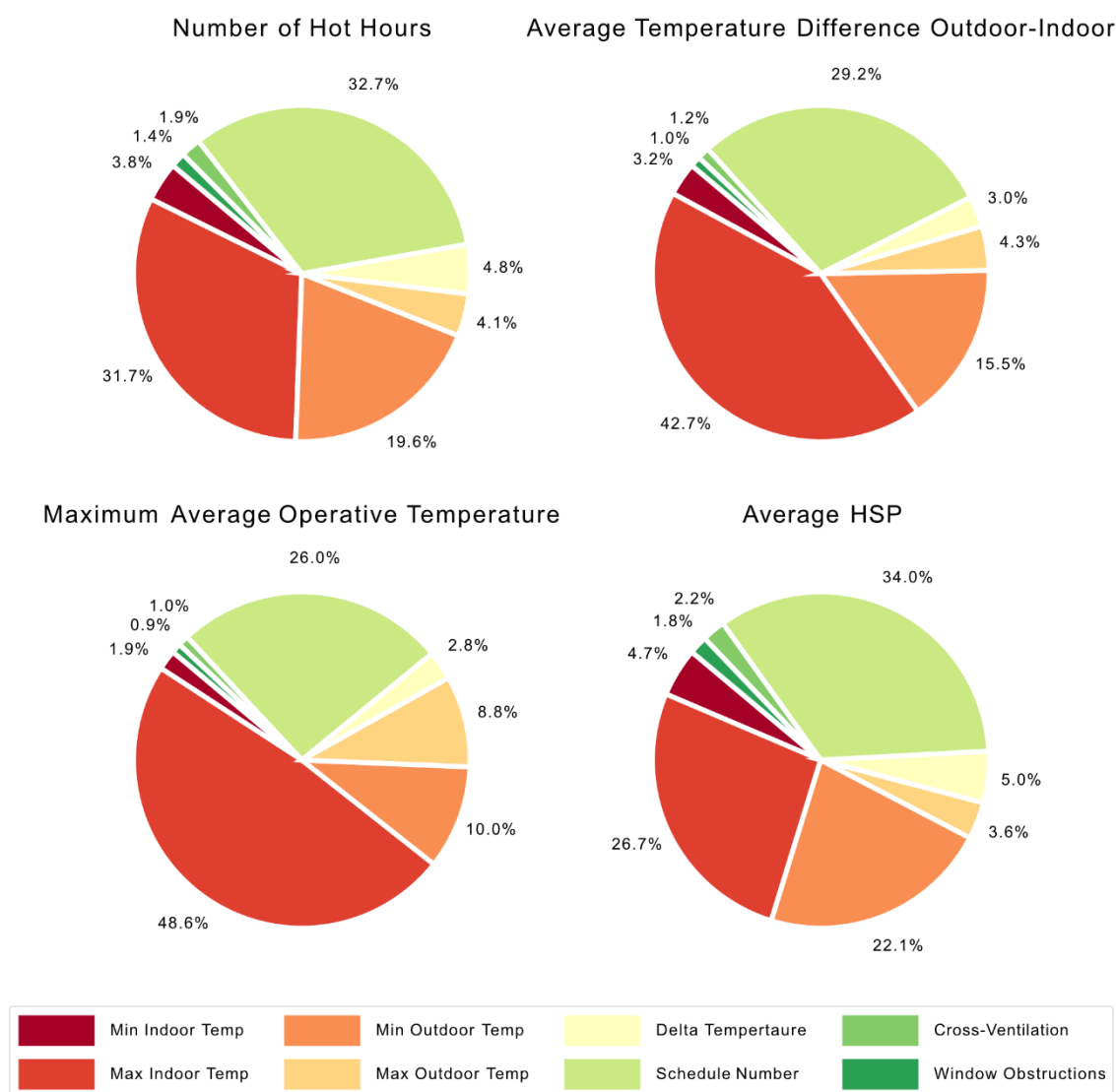
Figure 66 Sensitivity of natural ventilation parameters in terms of the outcome

In Annex 12 the sensitivity analysis calculation results are detailed. They are also visually represented on the pie charts in Figure 66. Although the values vary across the indicators, their respective order remains constant.

This chapter further demonstrated the adaptability of the selected methodology in integrating new sets of parameters. This flexibility facilitates the exploration of innovative solutions to a variety of challenges. The parametric approach, as employed here, has once again proven its effectiveness in performance-based design, particularly in the context of climate adaptation and heatwave resilience.

4.7. Section Summary

The data presented in this section results from conducting numerous performance simulations on a parametric "shoebox" building model. On one hand, this approach proved the feasibility of evaluating design decisions in the early stages. On the other hand, it highlighted the time-consuming and computationally intensive nature of such analyses.

The aggregation of this data facilitated in-depth comparisons, providing insightful findings that contribute to the future-proofing of building design. Most notably, it revealed the critical role of shading devices in enhancing climate adaptability and heatwave resilience. In contrast, the choice of materials and building orientation, regardless of the scenario, played a secondary role. This could potentially benefit the decision-making process by offering more flexibility in these aspects.

This section also gave particular focus to the impact of user behavior, specifically through window operability, thereby enabling natural ventilation via air exchange. The considerable variability of the results reveals the significant influence of the selected user actions.

To assess future climate scenarios, weather data files were updated and exchanged multiple times. The outcomes of such comparisons showed a consistent ranking of parameters, an observation that is meaningful regardless of if it was expected or not during this study. This consistency is valuable information for strategies aimed at climate adaptation and heatwave resilience.

5. Discussion

The study described in this master's thesis utilized various tools and concepts, bringing new insights into the topic of building performance simulation for climate adaptation and heatwave resilience. Simplifying the building model facilitated the comparability and adaptability of the results across various designs. The visual representation of data made the outcomes accessible to non-specialists, simplifying error detection and the identification of invalid data instances. However, the research process revealed several limitations in the chosen methodology.

5.1. Significance for Sustainable Building

The results of this thesis hold concrete implications for sustainable and future-oriented building design. Firstly, they provide insights into the significance of specific design decisions during the early stages of design, as well as the hierarchy of design parameters. Secondly, they examine the selected methodology to assess its utility in building design, including its application in the ECO+ Project.

Although the performance of designs featuring selected parameter values remained consistent across different years and scenarios, the variations between these values, and the relationships and proportions among them, underscored the significance of certain choices.

Furthermore, the chosen methodology facilitated the development of a design tool with a high degree of flexibility. This means it can be easily adjusted and adapted to evaluate different sets of parameters and their values, as well as to select various performance indicators, or external conditions provided in an EPW file. The adaptability of the methodology was tested in Chapter 4.6 (Influence of the Natural Ventilation Through Windows) where a completely different set of parameters was employed to focus on another aspect of building resilience and climate adaptation: the impact of human actions on natural ventilation in a passively cooled building.

In summary, after thousands of simulation iterations, analyzing the results and evaluating the methodology, the research questions can be answered:

"Which parameters are the most decisive when aiming at climate adaptability and heatwave resilience?"

Across all examined years and scenarios, the Window Shading Style consistently demonstrated the most significant impact on building performance and protection against heatwaves. The Window Solar Heat Gain Coefficient and the Window-To-Wall Ratio typically were in the second and third place respectively. The selection of materials and building orientation were thus less influential in this matter.

"Can parametric early-stage simulations facilitate informed decision-making for future-proofing buildings?"

Yes, they enable the rapid creation of variants and allow for comparisons to identify which design decisions can make a design future-proof. However, due to the time-intensive and computationally demanding nature of these simulations, other approaches might be more practical for this purpose.

5.2. Evaluation of the Methodology

The iterative approach (see Chapters 3.8 and 3.9) lead to establishment of a solid methodology and a well-defined scope. Saving large numbers of data, in the form of pictures, screenshots, plots, spreadsheets and models, made it possible to spot errors in simulation, inaccuracies in the model, or weaknesses of the chosen methodology during every iteration of the process.

The parameters initially selected to be evaluated proved to have high influence on the climate adaptation and heatwave resilience of a building design under various future scenarios. Distinguishing between scenarios in which a building requires mechanical ventilation and cooling, as opposed to only employing passive strategies for thermal comfort, allowed for a focused examination of the most important aspects of those two scenarios independently, disregarding irrelevant indicators for each. Finally, by comparing said scenarios, it was possible to evaluate the importance of the studied parameters and decide, which design choices would be advantageous for the building performance and user comfort regardless of the scenario and ventilation strategies.

5.3. Limitations

One of the most significant limitations of this study is the deliberate exclusion of green infrastructure's impact on climate adaptation strategies. It is widely acknowledged that green elements, such as green roofs, green façades and surrounding vegetation, play a crucial role in mitigating the effects of rising air temperatures and the increasing frequency of extreme weather events (Banihashemi et al., 2021; Dodman et al., 2022). However, due to the complexity of quantifying this influence of green infrastructure, the study intentionally focused on architectural and structural solutions, This should not be interpreted as undermining the importance of greenery; rather, its role is so significant that is should be deeper investigated in other research.

Secondly, limiting the analysis period to two hottest months of a year, while helping focus on the core idea, could lead to incorrect evaluations. The best design decisions in the context of climate adaptation and heatwave resilience could be possibly wrong considering the potential need for protection against cold temperatures in extremely cold winters.

Another limitation was that the method chosen to evaluate every potential parameter set, and therefore simulate numerous model iterations, resulted in high computational resource requirements. With the desire to evaluate more parameters and more of their possible values, the time needed to finish such a large number of simulations would make the methodology completely unfeasible.

On the other hand, it is vital to explore as many options as feasible to avoid overlooking critical factors or parameters. Due to the exponential increase in the number of simulation iterations with each added parameter value, this study had to exclude certain configurations of window properties and shading options.

In this situation, it might be not possible to find a balance between selecting a sufficiently high number of simulation parameters (as well as their values), so as to maximize the simulation accuracy keeping the total computation load within range of what can be performed with a home computer in a reasonable amount of time.

A significant issue that emerged later in the study was the need for a more 'parametric' selection of parameters, focusing on value changes rather than choosing a pre-defined

set. Parameters such as "Construction Set" or "Window Shading Style" appeared at the beginning to be very interesting to test, due to their similarity to early sustainable design decisions, but ultimately proved challenging to quantify and incorporate into sensitivity analysis.

Sensitivity analysis typically requires uniformly distributed values of parameters, or at least parameters that numerically represent the variation of the parameter (Campolongo & Cariboni, 2007). In this case, numerical values such as the U-Value, density, thermal capacity of a wall, or the percentage of window area covered by shading, would have been more appropriate choices.

The constraints associated with the chosen software, Rhino and Grasshopper, cannot be overlooked. While these tools offer visual programming workflows and ease of geometric manipulation, that is beneficial for architects and engineers, they have limitations including CPU-intensive computation, difficulty in stopping already running processes without data loss, and limited customization of the Ladybug Tools EnergyPlus and Radiance simulation methods.

Moreover, applying this workflow to larger projects or incorporating additional design stages would require updating the methodology with more advanced data processing tools and algorithms.

In summary, the limitations of this thesis resulted from the author's missing expertise in data science, computer science, numerical methods, and statistics. To further develop this topic, the personal knowledge gaps would need to be filled either by gaining more knowledge in the mentioned fields or by cooperating with specialists in related fields. The significance of the topic calls for continuation of this research and further studies potentially resulting in finding better solutions to issues related to climate change.

6. Outlook

Despite the described limitations, the time spent on this study allowed for developing a robust methodology and testing it thoroughly. The insights gained can already be considered to be valuable to decision makers involved in the planning of new buildings. The topic has emerged as both intriguing and significant, underscoring the need for further exploration.

As mentioned in Chapter 5.3 (Limitations), adopting a different approach to selecting input parameters could yield a more accurate sensitivity analysis. Numerous tools that could facilitate the evaluation of interrelations between parameters are available, enabling a more comprehensive global sensitivity analysis.

One such methodology is the Sobol method, which, through sensitivity analysis, provides various orders of indices (first-order, second-order, higher-order, total-order, etc.) in order to find the influence not only of each parameter alone but also in combination with others (Sobol′, 2001; Zhang et al., 2015). To implement this method, resources like the SaLiB open-source Python library could be employed. According to its documentation, standard usage begins with defining parameters and their ranges, executing a sampling function to generate inputs, and then assessing their outputs (*Basics — SALib's Documentation*, n.d.; Herman & Usher, 2017; Iwanaga et al., 2022). Thus, it would be advantageous to conduct performance simulations outside the Rhino and Grasshopper environment, enabling focus on specific desired output indicators.

Additionally, various statistical models and mathematical methods could be considered for output evaluation. Utilizing statistical regression methods for data analysis could also bring promising results, enabling the identification of relationships between parameters, and potentially reducing their number in future simulations (Montgomery et al., 2021). Principal Component Analysis, for instance, could potentially allow the inclusion of more parameters by clustering them into singular inputs (Jolliffe, 2002).

Moreover, the application of artificial intelligence (machine learning) in every aspect of the process, from defining parameters and indicators to simulation and result evaluation, could be particularly beneficial. A well-trained machine learning model could help reduce the time required for a large number of simulation iterations (Ali et al., 2023).

Furthermore, it could potentially allow for the application of output results and indications to other designs, possibly those more detailed and advanced in the planning process. However, the use of such technologies should be done thoughtfully and with a sufficiently high level of understanding them (De Wilde, 2023).

This work proved the necessity of designing for climate adaptation and building resilience against heatwaves. The performance of currently planned buildings may soon reveal that the methods used now are in this context insufficient. The early design stage, in which the most adjustments to the design are still possible, should be the time when future scenarios are especially considered. Buildings constructed now will exist in the future; therefore, their designs cannot rely solely on norms and data derived from past experiences and measurements. Emerging technologies allow for the integration of future predictions into the design process, enabling buildings to be adequately prepared for a range of potential future scenarios.

Bibliography

Ahuja, S., Chopson, P., Haymaker, J., & Augenbroe, G. (2015). *Practical energy and cost optimization methods for selecting massing, materials, and technologies.*

Aksamija, A. (2018). Methods for integrating parametric design with building performance analysis. *ARCC Conference Repository*.

Ali, A., Jayaraman, R., Mayyas, A., Alaifan, B., & Azar, E. (2023). Machine learning as a surrogate to building performance simulation: Predicting energy consumption under different operational settings. *Energy and Buildings*, *286*, 112940. https://doi.org/10.1016/j.enbuild.2023.112940

Alrasheed, M., & Mourshed, M. (2023). Domestic overheating risks and mitigation strategies: The state-of-the-art and directions for future research. *Indoor and Built Environment*, *32*(6), 1057–1077. https://doi.org/10.1177/1420326X231153856

Alwi, N. M., Flor, J.-F., Anuar, N. H., Mohamad, J., Hanafi, N. N. H., Muhammad, N. H., Zain, M. H. K. M., & Nasir, M. R. M. (2022). Retrofitting measures for climate resilience: Enhancing the solar performance of Malaysian school buildings with passive design concepts. *IOP Conference Series: Earth and Environmental Science*, *1102*(1), 012014. https://doi.org/10.1088/1755-1315/1102/1/012014

Ara Begum, R., Lempert, R., E. Ali, T. A. B., Bernauer, T., Cramer, W., Cui, X., Mach, K., Nagy, G., Stenseth, N. C., Sukumar, R., & Wester, P. (2022). Point of Departure and Key Concepts. In H. O. Pörtner, D. C. Roberts, M. Tignor, E. S. Poloczanska, K. Mintenbeck, A. Alegría, M. Craig, S. Langsdorf, S. Löschke, V. Möller, A. Okem, & B. Rama (Eds.), *Climate Change 2022: Impacts, Adaptation and Vulnerability. Contribution of Working Group II to the Sixth Assessment Report of the Intergovernmental Panel on Climate Change*. Cambridge University Press. https://doi.org/10.1017/9781009325844.003

Arrhenius, S. (1896). XXXI. *On the influence of carbonic acid in the air upon the temperature of the ground. The London, Edinburgh, and Dublin Philosophical Magazine and Journal of Science*, *41*(251), 237–276. https://doi.org/10.1080/14786449608620846

ASHRAE. (2021). 9.1 Human Thermoregulation. In *2021 ASHRAE® Handbook— Fundamentals (SI Edition)*. American Society of Heating, Refrigerating and Air-Conditioning Engineers, Inc. (ASHRAE). https://app.knovel.com/hotlink/pdf/id:kt012MGS14/ashrae-handbook-fundamentals/human-thermoregulation

Attia, S., Levinson, R., Ndongo, E., Holzer, P., Berk Kazanci, O., Homaei, S., Zhang, C., Olesen, B. W., Qi, D., Hamdy, M., & Heiselberg, P. (2021). Resilient cooling of buildings to protect against heat waves and power outages: Key concepts and definition. *Energy and Buildings*, *239*, 110869. https://doi.org/10.1016/j.enbuild.2021.110869

Attia, S., Walter, E., & Andersen, M. (2013). Identifying and modeling the integrated design process of net Zero Energy buildings. *High Performance Buildings-Design and Evaluation Methodologies*.

Augenbroe, G. (2011). The role of simulation in performance-based building. In J. L. M. Hensen & R. Lamberts (Eds.), *Building Performance Simulation for Design and Operation* (pp. 15–36).

Banihashemi, F., Erlwein, S., Harter, H., Meier-Dotzler, C., Zölch, T., Bauer, A., Jean-Louis, G., Lang, W., Linke, S., & Mittermüller, J. (2021). *Grüne und Graue Maßnahmen für die Siedlungsentwicklung Klimaschutz und Klimaanpassung in wachsenden Städten*.

Barnaby, C. S., & Crawley, U. B. (2011). Weather data for building performance simulation. In J. L. M. Hensen & R. Lamberts (Eds.), *Building Performance Simulation for Design and Operation* (pp. 37–55).

Basics—SALib's documentation. (n.d.). Retrieved 26 November 2023, from https://salib.readthedocs.io/en/latest/user_guide/basics.html

Belcher, S., Hacker, J., & Powell, D. (2005). Constructing design weather data for future climates. *Building Services Engineering Research and Technology*, *26*(1), 49–61. https://doi.org/10.1191/0143624405bt112oa

Benslimane, N., & Biara, R. W. (2019). The urban sustainable structure of the vernacular city and its modern transformation: A case study of the popular architecture in the saharian Region. *Energy Procedia*, *157*, 1241–1252. https://doi.org/10.1016/j.egypro.2018.11.290

Bocchini, P., & Frangopol, D. M. (2011). *Resilience-driven disaster management of civil infrastructure*.

Bougdah, H., & Sharples, S. (2009). *Environment, Technology and Sustainability* (0 ed.). Taylor & Francis. https://doi.org/10.4324/9780203878408

Bourgin, P.-Y., & Le-Clerc, S. (2022). A pragmatic approach to assess the climate resilience of hydro projects. *E3S Web of Conferences*, *346*, 04004. https://doi.org/10.1051/e3sconf/202234604004

Bruneau, M., Chang, S. E., Eguchi, R. T., Lee, G. C., O'Rourke, T. D., Reinhorn, A. M., Shinozuka, M., Tierney, K., Wallace, W. A., & Von Winterfeldt, D. (2003). A Framework to Quantitatively Assess and Enhance the Seismic Resilience of Communities. *Earthquake Spectra*, *19*(4), 733–752. https://doi.org/10.1193/1.1623497

Burman, E., Kimpian, J., & Mumovic, D. (2014). *Reconciling Resilience and Sustainability in Overheating and Energy Performance Assessments of Non-domestic Buildings*.

Burroughs, S. (2017). Development of a Tool for Assessing Commercial Building Resilience. *Procedia Engineering*, *180*, 1034–1043. https://doi.org/10.1016/j.proeng.2017.04.263

Cabeza, L. F., Bai, Q., Bertoldi, P., Kihila, J. M., Lucena, A. F. P., Mata, É., Mirasgedis, S., Novikova, A., & Saheb, Y. (2022). Buildings. In P. R. Shukla, J. Skea, R. Slade, A. A. Khourdajie, R. van Diemen, D. McCollum, M. Pathak, S. Some, P. Vyas, R. Fradera, M. Belkacemi, A. Hasija, G. Lisboa, S. Luz, & J. Malley (Eds.), *Climate change 2022: Mitigation of climate change. Contribution of working*

group III to the sixth assessment report of the intergovernmental panel on climate change. Cambridge University Press. https://doi.org/10.1017/9781009157926.011

Campolongo, F., & Cariboni, J. (2007). *Sensitivity analysis: How to detect important factors in large models*.

Candido, C. (2021). Wind, making the invisible visible: Design for and with natural ventilation. In D. Ryan, J. Ferng, & E. L'Heureux (Eds.), *Drawing Climate: Visualising Invisible Elements of Architecture* (pp. 36–51). Birkhäuser.

Chen, D., Rojas, M., Samset, B. H., Cobb, K., Diongue Niang, A., Edwards, P., Emori, S., Faria, S. H., Hawkins, E., Hope, P., Huybrechts, P., Meinshausen, M., Mustafa, S. K., Plattner, G.-K., & Tréguier, A.-M. (2021). Framing, context, and methods. In V. Masson-Delmotte, P. Zhai, A. Pirani, S. L. Connors, C. Péan, S. Berger, N. Caud, Y. Chen, L. Goldfarb, M. I. Gomis, M. Huang, K. Leitzell, E. Lonnoy, J. B. R. Matthews, T. K. Maycock, T. Waterfield, O. Yelekçi, R. Yu, & B. Zhou (Eds.), *Climate change 2021: The physical science basis. Contribution of working group I to the sixth assessment report of the intergovernmental panel on climate change* (pp. 147–286). Cambridge University Press. https://doi.org/10.1017/9781009157896.003

Cheung, T., Schiavon, S., Parkinson, T., Li, P., & Brager, G. (2019). Analysis of the accuracy on PMV – PPD model using the ASHRAE Global Thermal Comfort Database II. *Building and Environment, 153*, 205–217. https://doi.org/10.1016/j.buildenv.2019.01.055

Chinazzo, G., Rastogi, P., & Andersen, M. (2015). Assessing Robustness Regarding Weather Uncertainties for Energy- Efficiency-Driven Building Refurbishments. *Energy Procedia, 78*, 931–936. https://doi.org/10.1016/j.egypro.2015.11.021

Clarke, J. A. (2001). *Energy simulation in building design* (2nd ed). Butterworth-Heinemann.

Climate Change World Weather File Generator for World-Wide Weather Data—CCWorldWeatherGen—University of Southampton Blogs. (n.d.). Retrieved 12 September 2023, from https://energy.soton.ac.uk/climate-change-world-weather-file-generator-for-world-wide-weather-data-ccworldweathergen/

Climate Reanalyzer. (n.d.). Retrieved 19 July 2023, from https://climatereanalyzer.org/clim/t2_daily/

Climate.OneBuilding.Org. (n.d.). *Climate/Weather Data Sources*. Retrieved 8 September 2023, from https://climate.onebuilding.org/sources/default.html

Copernicus Climate Change Service (C3S). (2023). *European State of the Climate 2022*. Copernicus Climate Change Service (C3S). https://doi.org/10.24381/GVAF-H066

Crawley, D. B. (2008). *Building Performance Simulation: A Tool for Policymaking*.

de Dear, R., Brager, G., & Cooper, D. (1997). *Developing an Adaptive Model of Thermal Comfort and Preference. FINAL REPORT ASHRAE RP- 884*.

De Wilde, P. (2023). Building performance simulation in the brave new world of artificial intelligence and digital twins: A systematic review. *Energy and Buildings, 292*, 113171. https://doi.org/10.1016/j.enbuild.2023.113171

de Wilde, P., & Coley, D. (2012). The implications of a changing climate for buildings. *Building and Environment*, *55*, 1–7. https://doi.org/10.1016/j.buildenv.2012.03.014

Denton, F., Halsnæs, K., Akimoto, K., Burch, S., Diaz Morejon, C., Farias, F., Jupesta, J., Shareef, A., Schweizer-Ries, P., Teng, F., & Zusman, E. (2022). Accelerating the transition in the context of sustainable development. In P. R. Shukla, J. Skea, R. Slade, A. A. Khourdajie, R. van Diemen, D. McCollum, M. Pathak, S. Some, P. Vyas, R. Fradera, M. Belkacemi, A. Hasija, G. Lisboa, S. Luz, & J. Malley (Eds.), *Climate change 2022: Mitigation of climate change. Contribution of working group III to the sixth assessment report of the intergovernmental panel on climate change*. Cambridge University Press. https://doi.org/10.1017/9781009157926.019

Denton, F., Wilbanks, T. J., Abeysinghe, A. C., Burton, I., Gao, Q., Lemos, M. C., Masui, T., O'Brien, K. L., & Warner, K. (2014). Climate-resilient pathways: Adaptation, mitigation, and sustainable development. *Climate Change*, 1101–1131.

DGNB System. Districts criteria set. Version 2020. (2020). Deutsche Gesellschaft für Nachhaltiges Bauen (German Sustainable Building Council) – DGNB e.V.

DGNB System. New construction, Buildings, Criteria Set. Version 2020 International. (2020). Deutsche Gesellschaft für Nachhaltiges Bauen (German Sustainable Building Council) – DGNB e.V.

DGNB System. New construction, Buildings, Criteria Set. Version 2023 International. (2023). Deutsche Gesellschaft für Nachhaltiges Bauen (German Sustainable Building Council) – DGNB e.V.

Di Turi, S., & Ruggiero, F. (2017). Re-interpretation of an ancient passive cooling strategy: A new system of wooden lattice openings. *Energy Procedia*, *126*, 289–296. https://doi.org/10.1016/j.egypro.2017.08.159

Dickinson, R., & Brannon, B. (2016). Generating Future Weather Files for resilience. *Los Angeles*.

DIN 4108-4:2020-11, Wärmeschutz und Energie-Einsparung in Gebäuden_- Teil_4: Wärme- und feuchteschutztechnische Bemessungswerte. (n.d.). Beuth Verlag GmbH. https://doi.org/10.31030/3188939

DIN EN 15251:2012-12, Eingangsparameter für das Raumklima zur Auslegung und Bewertung der Energieeffizienz von Gebäuden_- Raumluftqualität, Temperatur, Licht und Akustik; Deutsche Fassung EN_15251:2007. (2012). Beuth Verlag GmbH. https://doi.org/10.31030/1912934

DIN EN ISO 7730:2006-05, Ergonomie der thermischen Umgebung_- Analytische Bestimmung und Interpretation der thermischen Behaglichkeit durch Berechnung des PMV- und des PPD-Indexes und Kriterien der lokalen thermischen Behaglichkeit (ISO_7730:2005); Deutsche Fassung EN_ISO_7730:2005. (2006). Beuth Verlag GmbH. https://doi.org/10.31030/9720035

Djongyang, N., Tchinda, R., & Njomo, D. (2010). Thermal comfort: A review paper. *Renewable and Sustainable Energy Reviews*, *14*(9), 2626–2640. https://doi.org/10.1016/j.rser.2010.07.040

Dodman, D., Hayward, B., Pelling, M., Castan Broto, V., Chow, W., Chu, E., Dawson, R., Khirfan, L., McPhearson, T., Prakash, A., Zheng, Y., & Ziervogel, G. (2022). Cities, Settlements and Key Infrastructure. In H. O. Pörtner, D. C. Roberts, M. Tignor, E. S. Poloczanska, K. Mintenbeck, A. Alegría, M. Craig, S. Langsdorf, S. Löschke, V. Möller, A. Okem, & B. Rama (Eds.), *Climate Change 2022: Impacts, Adaptation and Vulnerability. Contribution of Working Group II to the Sixth Assessment Report of the Intergovernmental Panel on Climate Change.* Cambridge University Press. https://doi.org/10.1017/9781009325844.008

Dodoo, A., & Gustavsson, L. (2016). Energy use and overheating risk of Swedish multi-storey residential buildings under different climate scenarios. *Energy*, *97*, 534–548. https://doi.org/10.1016/j.energy.2015.12.086

Ehlers, N., Schulze, K., Zong, C., Vollmer, M., Schroeter, B., & Lang, W. (2023). A holistic analysis of sustainability metrics at an urban district scale. *IOP Conference Series: Earth and Environmental Science*, *1196*(1), 012071. https://doi.org/10.1088/1755-1315/1196/1/012071

Encouraging resilient assets using BREEAM. (n.d.). Retrieved 31 December 2023, from https://files.bregroup.com/breeam/BREEAM_Resilience_BRE_115440.pdf

EnergyPlus. (n.d.). Retrieved 13 June 2023, from https://energyplus.net/

EnergyPlus Weather File (EPW) Format. (n.d.). Retrieved 18 April 2023, from https://designbuilder.co.uk/cahelp/Content/EnergyPlusWeatherFileFormat.htm

Ernstson, H., Van Der Leeuw, S. E., Redman, C. L., Meffert, D. J., Davis, G., Alfsen, C., & Elmqvist, T. (2010). Urban Transitions: On Urban Resilience and Human-Dominated Ecosystems. *AMBIO*, *39*(8), 531–545. https://doi.org/10.1007/s13280-010-0081-9

Escandón, R., Suárez, R., Sendra, J. J., Ascione, F., Bianco, N., & Mauro, G. M. (2019). Predicting the Impact of Climate Change on Thermal Comfort in A Building Category: The Case of Linear-type Social Housing Stock in Southern Spain. *Energies*, *12*(12), 2238. https://doi.org/10.3390/en12122238

The European Green Deal, European Commission (2019). https://eur-lex.europa.eu/legal-content/EN/TXT/?uri=COM:2019:640:FIN

European Commission. (2021). *Communication from the commission to the european parliament, the council, the european economic and social committee and the committee of the regions*. https://eur-lex.europa.eu/legal-content/EN/TXT/?uri=COM%3A2021%3A82%3AFIN

Eyring, V., Bony, S., Meehl, G. A., Senior, C. A., Stevens, B., Stouffer, R. J., & Taylor, K. E. (2016). Overview of the Coupled Model Intercomparison Project Phase 6 (CMIP6) experimental design and organization. *Geoscientific Model Development*, *9*(5), 1937–1958. https://doi.org/10.5194/gmd-9-1937-2016

Eyring, V., Gillett, N. P., Achuta Rao, K. M., Barimalala, R., Barreiro Parrillo, M., Bellouin, N., Cassou, C., Durack, P. J., Kosaka, Y., McGregor, S., Min, S., Morgenstern, O., & Sun, Y. (2021). Human influence on the climate system. In V. Masson-Delmotte, P. Zhai, A. Pirani, S. L. Connors, C. Péan, S. Berger, N. Caud, Y. Chen, L. Goldfarb, M. I. Gomis, M. Huang, K. Leitzell, E. Lonnoy, J. B. R. Matthews, T. K. Maycock, T. Waterfield, O. Yelekçi, R. Yu, & B. Zhou (Eds.), *Climate change 2021: The physical science basis. Contribution of working group*

I to the sixth assessment report of the intergovernmental panel on climate change (pp. 423–552). Cambridge University Press. https://doi.org/10.1017/9781009157896.005

Fanger, P. O. (1970). Thermal comfort. Analysis and applications in environmental engineering. *Thermal Comfort. Analysis and Applications in Environmental Engineering.*

Ferreira, A., Pinheiro, M. D., Brito, J. D., & Mateus, R. (2023). A critical analysis of LEED, BREEAM and DGNB as sustainability assessment methods for retail buildings. *Journal of Building Engineering*, *66*, 105825. https://doi.org/10.1016/j.jobe.2023.105825

Flores-Larsen, S., Bre, F., & Hongn, M. (2022). A performance-based method to detect and characterize heatwaves for building resilience analysis. *Renewable and Sustainable Energy Reviews*, *167*, 112795. https://doi.org/10.1016/j.rser.2022.112795

Flores-Larsen, S., Filippín, C., & Bre, F. (2023). New metrics for thermal resilience of passive buildings during heat events. *Building and Environment*, *230*, 109990. https://doi.org/10.1016/j.buildenv.2023.109990

Flourentzou, F. (2012). Measures of urban sustainability. In *Computer Modelling for Sustainable Urban Design* (pp. 177–201). Routledge.

Frazer, J. (2016). Parametric Computation: History and Future. *Architectural Design*, *86*(2), 18–23. https://doi.org/10.1002/ad.2019

Fuldauer, L. I., Thacker, S., Haggis, R. A., Fuso-Nerini, F., Nicholls, R. J., & Hall, J. W. (2022). Targeting climate adaptation to safeguard and advance the Sustainable Development Goals. *Nature Communications*, *13*(1), 3579. https://doi.org/10.1038/s41467-022-31202-w

Gallopín, G. C. (2006). Linkages between vulnerability, resilience, and adaptive capacity. *Global Environmental Change*, *16*(3), 293–303. https://doi.org/10.1016/j.gloenvcha.2006.02.004

Gesangyangji, Vimont, D. J., Holloway, T., & Lorenz, D. J. (2022). A methodology for evaluating the effects of climate change on climatic design conditions for buildings and application to a case study in Madison, Wisconsin. *Environmental Research: Infrastructure and Sustainability*, *2*(2), 025007. https://doi.org/10.1088/2634-4505/ac6e01

Gilani, S., & O'Brien, W. (2021). Natural ventilation usability under climate change in Canada and the United States. *Building Research & Information*, *49*(4), 367–386. https://doi.org/10.1080/09613218.2020.1760775

Gosling, S. N., Lowe, J. A., McGregor, G. R., Pelling, M., & Malamud, B. D. (2009). Associations between elevated atmospheric temperature and human mortality: A critical review of the literature. *Climatic Change*, *92*(3–4), 299–341. https://doi.org/10.1007/s10584-008-9441-x

Gremmelspacher, J. M., Sivolova, J., Naboni, E., & Nik, V. M. (2020). Future Climate Resilience Through Informed Decision Making in Retrofitting Projects. In O. Gervasi, B. Murgante, S. Misra, C. Garau, I. Blečić, D. Taniar, B. O. Apduhan, A. M. A. C. Rocha, E. Tarantino, C. M. Torre, & Y. Karaca (Eds.), *Computational*

Science and Its Applications – ICCSA 2020 (Vol. 12251, pp. 352–364). Springer International Publishing. https://doi.org/10.1007/978-3-030-58808-3_26

Grober, U. (2013). *Die Entdeckung der Nachhaltigkeit: Kulturgeschichte eines Begriffs*. Antje Kunstmann.

Guarda, E. L. A. da, Gabriel, E., Mansuelo Alves Domingos, R., Cleonice Durante, L., Julio Apolonio Callejas, I., Carlos Machado Sanches, J., & Andrade Carvalho Rosseti, K. D. (2019). Adaptive comfort assessment for different thermal insulations for building envelope against the effects of global warming in the mid-western Brazil. *IOP Conference Series: Earth and Environmental Science*, *329*(1), 012057. https://doi.org/10.1088/1755-1315/329/1/012057

Gulev, S. K., Thorne, P. W., Ahn, J., Dentener, F. J., Domingues, C. M., Gerland, S., Gong, D., Kaufman, D. S., Nnamchi, H. C., Quaas, J., Rivera, J. A., Sathyendranath, S., Smith, S. L., Trewin, B., von Schuckmann, K., & Vose, R. S. (2021). *Changing state of the climate system* (V. Masson-Delmotte, P. Zhai, A. Pirani, S. L. Connors, C. Péan, S. Berger, N. Caud, Y. Chen, L. Goldfarb, M. I. Gomis, M. Huang, K. Leitzell, E. Lonnoy, J. B. R. Matthews, T. K. Maycock, T. Waterfield, O. Yelekçi, R. Yu, & B. Zhou, Eds.; pp. 287–422). Cambridge University Press. https://www.ipcc.ch/report/ar6/wg1/downloads/report/IPCC_AR6_WGI_Chapter 02.pdf

Hamard, E. (2017). *Rediscovering of vernacular adaptative construction strategies for sustainable modern building: Application to cob and rammed earth*.

Hasan, A., & Reda, F. (2022). Special Issue "Net-Zero/Positive Energy Buildings and Districts". *Buildings*, *12*(3), 382. https://doi.org/10.3390/buildings12030382

Hasper, W., Kirtschig, T., Siddall, M., Johnston, D., Vallentin, G., & Harvie-Clark, J. (2021). Long-term performance of Passive House buildings. *Energy Efficiency*, *14*(1), 5. https://doi.org/10.1007/s12053-020-09913-0

Hawila, A. A. W., Pernetti, R., Pozza, C., & Belleri, A. (2022). Plus energy building: Operational definition and assessment. *Energy and Buildings*, *265*, 112069. https://doi.org/10.1016/j.enbuild.2022.112069

HB-Energy Primer. (n.d.). Retrieved 8 September 2023, from https://docs.ladybug.tools/hb-energy-primer/

Hegger, M., & Institut für internationale Architektur-Dokumentation (Eds.). (2008). *Energy manual: Sustainable architecture*. Birkhäuser ; Edition Detail.

Hensen, J. L. M., & Lamberts, R. (2011). Introduction to building performance simulation. In J. L. M. Hensen & R. Lamberts (Eds.), *Building Performance Simulation for Design and Operation* (pp. 1–14).

Herman, J., & Usher, W. (2017). SALib: An open-source Python library for Sensitivity Analysis. *The Journal of Open Source Software*, *2*(9), 97. https://doi.org/10.21105/joss.00097

Hersbach, H., Bell, B., Berrisford, P., Biavati, G., Horányi, A., Muñoz Sabater, J., Nicolas, J., Peubey, C., Radu, R., Rozum, I., Schepers, D., Simmons, A., Soci, C., Dee, D., & Thépaut, J.-N. (2023). *ERA5 hourly data on single levels from 1940 to present*. https://doi.org/10.24381/cds.adbb2d47

Hollberg, A. (2017). *A parametric method for building design optimization based on Life Cycle Assessment*.

Hollý, J., & Palková, A. (2019). Climate change impact – residential unit. *MATEC Web of Conferences*, *279*, 03007. https://doi.org/10.1051/matecconf/201927903007

Homaei, S., & Hamdy, M. (2021). Thermal resilient buildings: How to be quantified? A novel benchmarking framework and labelling metric. *Building and Environment*, *201*, 108022. https://doi.org/10.1016/j.buildenv.2021.108022

Honeybee Energy's documentation. (n.d.). Retrieved 13 June 2023, from https://www.ladybug.tools/honeybee-energy/docs/

Honeybee Primer. (n.d.). Retrieved 10 December 2023, from https://docs.ladybug.tools/honeybee-primer/

Hopfe, C. J., Emmerich, M. T., Marijt, R., & Hensen, J. (2012). Robust multi-criteria design optimisation in building design. *Proceedings of Building Simulation and Optimization, Loughborough, UK*, 118–125.

Hunt, A., & Watkiss, P. (2011). Climate change impacts and adaptation in cities: A review of the literature. *Climatic Change*, *104*(1), 13–49. https://doi.org/10.1007/s10584-010-9975-6

IPCC. (2021). Annex VII: Glossary [Matthews, J.B.R., V. Möller, R. van diemen, J.S. fuglestvedt, V. Masson-delmotte, C. Méndez, S. Semenov, A. Reisinger (eds.)]. In V. Masson-Delmotte, P. Zhai, A. Pirani, S. L. Connors, C. Péan, S. Berger, N. Caud, Y. Chen, L. Goldfarb, M. I. Gomis, M. Huang, K. Leitzell, E. Lonnoy, J. B. R. Matthews, T. K. Maycock, T. Waterfield, O. Yelekçi, R. Yu, & B. Zhou (Eds.), *Climate change 2021: The physical science basis. Contribution of working group I to the sixth assessment report of the intergovernmental panel on climate change* (pp. 2215–2256). Cambridge University Press. https://doi.org/10.1017/9781009157896.022

Iwanaga, T., Usher, W., & Herman, J. (2022). Toward SALib 2.0: Advancing the accessibility and interpretability of global sensitivity analyses. *Socio-Environmental Systems Modelling*, *4*, 18155. https://doi.org/10.18174/sesmo.18155

Jentsch, M. F., James, P. A. B., Bourikas, L., & Bahaj, A. S. (2013). Transforming existing weather data for worldwide locations to enable energy and building performance simulation under future climates. *Renewable Energy*, *55*, 514–524. https://doi.org/10.1016/j.renene.2012.12.049

Jia, H., & Chong, A. (n.d.). *epwshiftr: Create Future 'EnergyPlus' Weather Files using 'CMIP6' Data*.

Jolliffe, I. T. (2002). *Principal component analysis* (2nd ed). Springer.

Karamouz, M., & Zahmatkesh, Z. (2017). Quantifying Resilience and Uncertainty in Coastal Flooding Events: Framework for Assessing Urban Vulnerability. *Journal of Water Resources Planning and Management*, *143*(1), 04016071. https://doi.org/10.1061/(ASCE)WR.1943-5452.0000724

Koppe, C., Kovats, S., Jendritzky, G., Menne, B., & Breuer, D. J. (2004). *Heat waves: Risks and responses*. Regional Office for Europe, World Health Organization.

Kotireddy, R. R. (2018). *Towards Robust Low-Energy Houses*.

Ladybug Primer. (n.d.). Retrieved 10 August 2023, from https://docs.ladybug.tools/ladybug-primer/

Lee, J.-Y., Marotzke, J., Bala, G., Cao, L., Corti, S., Dunne, J. P., Engelbrecht, F., Fischer, E., Fyfe, J. C., Jones, C., Maycock, A., Mutemi, J., Ndiaye, O., Panickal, S., & Zhou, T. (2021). Future global climate: Scenario-based projections and near-term information. In V. Masson-Delmotte, P. Zhai, A. Pirani, S. L. Connors, C. Péan, S. Berger, N. Caud, Y. Chen, L. Goldfarb, M. I. Gomis, M. Huang, K. Leitzell, E. Lonnoy, J. B. R. Matthews, T. K. Maycock, T. Waterfield, O. Yelekçi, R. Yu, & B. Zhou (Eds.), *Climate change 2021: The physical science basis. Contribution of working group I to the sixth assessment report of the intergovernmental panel on climate change* (pp. 553–672). Cambridge University Press. https://doi.org/10.1017/9781009157896.006

LEED Climate Resilience Screening Tool for LEED v4 Projects | U.S. Green Building Council. (n.d.). Retrieved 31 December 2023, from https://www.usgbc.org/resources/leed-climate-resilience-screening-tool-leed-v4-projects

Li, B. (2017). *Use of building energy simulation software in early-stage of design process*.

Litsa, A., & Giarma, C. (2023). Beyond the building scale: Addressing energy related issues in urban areas' environmental performance assessment methods. *IOP Conference Series: Earth and Environmental Science*, *1196*(1), 012054. https://doi.org/10.1088/1755-1315/1196/1/012054

Lützkendorf, T. (2019). Sustainability in Building Construction – A Multilevel Approach. *IOP Conference Series: Earth and Environmental Science*, *290*(1), 012004. https://doi.org/10.1088/1755-1315/290/1/012004

Mahdavi, A. (2011). People in building performance simulation. In J. L. M. Hensen & R. Lamberts (Eds.), *Building Performance Simulation for Design and Operation* (pp. 56–72).

Malalgoda, C., Amaratunga, D., & Haigh, R. (2014). Challenges in Creating a Disaster Resilient Built Environment. *Procedia Economics and Finance*, *18*, 736–744. https://doi.org/10.1016/S2212-5671(14)00997-6

Manzoor, B., Othman, I., Sadowska, B., & Sarosiek, W. (2022). Zero-Energy Buildings and Energy Efficiency towards Sustainability: A Bibliometric Review and a Case Study. *Applied Sciences*, *12*(4), 2136. https://doi.org/10.3390/app12042136

Marx, D., Reitberger, R., Kleeberger, M., & Lang, W. (2023). Automated workflow for simulating the effect of green façades on indoor thermal comfort. *Journal of Physics: Conference Series*, *2600*(9), 092007. https://doi.org/10.1088/1742-6596/2600/9/092007

Meteonorm 8. (2023a). *Meteonorm 8 Handbook part I: Software*. https://meteonorm.com/assets/downloads/mn82_software.pdf

Meteonorm 8. (2023b). *Meteonorm 8 Handbook part II: Theory*. https://meteonorm.com/assets/downloads/mn82_theory.pdf

Moazami, A., Nik, V. M., Carlucci, S., & Geving, S. (2019). Impacts of future weather data typology on building energy performance – Investigating long-term patterns

of climate change and extreme weather conditions. *Applied Energy*, *238*, 696–720. https://doi.org/10.1016/j.apenergy.2019.01.085

Moench, M. (2014). Experiences applying the climate resilience framework: Linking theory with practice. *Development in Practice*, *24*(4), 447–464. https://doi.org/10.1080/09614524.2014.909385

Möller, V., van Diemen, R., Matthews, J. B. R., Méndez, S., C. Semenov, Fuglestvedt, J. S., & Reisinger, A. (eds.). (2022a). Glossary. In H. O. Pörtner, D. C. Roberts, M. Tignor, E. S. Poloczanska, K. Mintenbeck, A. Alegría, M. Craig, S. Langsdorf, S. Löschke, V. Möller, A. Okem, & B. Rama (Eds.), *Climate Change 2022: Impacts, Adaptation and Vulnerability. Contribution of Working Group II to the Sixth Assessment Report of the Intergovernmental Panel on Climate Change*. Cambridge University Press. https://doi.org/10.1017/9781009325844.029

Möller, V., van Diemen, R., Matthews, J. B. R., Méndez, S., C. Semenov, Fuglestvedt, J. S., & Reisinger, A. (eds.). (2022b). Glossary. In H. O. Pörtner, D. C. Roberts, M. Tignor, E. S. Poloczanska, K. Mintenbeck, A. Alegría, M. Craig, S. Langsdorf, S. Löschke, V. Möller, A. Okem, & B. Rama (Eds.), *Climate Change 2022: Impacts, Adaptation and Vulnerability. Contribution of Working Group II to the Sixth Assessment Report of the Intergovernmental Panel on Climate Change*. Cambridge University Press. https://doi.org/10.1017/9781009325844.029

Montgomery, D. C., Peck, E. A., & Vining, G. G. (2021). *Introduction to linear regression analysis*. John Wiley & Sons.

Navarro, D., Lizundia-Loiola, J., Paz, J., Abajo, B., Cantergiani, C., García, G., & Feliu, E. (2022). *Climate data and maps update* (Issue ESPON 2020 Cooperation Programme) [Final report]. ESPON EGTC / European Spatial Planning Observation Network (ESPON). https://www.espon.eu/projects/espon-2020/monitoring-and-tools/climate-data-and-maps-update

Negendahl, K., & Nielsen, T. R. (2015). Building energy optimization in the early design stages: A simplified method. *Energy and Buildings*, *105*, 88–99. https://doi.org/10.1016/j.enbuild.2015.06.087

Nguyen, A. T., Truong, N. S. H., Rockwood, D., & Tran Le, A. D. (2019). Studies on sustainable features of vernacular architecture in different regions across the world: A comprehensive synthesis and evaluation. *Frontiers of Architectural Research*, *8*(4), 535–548. https://doi.org/10.1016/j.foar.2019.07.006

Nguyen, A.-T., Reiter, S., & Rigo, P. (2014). A review on simulation-based optimization methods applied to building performance analysis. *Applied Energy*, *113*, 1043–1058. https://doi.org/10.1016/j.apenergy.2013.08.061

Okeil, A. (2010). A holistic approach to energy efficient building forms. *Energy and Buildings*, *42*(9), 1437–1444. https://doi.org/10.1016/j.enbuild.2010.03.013

ÖKOBAUDAT. (n.d.). Retrieved 8 September 2023, from https://oekobaudat.de/

Olonscheck, M., Holsten, A., & Kropp, J. P. (2011). Heating and cooling energy demand and related emissions of the German residential building stock under climate change. *Energy Policy*, *39*(9), 4795–4806. https://doi.org/10.1016/j.enpol.2011.06.041

Omrany, H., Chang, R., Soebarto, V., Zhang, Y., Ghaffarianhoseini, A., & Zuo, J. (2022). A bibliometric review of net zero energy building research 1995–2022. *Energy and Buildings*, *262*, 111996. https://doi.org/10.1016/j.enbuild.2022.111996

O'Neill, B. C., Tebaldi, C., van Vuuren, D. P., Eyring, V., Friedlingstein, P., Hurtt, G., Knutti, R., Kriegler, E., Lamarque, J.-F., Lowe, J., Meehl, G. A., Moss, R., Riahi, K., & Sanderson, B. M. (2016). The scenario model intercomparison project (ScenarioMIP) for CMIP6. *Geoscientific Model Development*, *9*(9), 3461–3482. https://doi.org/10.5194/gmd-9-3461-2016

Orosa, J. A., & Oliveira, A. C. (2011). A new thermal comfort approach comparing adaptive and PMV models. *Renewable Energy*, *36*(3), 951–956. https://doi.org/10.1016/j.renene.2010.09.013

Paulson, B. C. (1976). Designing to Reduce Construction Costs. *Journal of the Construction Division*, *102*(4), 587–592.

Phillips, S. (2010). Parametric design: A brief history. *arcCA Magazine*, *10.1*, 24–28.

Rahif, R., Hamdy, M., Homaei, S., Zhang, C., Holzer, P., & Attia, S. (2022). Simulation-based framework to evaluate resistivity of cooling strategies in buildings against overheating impact of climate change. *Building and Environment*, *208*, 108599. https://doi.org/10.1016/j.buildenv.2021.108599

Ranasinghe, R., Ruane, A. C., Vautard, R., Arnell, N., Coppola, E., Cruz, F. A., Dessai, S., Islam, A. S., Rahimi, M., Ruiz Carrascal, D., Sillmann, J., Sylla, M. B., Tebaldi, C., Wang, W., & Zaaboul, R. (2021). Climate change information for regional impact and for risk assessment. In V. Masson-Delmotte, P. Zhai, A. Pirani, S. L. Connors, C. Péan, S. Berger, N. Caud, Y. Chen, L. Goldfarb, M. I. Gomis, M. Huang, K. Leitzell, E. Lonnoy, J. B. R. Matthews, T. K. Maycock, T. Waterfield, O. Yelekçi, R. Yu, & B. Zhou (Eds.), *Climate change 2021: The physical science basis. Contribution of working group I to the sixth assessment report of the intergovernmental panel on climate change* (pp. 1767–1926). Cambridge University Press. https://doi.org/10.1017/9781009157896.014

Rasheed, A., & Robinson, D. (2012). The Urban Climate. In *Computer Modelling for Sustainable Urban Design* (pp. 75–112). Routledge.

Razavi, S., & Gupta, H. V. (2015). What do we mean by sensitivity analysis? The need for comprehensive characterization of "global" sensitivity in E arth and E nvironmental systems models. *Water Resources Research*, *51*(5), 3070–3092. https://doi.org/10.1002/2014WR016527

Rentfro, S., & Gumpertz, S. (2020). *Calculating Fenestration System U-Factor, SHGC, and VT using partially automated workflows*.

Rey-Hernández, J. M., Yousif, C., Gatt, D., Velasco-Gómez, E., San José-Alonso, J., & Rey-Martínez, F. J. (2018). Modelling the long-term effect of climate change on a zero energy and carbon dioxide building through energy efficiency and renewables. *Energy and Buildings*, *174*, 85–96. https://doi.org/10.1016/j.enbuild.2018.06.006

Robinson, D., & Bruse, M. (2012). Pedestrian comfort. In *Computer modelling for sustainable urban design* (pp. 113–128). Routledge.

Robinson, D., Campbell, N., Gaiser, W., Kabel, K., Le-Mouel, A., Morel, N., Page, J., Stankovic, S., & Stone, A. (2007). SUNtool – A new modelling paradigm for

simulating and optimising urban sustainability. *Solar Energy*, *81*(9), 1196–1211. https://doi.org/10.1016/j.solener.2007.06.002

Robinson, D., & Haldi, F. (2008). An integrated adaptive model for overheating risk prediction. *Journal of Building Performance Simulation*, *1*(1), 43–55. https://doi.org/10.1080/19401490801906460

Robinson, D., Haldi, F., Kampf, J., & Perez, D. (2012). Building Modelling. In *Computer Modelling for Sustainable Urban Design* (pp. 131–166). Routledge.

Robinson, P. J. (2001). On the Definition of a Heat Wave. *Journal of Applied Meteorology*, *40*(4), 762–775. https://doi.org/10.1175/1520-0450(2001)040<0762:OTDOAH>2.0.CO;2

Rodrigues, E., Fernandes, M. S., & Carvalho, D. (2023). Future weather generator for building performance research: An open-source morphing tool and an application. *Building and Environment*, *233*, 110104. https://doi.org/10.1016/j.buildenv.2023.110104

Rodriguez-Nikl, T. (2015). Linking disaster resilience and sustainability. *Civil Engineering and Environmental Systems*, *32*(1–2), 157–169. https://doi.org/10.1080/10286608.2015.1025386

Schaudienst, F., & Vogdt, F. U. (2017). Fanger's model of thermal comfort: A model suitable just for men? *Energy Procedia*, *132*, 129–134. https://doi.org/10.1016/j.egypro.2017.09.658

Schwartz, Y., Raslan, R., Korolija, I., & Mumovic, D. (2021). A decision support tool for building design: An integrated generative design, optimisation and life cycle performance approach. *International Journal of Architectural Computing*, *19*(3), 401–430. https://doi.org/10.1177/1478077121999802

Seabold, S., & Perktold, J. (2010). *Statsmodels: Econometric and Statistical Modeling with Python*. 92–96. https://doi.org/10.25080/Majora-92bf1922-011

Seaborn: Statistical data visualization—Seaborn 0.13.0 documentation. (n.d.). Retrieved 31 December 2023, from https://seaborn.pydata.org/index.html

Seneviratne, S. I., Zhang, X., Adnan, M., Badi, W., Dereczynski, C., Di Luca, A., Ghosh, S., Iskandar, I., Kossin, J., Lewis, S., Otto, F., Pinto, I., Satoh, M., Vicente-Serrano, S. M., Wehner, M., & Zhou, B. (2021). Weather and climate extreme events in a changing climate. In V. Masson-Delmotte, P. Zhai, A. Pirani, S. L. Connors, C. Péan, S. Berger, N. Caud, Y. Chen, L. Goldfarb, M. I. Gomis, M. Huang, K. Leitzell, E. Lonnoy, J. B. R. Matthews, T. K. Maycock, T. Waterfield, O. Yelekçi, R. Yu, & B. Zhou (Eds.), *Climate change 2021: The physical science basis. Contribution of working group I to the sixth assessment report of the intergovernmental panel on climate change* (pp. 1513–1766). Cambridge University Press. https://doi.org/10.1017/9781009157896.013

Sharifi, A. (2022). Cities in the Context of Global Change: Challenges and the Need for Smart and Resilient Cities. In P. Salehi & Ayyoob (Eds.), *Resilient Smart Cities: Theoretical and Empirical Insights*. Springer International Publishing. https://doi.org/10.1007/978-3-030-95037-8

Sharma, D., Singh, R., & Singh, R. (2014). Building urban climate resilience: Learning from the ACCCRN experience in India. *International Journal of Urban*

Sustainable Development, *6*(2), 133–153. https://doi.org/10.1080/19463138.2014.937720

Sheil, B. (2020). From Making Digital Architecture to Making Resilient Architecture. In J. Burry, J. Sabin, B. Sheil, & M. Skavara (Eds.), *MAKING RESILIENT ARCHITECTURE*.

Sijakovic, M., Peric, A., & Ayuso Ollero, P. (2021). Towards resilient design of the building asset: The BREEAM-based evaluation of the Z Hotel Holborn, London. *International Journal of Disaster Resilience in the Built Environment*, *12*(1), 85–100. https://doi.org/10.1108/IJDRBE-05-2020-0038

Simulated historical climate & weather data for Bamberg—Meteoblue. (n.d.). Retrieved 15 December 2023, from https://www.meteoblue.com/en/weather/historyclimate/climatemodelled/bamberg_germany_2952984

Sobek, W. (2022). *Non nobis-über das Bauen in der Zukunft—Buch 1. Ausgehen muss man von dem, was ist*. Avedition.

Sobol′, I. M. (2001). Global sensitivity indices for nonlinear mathematical models and their Monte Carlo estimates. *Mathematics and Computers in Simulation*, *55*(1–3), 271–280. https://doi.org/10.1016/S0378-4754(00)00270-6

Spitler, J. D. (2011). Thermal load and energy performance prediction. In J. L. M. Hensen & R. Lamberts (Eds.), *Building Performance Simulation for Design and Operation* (pp. 73–131).

Stagrum, A. E., Andenæs, E., Kvande, T., & Lohne, J. (2020). Climate Change Adaptation Measures for Buildings—A Scoping Review. *Sustainability*, *12*(5), 1721. https://doi.org/10.3390/su12051721

Statsmodels 0.15.0 (+180). (n.d.). Retrieved 31 December 2023, from https://www.statsmodels.org/dev/index.html

Stead, D. (2014). Urban planning, water management and climate change strategies: Adaptation, mitigation and resilience narratives in the Netherlands. *International Journal of Sustainable Development & World Ecology*, *21*(1), 15–27.

Takewaki, I., Moustafa, A., & Fujita, K. (2013). *Improving the Earthquake Resilience of Buildings: The worst case approach*. Springer London. https://doi.org/10.1007/978-1-4471-4144-0

Tokgoz, B. E., & Gheorghe, A. V. (2013). Resilience quantification and its application to a residential building subject to hurricane winds. *International Journal of Disaster Risk Science*, *4*(3), 105–114. https://doi.org/10.1007/s13753-013-0012-z

Tyler, S., & Moench, M. (2012). A framework for urban climate resilience. *Climate and Development*, *4*(4), 311–326. https://doi.org/10.1080/17565529.2012.745389

United Nations. (1987). Report of the World Commission on Environment and Development: Our common future. *Accessed Feb*, *10*, 1–300.

United Nations. (2015). *Resolution adopted by the General Assembly on 25 September 2015, Transforming our world: The 2030 Agenda for Sustainable Development (A/RES/70/1)*.

United Nations Framework Convention on Climate Change (UNFCCC). (2016). *The Paris Agreement*.

Van Hoof, J. (2008). Forty years of Fanger's model of thermal comfort: Comfort for all? *Indoor Air*, *18*(3), 182–201. https://doi.org/10.1111/j.1600-0668.2007.00516.x

Van Treeck, C. (2011). Indoor thermal quality performance prediction. In J. L. M. Hensen & R. Lamberts (Eds.), *Building Performance Simulation for Design and Operation* (pp. 169–223).

Van Vuuren, D. P., Edmonds, J., Kainuma, M., Riahi, K., Thomson, A., Hibbard, K., Hurtt, G. C., Kram, T., Krey, V., Lamarque, J.-F., Masui, T., Meinshausen, M., Nakicenovic, N., Smith, S. J., & Rose, S. K. (2011). The representative concentration pathways: An overview. *Climatic Change*, *109*(1–2), 5–31. https://doi.org/10.1007/s10584-011-0148-z

Vollmer, M., Theilig, K., Takser, I., Reitberger, R., & Lang, W. (2023). Life cycle-based parametric optimization of buildings towards climate neutrality and its implications for environmental protection. *IOP Conference Series: Earth and Environmental Science*, *1196*(1), 012050. https://doi.org/10.1088/1755-1315/1196/1/012050

Wagner, A., Gossauer, E., Moosmann, C., Gropp, Th., & Leonhart, R. (2007). Thermal comfort and workplace occupant satisfaction—Results of field studies in German low energy office buildings. *Energy and Buildings*, *39*(7), 758–769. https://doi.org/10.1016/j.enbuild.2007.02.013

Wang, H., & Chen, Q. (2014). Impact of climate change heating and cooling energy use in buildings in the United States. *Energy and Buildings*, *82*, 428–436. https://doi.org/10.1016/j.enbuild.2014.07.034

WeatherShift. (n.d.). Retrieved 26 April 2023, from https://www.weathershift.com/

Wetter, M. (2004). *Simulation-Based Building Energy Optimization* [Phd dissertation]. University of California, Berkeley.

Wohngebäude nach Baujahr | Statistikportal.de. (n.d.). Retrieved 20 December 2023, from https://www.statistikportal.de/de/wohngebaeude-nach-baujahr

Wu, Y., Zhang, S., Liu, H., & Cheng, Y. (2023). Thermal sensation and percentage of dissatisfied in thermal environments with positive and negative vertical air temperature differences. *Energy and Built Environment*, *4*(6), 629–638. https://doi.org/10.1016/j.enbenv.2022.06.002

Zeng, Z., Tan, H., Hu, Y., Rastogi, P., Wang, J., & Muehleisen, R. (2023). *A critical analysis of future weather data for building and energy modeling*.

Zhang, X., Trame, M., Lesko, L., & Schmidt, S. (2015). Sobol Sensitivity Analysis: A Tool to Guide the Development and Evaluation of Systems Pharmacology Models. *CPT: Pharmacometrics & Systems Pharmacology*, *4*(2), 69–79. https://doi.org/10.1002/psp4.6

Table of Figures

Table of Tables

Annex

5.2   Risk of heat stress on population

The maps of risk of heat stress on population are shown in Map 2 for the baseline climate (first column) and for the very high emissions scenario (second column) as well as considering the risk calculation with absolute exposure (first row) and with relative exposure (second row). The indicators used in this impact chain for all the risk components can be found in Table 2.

The Map 2 shows that the risk is expected to increase from the baseline climate (1981-2010) to the very high emissions scenario at the end of the century (RCP8.5 in 2070-2100), and it shows a distinct north-south pattern, with southern areas being the most affected for RCP8.5 in the 2070-2100 period.

A result of interest arises from comparing the risk in the very high emissions scenario at the end of the century with absolute exposure and the risk with relative exposure. This is the case for example in Paris, where the total population is divided between the four NUTS3 that form the metropolitan area, resulting in a limited absolute exposure and therefore a lower risk, while the population density is considerably high, making the relative exposure very high and therefore the risk with relative exposure very high.

Maps of all risk components (hazard, exposure, sensitivity, adaptive capacity, vulnerability and risk) as well as the low emissions and intermediate emissions scenarios (RCP2.6 and RCP4.5 respectively) can be found in the high-resolution map annex.

Map 2 Risk scenarios of heat stress on population. In rows, absolute and relative exposure. In columns, baseline climate and very high emissions scenario.

meteoblue
weather ☀ close to you
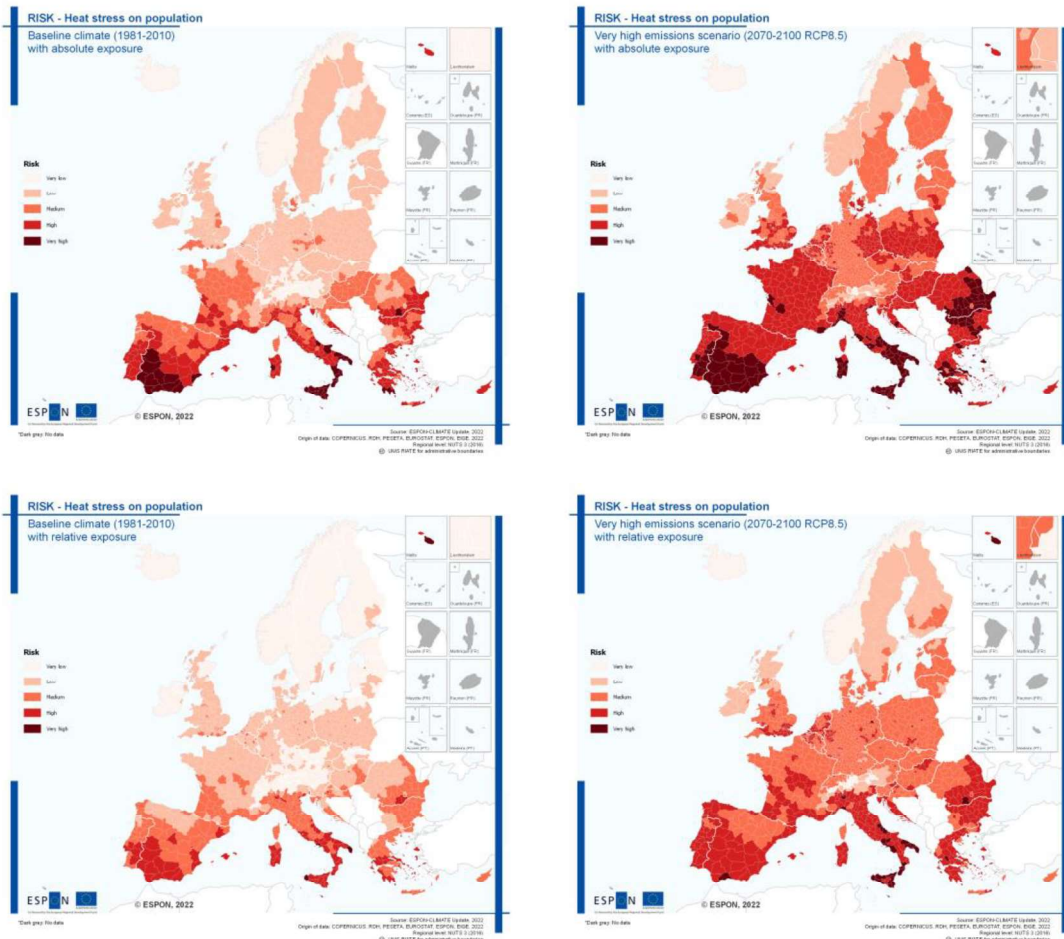
Simulated historical climate
& weather data for Bamberg

Bavaria, Germany, 49.9°N 10.9°E, 243m asl

The meteoblue climate diagrams are based on 30 years of hourly weather model simulations and available for every place on Earth. They give good indications of typical climate patterns and expected conditions (temperature, precipitation, sunshine and wind). The simulated weather data have a spatial resolution of approximately 30 km and may not reproduce all local weather effects, such as thunderstorms, local winds, or tornadoes, and local differences as they occur in urban, mountainous, or coastal areas.

You can explore the climate for any location like the Amazon rainforest, West-Africa savannas, Sahara desert, Siberian Tundra or the Himalaya.

Hourly historical weather data since 1940 for Bamberg can be purchased with history+. Download variables such as temperature, wind, clouds and precipitation as CSV for any place on Earth.

Average temperatures and precipitation
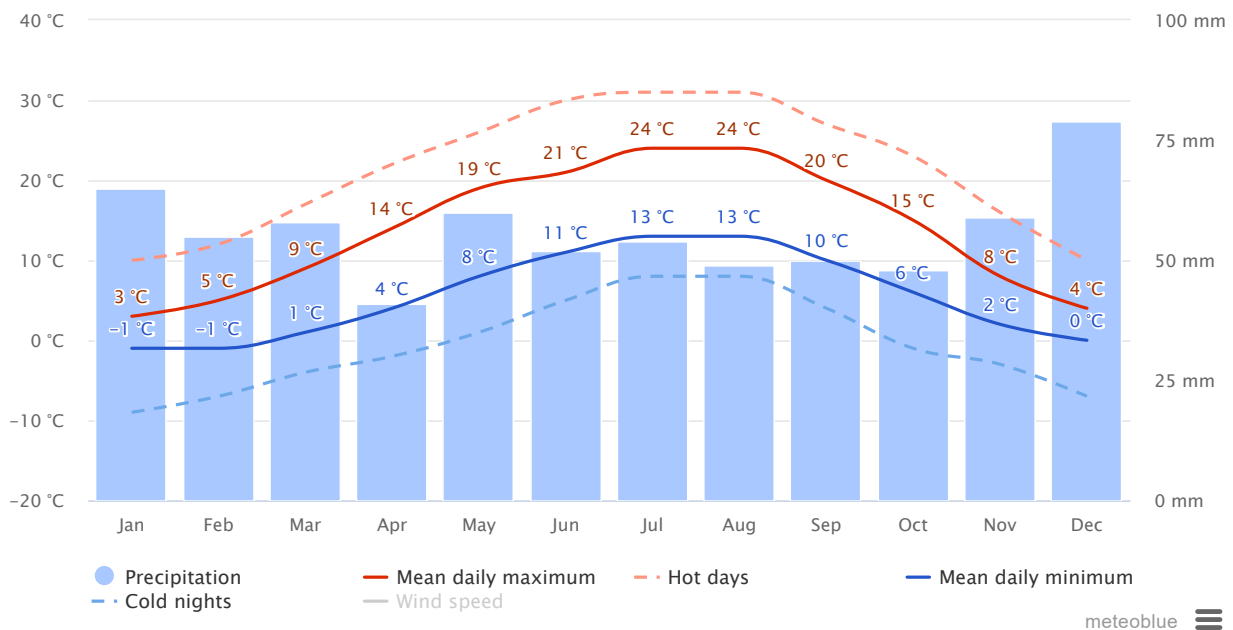
The "mean daily maximum" (solid red line) shows the maximum temperature of an average day for every month for Bamberg. Likewise, "mean daily minimum" (solid blue line) shows the average minimum temperature. Hot days and cold nights (dashed red and blue lines) show the average of the hottest day and coldest night of each month of the last 30 years. For vacation planning, you can expect the mean temperatures, and be prepared for hotter and colder days. Wind speeds are not displayed per default, but can be enabled at the bottom of the graph.

The precipitation chart is useful to plan for seasonal effects such as monsoon climate in India or wet season in Africa. Monthly precipita tions above 150mm are mostly wet, below 30mm mostly dry. Note: Simulated precipitation amounts in tropical regions and complex terrain tend to be lower than local measurements.

Cloudy, sunny, and precipitation days
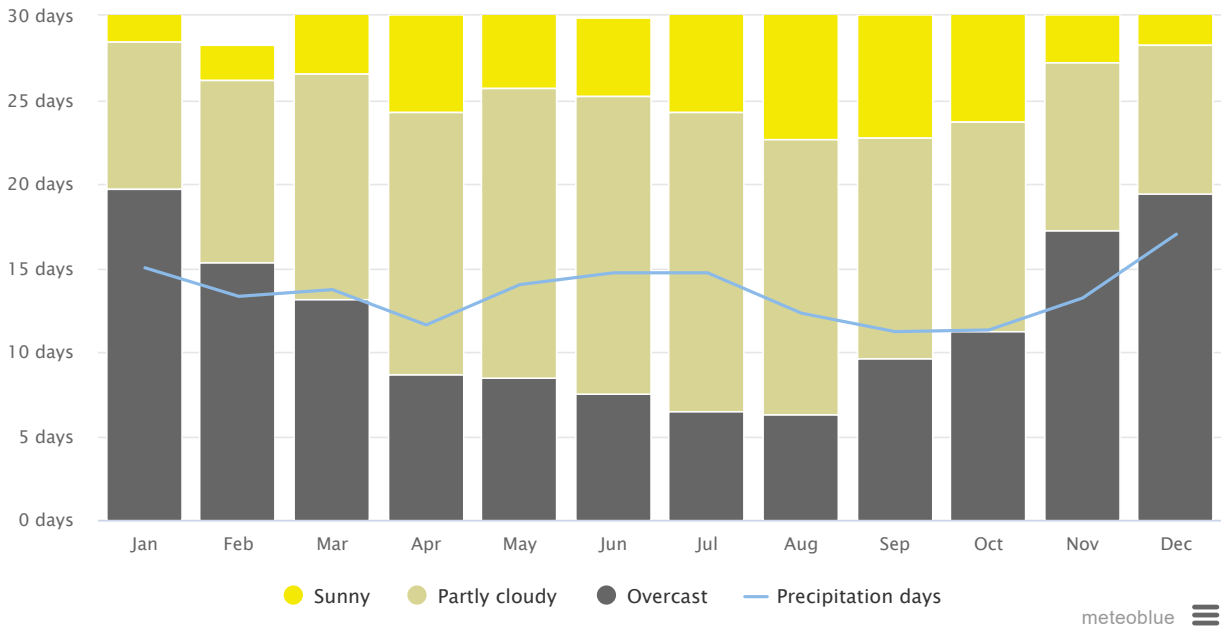
The graph shows the monthly number of sunny, partly cloudy, overcast and precipitation days. Days with less than 20% cloud cover are considered as sunny, with 20-80% cloud cover as partly cloudy and with more than 80% as overcast. While Reykjavík on Iceland has mostly cloudy days, Sossusvlei in the Namib desert is one of the sunniest places on earth.

Note: In tropical climates like in Malaysia or Indonesia the number of precipitation days may be overestimated by a factor up to 2.

Maximum temperatures
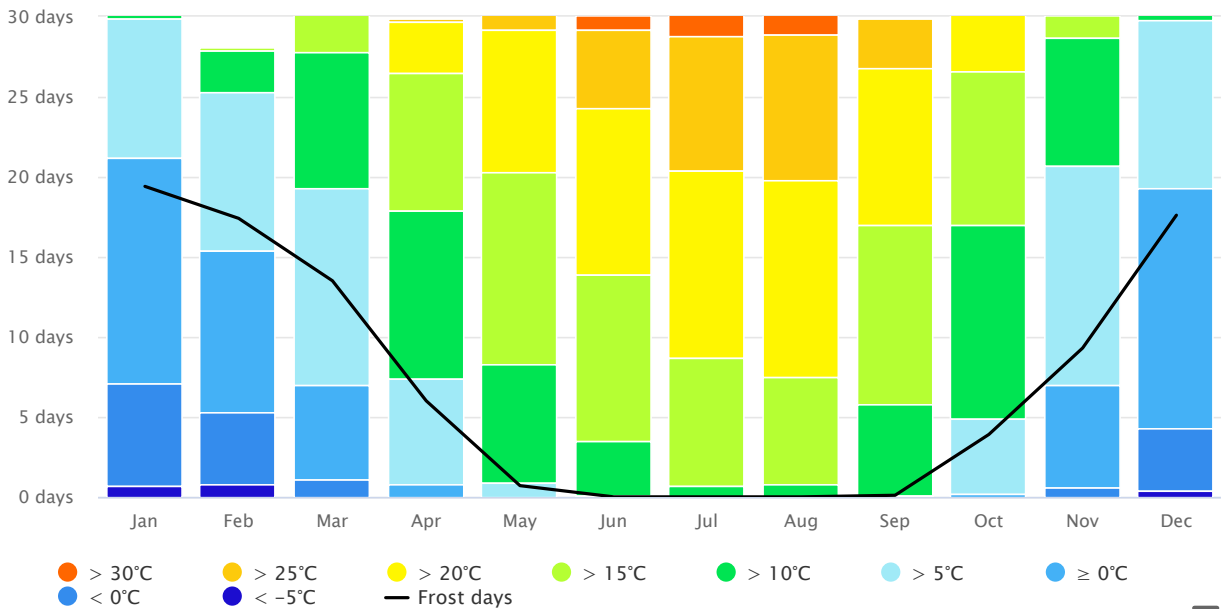
The maximum temperature diagram for Bamberg displays how many days per month reach certain temperatures. Dubai, one of the hottest cities on earth, has almost none days below 40°C in July. You can also see the cold winters in Moscow with a few days that do not even reach -10°C as daily maximum.

Precipitation amounts
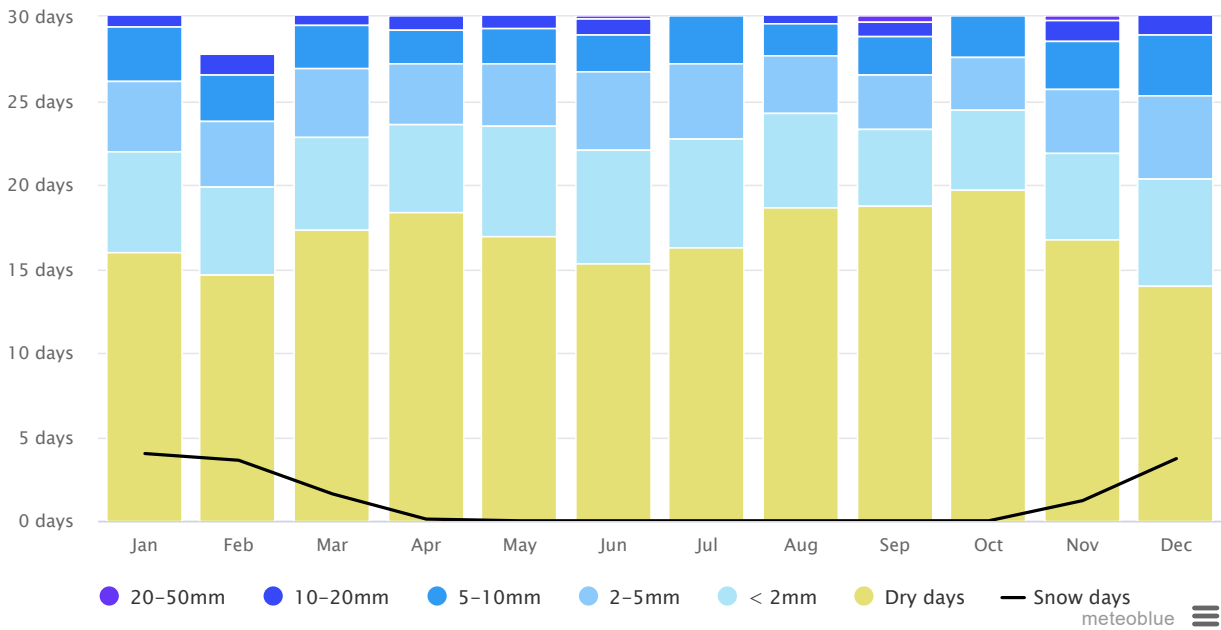
The precipitation diagram for Bamberg shows on how many days per month, certain precipitation amounts are reached. In tropical and monsoon climates, the amounts may be underestimated.

Wind speed
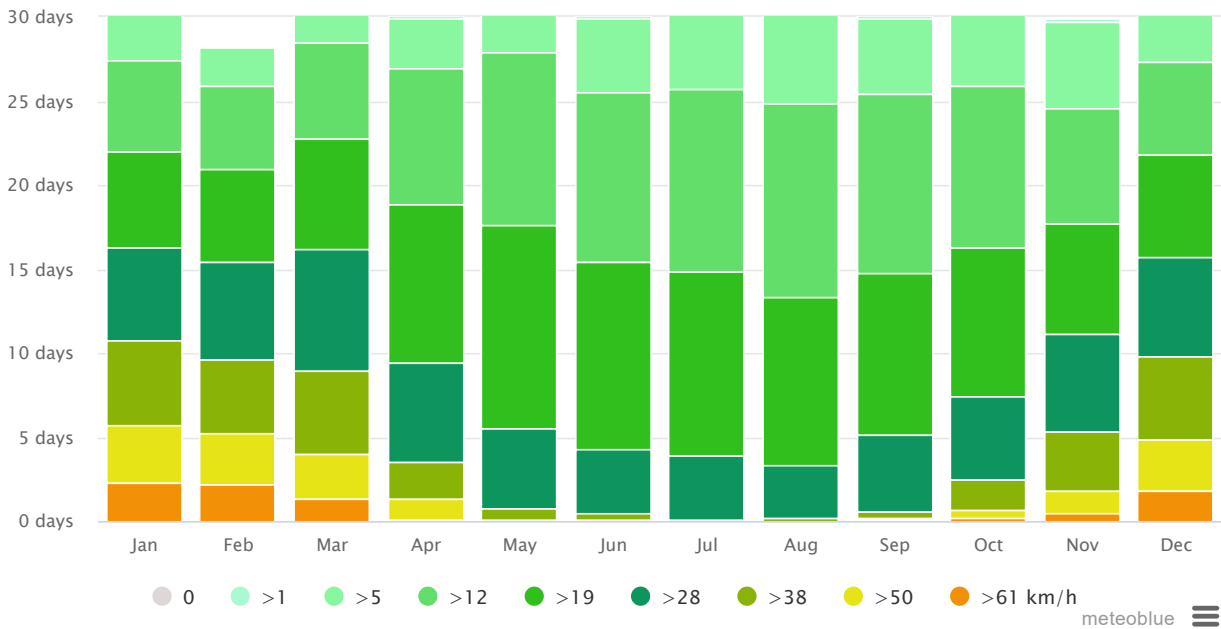
The diagram for Bamberg shows the days per month, during which the wind reaches a certain speed. An interesting example is the Tibetan Plateau, where the monsoon creates steady strong winds from December to April, and calm winds from June to October.

Wind speed units can be changed in the preferences (top right).

Wind rose
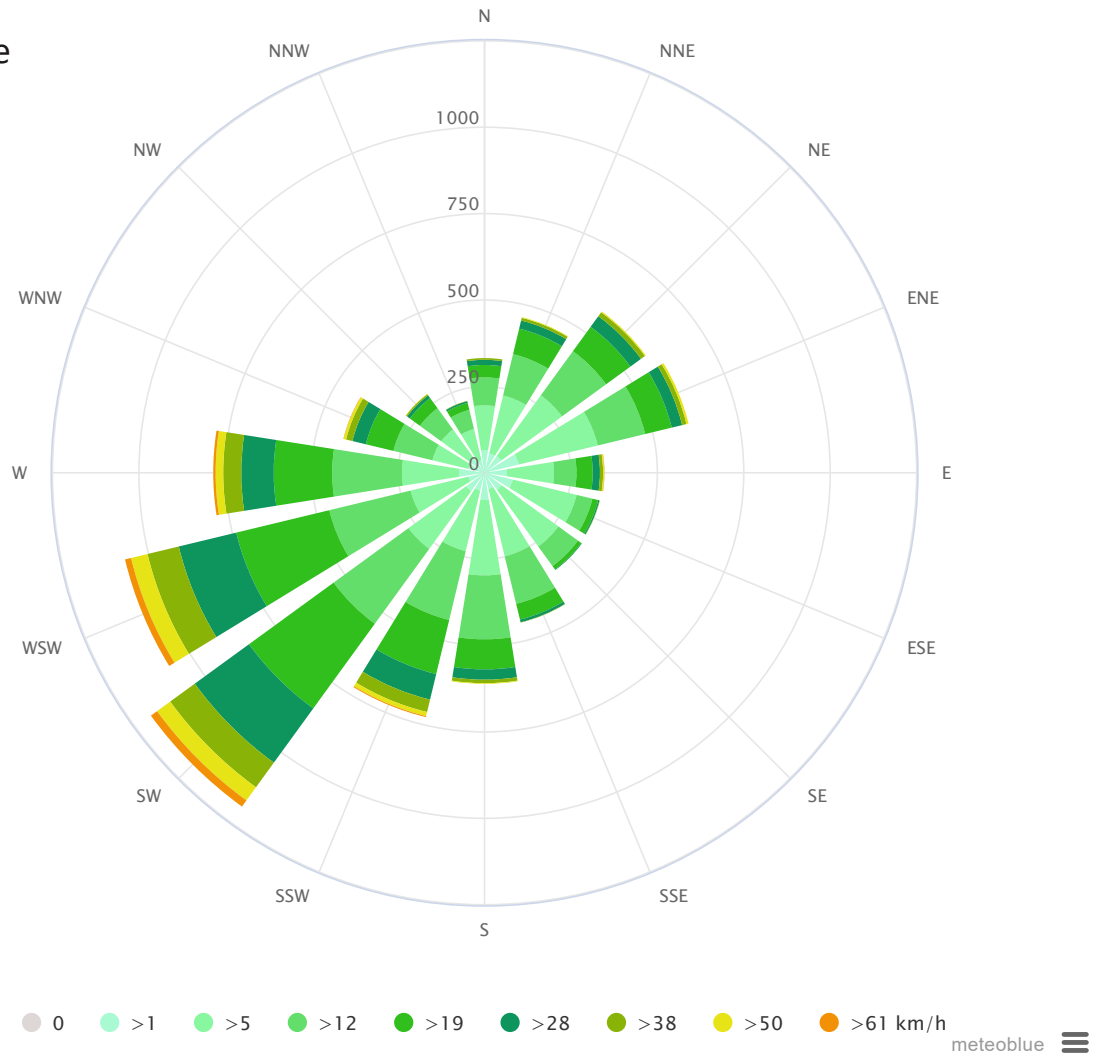
The wind rose for Bamberg shows how many hours per year the wind blows from the indicated direction. Example SW: Wind is blowing from South-West (SW) to North-East (NE). Cape Horn, the southernmost land point of South America, has a characteristic strong westwind, which makes crossings from East to West very difficult especially for sailing boats.

General information

Since 2007, meteoblue has been archiving weather model data. In 2014 we started to calculate weather models with historical data from 1985 onwards and generated a continuous 30-year global history with hourly weather data. The climate diagrams are the first simulated climate data-set made public on the net. Our weather history covers any place on earth at any given time regardless of availability of weather stations.

The data is derived from our global NEMS weather model at approximately 30km resolution and cannot reproduce detail local weather effects, such as heat islands, cold air flows, thunderstorms or tornadoes. For locations and events which require very high precision (such as energy generation, insurance, town planning, etc.), we offer high resolution simulations with hourly data through point+, hisTory+ and our API.

License

Construction sets are based on Eco+ material sets, but may differ from the original list.

V01_Sandlime

material	thickness [m]	conductivity [W/m*K]	density [kg/m3]	spec heat [J/kg*K]	part of the layer
EXTERNAL WALL					
Lime plaster	0.020	0.85	1800	970	
Expanded polystyrene 220	0.220	0.035	15	1450	
Sand-lime brick	0.180	0.99	1800	1300	
Gypsum interior plaster	0.020	0.85	1800	970	
INTERNAL WALL					
Fire-resistant plasterboard	0.025	0.58	800	1089	
Aluminium frame	0.075	237	2700	910	*0.2
Mineral wool 75	0.075	0.035	26	840	*0.8
Fire-resistant plasterboard	0.025	0.58	800	1089	
ROOF					
Green roof extensive	0.150	0.35	1100	1200	
Bitumen sheets 01	0.010				
Bitumen sheets 003	0.003	0.5	1700	1000	
Expanded polystyrene 240	0.240	0.035	15	1450	
Bitumen sheets 001	0.001	0.5	1700	1000	
Concrete C20/25 18	0.180	1.3	2297	1000	*0.98
Reinforcement steel wire 18		45	7850	420	*0.02
FOUNDATION					
Cement screed	0.060	1.4	2000	1000	
Damp insulation PE	0.000	0.34	950	2300	
Expanded polystyrene 30	0.030	0.035	15	1450	
Mineral wool 40	0.040	0.035	85	840	
Bitumen sheets 002	0.002	0.5	1700	1000	
Concrete C20/25 30	0.300	1.3	2297	1000	*0.98
Reinforcement steel wire 30	0.000	45	7850	420	*0.02
Extruded polystyrene	0.140	0.033	32	1500	
INTERNAL WALL					
Cement screed	0.060	1.4	2000	1000	
Damp insulation PE	0.000	0.34	950	2300	
Expanded polystyrene 30	0.030	0.035	15	1450	
Mineral wool 40	0.040	0.035	85	840	
Concrete C20/25 18	0.180	1.3	2297	1000	*0.98
Reinforcement steel wire 18		45	7850	420	*0.02

Construction sets are based on Eco+ material sets, but may differ from the original list.

V02_Brick

material	thickness [m]	conductivity [W/m*K]	density [kg/m3]	spec heat [J/kg*K]	part of the layer
EXTERNAL WALL					
Lime plaster	0.020	0.85	1800	970	
Expanded polystyrene 60	0.060	0.035	15	1450	
Brick (filled with insulating material)	0.365	0.075	605	1000	
Gypsum interior plaster	0.020	0.85	1800	970	
INTERNAL WALL					
Fire-resistant plasterboard	0.025	0.58	800	1089	
Aluminium frame	0.075	237	2700	910	*0.2
Mineral wool 75	0.075	0.035	26	840	*0.8
Fire-resistant plasterboard	0.025	0.58	800	1089	
ROOF					
Green roof extensive	0.150	0.35	1100	1200	
Bitumen sheets 01	0.010				
Bitumen sheets 003	0.003	0.5	1700	1000	
Expanded polystyrene	0.240	0.035	15	1450	
Bitumen sheets 001	0.001	0.5	1700	1000	
Concrete C20/25 18	0.180	1.3	2297	1000	*0.98
Reinforcement steel wire 18		45	7850	420	*0.02
FOUNDATION					
Cement screed	0.060	1.4	2400	1000	
Damp insulation PE	0.000	0.34	950	2300	
Expanded polystyrene	0.030	0.035	15	1450	
Mineral wool 40	0.040	0.035	85	840	
Bitumen sheets 002	0.002	0.5	1700	1000	
Concrete C20/25 30	0.300	1.3	2297	1000	*0.98
Reinforcement steel wire 30	0.000	45	7850	420	*0.02
Extruded polystyrene	0.140	0.033	32	1500	
INTERNAL WALL					
Cement screed	0.060	1.4	2400	1000	
Damp insulation PE	0.000	0.34	950	2300	
Expanded polystyrene	0.030	0.035	15	1450	
Mineral wool 40	0.040	0.035	85	840	
Concrete C20/25 18	0.180	1.3	2297	1000	*0.98
Reinforcement steel wire 18		45	7850	420	*0.02

Construction sets are based on Eco+ material sets, but may differ from the original list.

V03_WoodMassive

material	thickness [m]	conductivity [W/m*K]	density [kg/m3]	spec heat [J/kg*K]	part of the layer
EXTERNAL WALL					
Coniferous lumber - kiln dried 24	0.024	0.13	485	1700	
Coniferous lumber - kiln dried 30	0.030	0.13	485	1700	
Damp insulation PE 1	0.001	0.34	950	2300	
Wood fiber insulation 160	0.160	0.05	162	2100	*0.99
KVH structural timber	0.160	0.13	493.0	1,600.0	*0.01
Coniferous lumber - kiln dried 30	0.030	0.13	485	1700	
Wood fiber insulation 40	0.040	0.05	162	2100	
Coniferous lumber - kiln dried 24	0.024	0.13	485	1700	
INTERNAL WALL					
Clay panel	0.022	0.13	700	1450	
Aluminium frame	0.075	237	2700	910	
Mineral wool 75	0.075	0.035	26	840	
Clay panel	0.022	0.13	700	1450	
ROOF					
Green roof extensive	0.150	0.35	1100	1200	
Bitumen sheets 01	0.010				
Bitumen sheets 003	0.003	0.5	1700	1000	
Wood fiber insulation 160	0.160	0.05	162	2100	
Bitumen sheets 001	0.000	0.5	1700	1000	
Glued laminated timber 180	0.180	0.13	507	2100	*0.70
FOUNDATION					
Cement screed	0.060	1.4	2400	1000	
Damp insulation PE	0.000	0.34	950	2300	
Wood fiber insulation 30	0.030	0.05	162	2100	
Wood fiber insulation 40	0.040	0.05	162	2100	
Bitumen sheets 002	0.002	0.5	1700	1000	
Concrete C20/25 30	0.300	1.3	2297	1000	*0.98
Reinforcement steel wire 30	0.000	45	7850	420	*0.02
Extruded polystyrene	0.140	0.033	32	1500	
INTERNAL WALL					
Cement screed	0.060	1.4	2400	1000	
Damp insulation PE	0.000	0.34	950	2300	
Wood fiber insulation 30	0.030	0.05	162	2100	
Aerated concrete granulate	0.060	0.8	400	1000	
Damp insulation PE	0.001	0.34	950	2300	
Glued laminated timber 180	0.180	0.13	507	2100	

Construction sets are based on Eco+ material sets, but may differ from the original list.

V04_WoodLight

material	thickness [m]	conductivity [W/m*K]	density [kg/m3]	spec heat [J/kg*K]	part of the layer
EXTERNAL WALL					
Coniferous lumber - kiln dried 24	0.024	0.13	485	1700	
Expanded polystyrene	0.030	0.13	485	1700	
Damp insulation PE 1	0.001	0.34	950	2300	
KVH structural timber	0.200	0.13	493.0	1,600.0	*0.99
Wood fiber insulation 160	0.200	0.05	162	2100	*0.01
Damp insulation PE 1	0.001	0.34	950	2300	
Coniferous lumber - kiln dried 30	0.030	0.13	485	1700	*0.01
Wood fiber insulation 40	0.030	0.05	162	2100	*0.99
Coniferous lumber - kiln dried 24	0.024				
INTERNAL WALL					
Clay panel	0.022	0.13	700	1450	
Aluminium frame	0.075	237	2700	910	
Mineral wool 75	0.075	0.035	26	840	
Clay panel	0.022	0.13	700	1450	
ROOF					
Green roof extensive	0.150	0.35	1100	1200	
Bitumen sheets 01	0.010				
Bitumen sheets 003	0.003	0.5	1700	1000	
Wood fiber insulation 260	0.260	0.05	162	2100	
Bitumen sheets 001	0.000	0.5	1700	1000	
3- and 5-layer solid wood panel	0.028	0.12	510	1600	
Glued laminated timber 140	0.140	0.13	507	2100	
3- and 5-layer solid wood panel	0.028	0.13	450	2100	
FOUNDATION					
Cement screed	0.060	1.4	2400	1000	
Damp insulation PE	0.000	0.34	950	2300	
Wood fiber insulation 30	0.030	0.05	162	2100	
Wood fiber insulation 40	0.040	0.05	162	2100	
Bitumen sheets 002	0.002	0.34	950	2300	
Concrete C20/25 30	0.300	1.3	2297	1000	*0.98
Reinforcement steel wire 30	0.000	45	7850	420	*0.02
Extruded polystyrene	0.140	0.033	32	1500	
INTERNAL WALL					
Cement screed	0.060	1.4	2400	1000	
Damp insulation PE	0.000	0.34	950	2300	
Wood fiber insulation 30	0.040	0.05	162	2100	
Aerated concrete granulate	0.060	0.8	400	1000	
Cross laminated timber	0.028	0.13	489	2100	
Glued laminated timber 220	0.220	0.13	507	2100	*0.70

Original material list of the ECO+ Project

V01_Sandlime

	Bezeichnur		Bauteilaufbau	Nutzungs dauer	Datensatz
	-	[mm]	Material	[a]	
External Wall	**AW-01**				
		20.0	Außenputz	40.0	Kalkputzmörtel
		220.0	Wärmedämmung	40.0	EPS-Hartschaum (Rohdichte 15 kg/m³)
		180.0	Kalk-Sandstein	50.0	Kalksandstein
		20.0	Innenputz	50.0	Gipsputz (innen)
Internal Wall	**IW-01**				
	GK Metallst	25.0	Gipskartonplatte 2 x 12,5mm	50.0	GIPSPLATTE - FEUERSCHUTZ / Tool
		75.0	Metallständer (e=0,625m)	50.0	Aluminiumblech
		75.0	Mineralwolle	50.0	Mineralwolle (Innenausbau-Dämmung)
		25.0	Gipskartonplatte 2 x 12,5mm	50.0	GIPSPLATTE - FEUERSCHUTZ / Tool
Roof	**DA-01**				
	Warmdach	150.0	Extensive Dachbegrünung	40.0	Gründach extensiv (ohne Geländer)
		10.0	Schutz, Drän- und Filterschicht	40.0	
		3.0	Dachabdichtung	40.0	Bitumenbahnen G 200 S4
		240.0	Wärmedämmung	50.0	EPS-Hartschaum (Rohdichte 15 kg/m³)
		1.0	Abdichtung	50.0	Bitumenbahnen G 200 S4
		180.0	Stahlbeton 2 % Bewehrungsstahl	50.0	Transportbeton C20/25
			Bewehrungsdstahl	50.0	Bewehrungsstahl
Founda- tion	**G-01**				
	Bodenplatte	60.0	Zementestrich	50.0	Zementestrich
		0.4	Trennlage	50.0	Dampfbremse PE
		30.0	Trittschalldämmung	50.0	EPS-Hartschaum (Rohdichte 15 kg/m³)
		40.0	Wärmedämmung	50.0	Mineralwolle (Boden-Dämmung)
		2.0	Abdichtung	50.0	Bitumenbahnen G 200 S4
		300.0	Stahlbeton 2 % Bewehrungsstahl	50.0	Transportbeton C20/25
			Bewehrungsstahl	50.0	Bewehrungsstahl
		140.0	Wärmedämmung	50.0	Extrudierter Polystyrol Dämmstoff (XPS)
Ceiling	**DE-01**				
		60.0	Zementestrich	50.0	Zementestrich
		0.4	Trennlage	50.0	Dampfbremse PE
		30.0	Trittschalldämmung	50.0	EPS-Hartschaum (Rohdichte 15 kg/m³)
		40.0	Wärmedämmung	50.0	Mineralwolle (Boden-Dämmung)
		180.0	Stahlbeton 2 % Bewehrungsstahl	50.0	Transportbeton C20/25
			Bewehrungsstahl	50.0	Bewehrungsstahl
Window	**FE-01**				
			Flügelrahmen Kunststoff	40.0	Flügelrahmen PVC-U
			Blendrahmen Kunststoff	40.0	Blendrahmen PVC-U
			Dreischeiben-Isolierverglasung	30.0	Dreifachverglasung

Original material list of the ECO+ Project

V02_Brick

	Bezeichnur	Bauteilaufbau		Nutzungs dauer	Datensatz
	-	[mm]	Material	[a]	
	AW-01				
		20.0	Außenputz	40.0	Kalkputzmörtel
		60.0	Wärmedämmung	40.0	EPS-Hartschaum (Rohdichte 15 kg/m³)
External Wall		365.0	Wärmedämm-Ziegel	50.0	Mauerziegel (mit Dämmstoff gefüllt)
		20.0	Innenputz	50.0	Gipsputz (innen)
	IW-01				
	GK Metallst	25.0	Gipskartonplatte 2 x 12,5mm	50.0	GIPSPLATTE - FEUERSCHUTZ / Tool
		75.0	Metallständer (e=0,625m)	50.0	Aluminiumblech
Internal Wall		75.0	Mineralwolle	50.0	Mineralwolle (Innenausbau-Dämmung)
		25.0	Gipskartonplatte 2 x 12,5mm	50.0	GIPSPLATTE - FEUERSCHUTZ / Tool
	DA-01				
	Warmdach	150.0	Extensive Dachbegrünung	40.0	Gründach extensiv (ohne Geländer)
		10.0	Schutz, Drän- und Filterschicht	40.0	
Roof		3.0	Dachabdichtung	40.0	Bitumenbahnen G 200 S4
		240.0	Wärmedämmung	50.0	EPS-Hartschaum (Rohdichte 15 kg/m³)
		1.0	Abdichtung	50.0	Bitumenbahnen G 200 S4
		180.0	Stahlbeton 2 % Bewehrungsstahl	50.0	Transportbeton C20/25
			Bewehrungsstahl	50.0	Bewehrungsstahl
	G-01				
	Bodenplatte	60.0	Zementestrich	50.0	Zementestrich
		0.4	Trennlage	50.0	Dampfbremse PE
		30.0	Trittschalldämmung	50.0	EPS-Hartschaum (Rohdichte 15 kg/m³)
Founda-tion		40.0	Wärmedämmung	50.0	Mineralwolle (Boden-Dämmung)
		2.0	Abdichtung	50.0	Bitumenbahnen G 200 S4
		300.0	Stahlbeton 2 % Bewehrungsstahl	50.0	Transportbeton C20/25
			Bewehrungsdstahl	50.0	Bewehrungsstahl
		140.0	Wärmedämmung	50.0	Extrudierter Polystyrol Dämmstoff (XPS)
	DE-01				
		60.0	Zementestrich	50.0	Zementestrich
		0.4	Trennlage	50.0	Dampfbremse PE
		30.0	Trittschalldämmung	50.0	EPS-Hartschaum (Rohdichte 15 kg/m³)
Ceiling		40.0	Wärmedämmung	50.0	Mineralwolle (Boden-Dämmung)
		180.0	Stahlbeton 2 % Bewehrungsstahl	50.0	Transportbeton C20/25
			Bewehrungsstahl	50.0	Bewehrungsstahl
	FE-01				
			Flügelrahmen Kunststoff	40.0	Flügelrahmen PVC-U
			Blendrahmen Kunststoff	40.0	Blendrahmen PVC-U
			Dreischeiben-Isolierverglasung	30.0	Dreifachverglasung
Window					

Original material list of the ECO+ Project

V03_WoodMassive

Bezeichnung		Bauteilaufbau	Nutzungs dauer	Datensatz
-	[mm]	Material	[a]	
AW-01				
	24.0	Holz Aussenwandverkleidung	40.0	Nadelschnittholz - getrocknet (Durchschnitt DE)
	30.0	Holz Lattung versetzt	40.0	Nadelschnittholz - getrocknet (Durchschnitt DE)
	1.0	Windbremse	30.0	Dampfbremse PE
	160.0	Wärmedämmung	50.0	Holzfaserdämmstoffplatte Trockenverfahren (Durchschnitt
	160.0	Konstruktionsvollholz (60/200; e=0,625m)	50.0	Konstruktionsvollholz (Durchschnitt DE)
	30.0	Querlattung Holz (e=400m)	50.0	Nadelschnittholz - getrocknet (Durchschnitt DE)
	40.0	Wärmedämmung	50.0	Holzfaserdämmstoffplatte Trockenverfahren (Durchschnitt
	24.0	Holz Innenwandverkleidung	50.0	Nadelschnittholz - getrocknet (Durchschnitt DE)

External Wall — AW-01

Bezeichnung	[mm]	Material	[a]	Datensatz
IW-01				
Lehmbaupla	22.0	Lehmbauplatte	50.0	Lehmbauplatte
	75.0	Metallständer (e=0,625m)	50.0	Aluminiumblech
	75.0	Mineralwolle	50.0	Mineralwolle (Innenausbau-Dämmung)
	22.0	Lehmbauplatte	50.0	Lehmbauplatte

Internal Wall — IW-01

Bezeichnung	[mm]	Material	[a]	Datensatz
DA-01				
Warmdach	150.0	Extensive Dachbegrünung	40.0	Gründach extensiv (ohne Geländer)
	10.0	Schutz, Drän- und Filterschicht	40.0	
	3.0	Dachabdichtung	40.0	Bitumenbahnen G 200 S4
	160.0	Holzfaserdämmung (λ = 0,039 W/mK)	50.0	Holzfaserdämmstoffplatte Trockenverfahren (Durchschnitt
	0.1	Abdichtungsbahn	50.0	Bitumenbahnen G 200 S4
	180.0	Brettschichtholz	50.0	Brettschichtholz - Standardformen (Durchschnitt DE)

Roof — DA-01

Bezeichnung	[mm]	Material	[a]	Datensatz
G-01				
Bodenplatte	60.0	Zementestrich	50.0	Zementestrich
	0.4	Trennlage	50.0	Dampfbremse PE
	30.0	Trittschalldämmung	50.0	Holzfaserdämmstoffplatte Trockenverfahren (Durchschnitt
	40.0	Wärmedämmung	50.0	Holzfaserdämmstoffplatte Trockenverfahren (Durchschnitt
	2.0	Abdichtung	50.0	Bitumenbahnen G 200 S4
	300.0	Stahlbeton 2 % Bewehrungsstahl	50.0	Transportbeton C20/25
		Bewehrungsstahl	50.0	Bewehrungsstahl
	140.0	Wärmedämmung	50.0	Extrudierter Polystyrol Dämmstoff (XPS)

Foundation — G-01

Bezeichnung	[mm]	Material	[a]	Datensatz
DE-01				
	60.0	Zementestrich	50.0	Zementestrich
	0.4	Trennlage	50.0	Dampfbremse PE
	30.0	Trittschalldämmung	50.0	Holzfaserdämmstoffplatte Trockenverfahren (Durchschnitt
	60.0	Splittschüttung (m' ≥ 90 kg/m2)	50.0	Porenbeton Granulat
	1.0	Trennlage	50.0	Dampfbremse PE
	180.0	Brettsperrholz	50.0	Brettschichtholz - Standardformen (Durchschnitt DE)

Ceiling — DE-01

Bezeichnung	[mm]	Material	[a]	Datensatz
FE-01				
		Flügelrahmen Holz	50.0	Holz-Flügelrahmen
		Blendrahmen Holz	50.0	Holz-Blendrahmen
		Dreischeiben-Isolierverglasung	30.0	Dreifachverglasung

Window — FE-01

Original material list of the ECO+ Project

V04_WoodLight

Bezeichnun	[mm]	Bauteilaufbau / Material	Nutzungs dauer [a]	Datensatz
-				
AW-01				
	24.0	Holz Aussenwandverkleidung	40.0	Nadelschnittholz - getrocknet (Durchschnitt DE)
	30.0	Holz Lattung versetzt	40.0	Nadelschnittholz - getrocknet (Durchschnitt DE)
	1.0	Windbremse	40.0	Dampfbremse PE
	200.0	Konstruktionsvollholz (60/200; e=0,625m)	50.0	Konstruktionsvollholz (Durchschnitt DE)
	200.0	Wärmedämmung	50.0	Holzfaserdämmstoffplatte Trockenverfahren (Durchschnitt
	1.0	Dampfbremse	50.0	Dampfbremse PE
	30.0	Querlattung Holz (e=400m)	50.0	Nadelschnittholz - getrocknet (Durchschnitt DE)
	30.0	Wärmedämmung	50.0	Holzfaserdämmstoffplatte Trockenverfahren (Durchschnitt
	24.0	Holz Innenwandverkleidung	50.0	Nadelschnittholz - getrocknet (Durchschnitt DE)

Bezeichnun	[mm]	Material	[a]	Datensatz
IW-01				
Lehmbaupla	22.0	Lehmbauplatte	50.0	Lehmbauplatte
	75.0	Metallständer (e=0,625m)	50.0	Aluminiumblech
	75.0	Mineralwolle	50.0	Mineralwolle (Innenausbau-Dämmung)
	22.0	Lehmbauplatte	50.0	Lehmbauplatte

Bezeichnun	[mm]	Material	[a]	Datensatz
DA-01				
Warmdach	150.0	Extensive Dachbegrünung	40.0	Gründach extensiv (ohne Geländer)
	10.0	Schutz, Drän- und Filterschicht	40.0	
	3.0	Dachabdichtungsbahn	40.0	Bitumenbahnen G 200 S4
	260.0	Holzfaserdämmung (λ = 0,039 W/mK)	50.0	Holzfaserdämmstoffplatte Trockenverfahren (Durchschnitt
	0.1	Abdichtungsbahn	50.0	Bitumenbahnen G 200 S4
	28.0	Dreischichtplatte auf Trägerplatte geklebt	50.0	3- und 5-Schicht Massivholzplatte (Durchschnitt DE)
	140.0	Brettschichtholzträger (80/140; e=0,3125m)	50.0	Brettschichtholz - Standardformen (Durchschnitt DE)
	28.0	Dreischichtplatte auf Trägerplatte geklebt	50.0	

Bezeichnun	[mm]	Material	[a]	Datensatz
G-01				
Bodenplatte	60.0	Zementestrich	50.0	Zementestrich
	0.4	Trennlage	50.0	Dampfbremse PE
	30.0	Trittschalldämmung	50.0	Holzfaserdämmstoffplatte Trockenverfahren (Durchschnitt
	40.0	Wärmedämmung	50.0	Holzfaserdämmstoffplatte Trockenverfahren (Durchschnitt
	2.0	Abdichtung	50.0	Dampfbremse PE
	300.0	Stahlbeton 2 % Bewehrungsstahl	50.0	Transportbeton C20/25
		Bewehrungsstahl	50.0	Bewehrungsstahl
	140.0	Wärmedämmung	50.0	Extrudierter Polystyrol Dämmstoff (XPS)

Bezeichnun	[mm]	Material	[a]	Datensatz
DE-01				
	60.0	Zementestrich	50.0	Zementestrich
	0.4	Trennlage	50.0	Dampfbremse PE
	40.0	Trittschalldämmung	50.0	Holzfaserdämmstoffplatte Trockenverfahren (Durchschnitt
	60.0	Splittschüttung	50.0	Porenbeton Granulat
	28.0	Dreischichtplatte	50.0	Brettsperrholz (Durchschnitt DE)
	220.0	Brettschichtholz Träger (100/220; e=0,3125m)	50.0	Brettschichtholz - Standardformen (Durchschnitt DE)

Bezeichnun	[mm]	Material	[a]	Datensatz
FE-01				
		Flügelrahmen Holz	50.0	Holz-Flügelrahmen
		Blendrahmen Holz	50.0	Holz-Blendrahmen
		Dreischeiben-Isolierverglasung	30.0	Dreifachverglasung

External Wall — AW-01
Internal Wall — IW-01
Roof — DA-01
Foundation — G-01
Ceiling — DE-01
Window — FE-01

Annex 5 Average values of the energy performance simulations for the scenario RCP8.5 of the year 2100

Input Parameter	Value	Total End Use Energy Intensity [kWh/m^2]	Total Cooling Energy Intensity [kWh/m^2]	Peak Hour Cooling Energy Intensity [kWh/m^2]
in:Construction Set	1	44.55956	37.21067	0.073624
in:Construction Set	2	44.58149	37.23259	0.074528
in:Construction Set	3	45.136	37.78711	0.079655
in:Construction Set	4	45.15405	37.80516	0.080711
in:Building rotation	0	46.29009	38.9412	0.081351
in:Building rotation	30	45.56704	38.21814	0.079645
in:Building rotation	60	43.30833	35.95943	0.074501
in:Building rotation	120	43.49139	36.1425	0.071871
in:Building rotation	150	45.63203	38.28313	0.078279
in:Window shading style	0	51.55138	44.20248	0.090205
in:Window shading style	1	39.30847	31.95958	0.066252
in:Window shading style	2	47.79445	40.44556	0.082843
in:Window shading style	3	40.7768	33.42791	0.069218
in:Window U-Factor	0.6	44.95581	37.60692	0.076874
in:Window U-Factor	1.2	44.75974	37.41084	0.077385
in:Window SHGC	0.4	39.94019	32.5913	0.068226
in:Window SHGC	0.6	45.00083	37.65193	0.077093
in:Window SHGC	0.8	49.63231	42.28341	0.08607
in:Windows-To-Wall-Ratio	0.2	39.69267	32.34378	0.066747
in:Windows-To-Wall-Ratio	0.3	44.96839	37.6195	0.07701
in:Windows-To-Wall-Ratio	0.4	49.91226	42.56337	0.087631
Overall mean	-	44.85778	37.50888	0.07713

Annex 6 Average values of the thermal comfort simulations for the scenario RCP8.5 of the year 2100

Input Parameter	Value	Number of hot hours	Average Temperature Difference Outdoor-Indoor	Maximum Average Operative Temperature	Average HSP
in:Construction Set	1	1487.908	13.02214	43.68546	95.02636
in:Construction Set	2	1487.594	13.07332	43.9738	96.03792
in:Construction Set	3	1474.181	12.68224	47.0379	96.30409
in:Construction Set	4	1458.094	12.65522	48.55805	95.71397
in:Building rotation	0	1479.247	13.65716	46.97088	96.79922
in:Building rotation	30	1478.424	13.26983	46.487	96.27879
in:Building rotation	60	1474.611	12.06561	44.86805	94.63478
in:Building rotation	120	1474.253	12.04981	44.38789	94.74976
in:Building rotation	150	1478.188	13.24873	46.35519	96.39038
in:Window shading style	0	1485.625	16.28543	50.28962	99.09577
in:Window shading style	1	1464.347	10.06497	42.44192	91.22607
in:Window shading style	2	1483.436	14.34134	47.97079	98.13627
in:Window shading style	3	1474.369	10.74117	42.55289	94.62423
in:Window U-Factor	0.6	1481.807	13.56064	46.42598	96.82589
in:Window U-Factor	1.2	1472.082	12.15582	45.20162	94.71528
in:Window SHGC	0.4	1466.431	10.31934	42.40734	92.12288
in:Window SHGC	0.6	1480.196	12.91268	45.77316	96.72585
in:Window SHGC	0.8	1484.206	15.34266	49.26091	98.46303
in:Windows-To-Wall-Ratio	0.2	1471.906	10.72459	42.56925	92.77059
in:Windows-To-Wall-Ratio	0.3	1478.279	12.94433	45.84117	96.50684
in:Windows-To-Wall-Ratio	0.4	1480.648	14.90576	49.03099	98.03432
Overall mean	-	1476.944	12.85822	45.81380	95.77058

Annex 7 Average values of the thermal comfort simulations for the scenario RCP2.5 of the year 2100

Input Parameter	Value	Number of hot hours	Average Temperature Difference Outdoor-Indoor	Maximum Average Operative Temperature	Average HSP
in:Construction Set	1	1378.189	12.76831	39.00934	84.05286
in:Construction Set	2	1375.075	12.80017	39.33768	84.84567
in:Construction Set	3	1280.261	12.5769	41.33731	80.52561
in:Construction Set	4	1243.514	12.59985	42.46983	78.47429
in:Building rotation	0	1359.417	13.4126	42.037	85.90948
in:Building rotation	30	1342.997	13.05202	41.48752	84.11576
in:Building rotation	60	1274.465	11.95371	39.95876	77.6679
in:Building rotation	120	1277.743	11.96828	38.369	77.93462
in:Building rotation	150	1341.677	13.04493	40.84042	84.24528
in:Window shading style	0	1455.664	15.92585	45.58943	95.28648
in:Window shading style	1	1132.925	10.04215	36.86773	64.72962
in:Window shading style	2	1423.164	14.08894	43.24142	91.25833
in:Window shading style	3	1265.286	10.68828	36.45558	76.624
in:Window U-Factor	0.6	1368.379	13.36222	41.16896	86.11828
in:Window U-Factor	1.2	1270.14	12.0104	39.90812	77.83093
in:Window SHGC	0.4	1363.719	12.73793	40.55105	85.44147
in:Window SHGC	0.6	1434.625	15.0417	44.53715	92.69818
in:Window SHGC	0.8	1159.435	10.27929	36.52742	67.78416
in:Windows-To-Wall-Ratio	0.2	1201.9	10.67561	36.84326	70.84529
in:Windows-To-Wall-Ratio	0.3	1350.656	12.76352	40.5931	84.48499
in:Windows-To-Wall-Ratio	0.4	1405.223	14.6198	44.17926	90.59354
Overall mean	-	1319.260	12.68631	40.53854	81.97461

Annex 8 Average values of the thermal comfort simulations for the scenario RCP4.5 of the year 2100 – comparison of natural ventilation strategies.

Input Parameter	Value	Number of hot hours	Average Temperature Difference Outdoor-Indoor	Maximum Average Operative Temperature	Average HSP
in:Min indoor temp	-100	1329.601	21.0229	64.38719	86.4894
in:Min indoor temp	20	1335.508	21.17849	64.46105	87.07968
in:Min indoor temp	25	1364.235	21.80358	64.78368	90.01968
in:Max indoor temp	30	1475.098	25.75815	68.35044	97.26239
in:Max indoor temp	35	1369.029	22.91413	66.98671	89.13214
in:Max indoor temp	100	1185.217	15.33269	58.29476	77.19423
in:Min outdoor temp	-100	1266.407	19.63072	63.59718	80.46723
in:Min outdoor temp	20	1445.048	23.42474	65.66627	97.08125
in:Min outdoor temp	15	1317.888	20.94951	64.36846	86.04028
in:Max outdoor temp	25	1364.099	21.92772	65.29367	89.41152
in:Max outdoor temp	30	1338.418	21.18818	64.86607	87.44697
in:Max outdoor temp	100	1326.827	20.88907	63.47217	86.73028
in:Delta tempertaure	-100	1328.479	21.08949	64.34951	86.60904
in:Delta tempertaure	0	1328.964	21.10257	64.35668	86.64571
in:Delta tempertaure	5	1371.9	21.81291	64.92573	90.33401
in:Schedule Number	0	1181.584	17.31404	61.40062	73.48829
in:Schedule Number	1	1367.214	22.24819	65.44391	90.99901
in:Schedule Number	2	1480.545	24.44273	66.78738	99.10146
in:Cross-Ventilation	0	1347.528	21.40624	64.59687	88.28269
in:Cross-Ventilation	1	1338.701	21.26374	64.49107	87.44315
in:Window obstructions	0.4	1346.359	21.39663	64.59214	88.19537
in:Window obstructions	0.65	1339.87	21.27335	64.4958	87.53047
Overall mean	-	1343.115	21.3350	64.54397	87.86292

Annex 9 Summary of sensitivities Energy Performance simulation results

	Total End Use Energy Intensity [kWh/m^2]		Total Cooling Energy Intensity [kWh/m^2]		Peak Hour Cooling Energy Intensity [kWh/m^2]	
	Sensitivity	Normalized	Sensitivity	Normalized	Sensitivity	Normalized
P1	0.198163	0.00947	0.198164	0.00947	0.002363	0.053371
P2	1.326365	0.063386	1.326365	0.063386	0.003972	0.08973
P3	9.248844	0.441993	9.248844	0.441993	0.018056	0.407899
P4	0.196073	0.00937	0.196073	0.00937	0.000512	0.011555
P5	4.846057	0.231588	4.846057	0.231588	0.008922	0.201559
P6	5.109795	0.244192	5.109795	0.244192	0.010442	0.235885

Annex 10 Summary of sensitivities Thermal Comfort simulation results

	Number of hot hours		Avg. Temp. Difference Outdoor-Indoor		Maximum Average Operative Temperature		Average HSP	
	Sensitivity	Norm.	Sensitivity	Norm.	Sensitivity	Norm.	Sensitivity	Norm.
P1	9.938	0.192	0.156	0.014	1.624	0.096	0.623	0.040
P2	2.232	0.043	0.702	0.061	1.138	0.067	0.980	0.063
P3	16.478	0.319	4.699	0.406	6.265	0.371	6.097	0.391
P4	9.725	0.188	1.405	0.121	1.224	0.072	2.111	0.135
P5	8.887	0.172	2.512	0.217	3.427	0.203	3.170	0.203
P6	4.371	0.085	2.091	0.181	3.231	0.191	2.632	0.169

Annex 11 Summary of sensitivities Thermal Comfort simulation results

	Number of hot hours		Avg. Temp. Difference Outdoor-Indoor		Maximum Average Operative Temperature		Average HSP	
	Sensitivity	Norm.	Sensitivity	Norm.	Sensitivity	Norm.	Sensitivity	Norm.
P1	44.892	0.066	0.093	0.009	1.153	0.061	2.388	0.039
P2	38.041	0.056	0.638	0.059	1.535	0.081	3.705	0.061
P3	256.952	0.379	4.444	0.408	7.294	0.386	23.907	0.394
P4	98.239	0.145	1.352	0.124	1.261	0.067	8.287	0.137
P5	137.595	0.203	2.381	0.219	4.005	0.212	12.457	0.206
P6	101.661	0.150	1.972	0.181	3.668	0.194	9.874	0.163

Annex 12 Summary of sensitivities Thermal Comfort simulation results – Natural Ventilation strategies

	Number of hot hours		Avg. Temp. Difference Outdoor-Indoor		Maximum Average Operative Temperature		Average HSP	
	Sensitivity	Norm.	Sensitivity	Norm.	Sensitivity	Norm.	Sensitivity	Norm.
PV1	17.317	0.038	0.390	0.032	0.198	0.019	1.765	0.047
PV2	144.940	0.317	5.213	0.427	5.028	0.486	10.034	0.267
PV3	89.320	0.196	1.897	0.155	1.035	0.100	8.307	0.221
PV4	18.636	0.041	0.519	0.043	0.911	0.088	1.341	0.036
PV5	21.710	0.048	0.362	0.030	0.288	0.028	1.862	0.050
PV6	149.480	0.327	3.564	0.292	2.693	0.260	12.807	0.340
PV7	8.827	0.019	0.142	0.012	0.106	0.010	0.840	0.022
PV8	6.488	0.014	0.123	0.010	0.096	0.009	0.665	0.018